



**University of California
High-Performance
AstroComputing Center
(UC-HiPACC)**

**International Summer School
on AstroComputing 2012**

AstroInformatics



Lecture II

Simulating Galaxies and the Universe

**Joel R. Primack, UCSC
(Director, UC-HiPACC)**

The background of the slide is a complex, glowing orange-red network of filaments and nodes, representing a simulation of the cosmic web or galaxy distribution. The filaments are interconnected and vary in thickness, with brighter spots indicating denser regions.

Simulating Galaxies and the Universe

Joel R. Primack

University of California, Santa Cruz

This picture is beautiful but misleading, since it only shows about 0.5% of the cosmic density.

The other 99.5% of the universe is invisible.

All Other Atoms 0.01%
H and He 0.5%

} Visible Matter 0.5%

Invisible Atoms 4%

Cold Dark Matter 25%

Dark Energy 70%

Imagine that the entire universe is an ocean of dark energy. On that ocean sail billions of ghostly ships made of dark matter...

Matter and Energy Content of the Universe

Λ CDM

Double Dark Theory

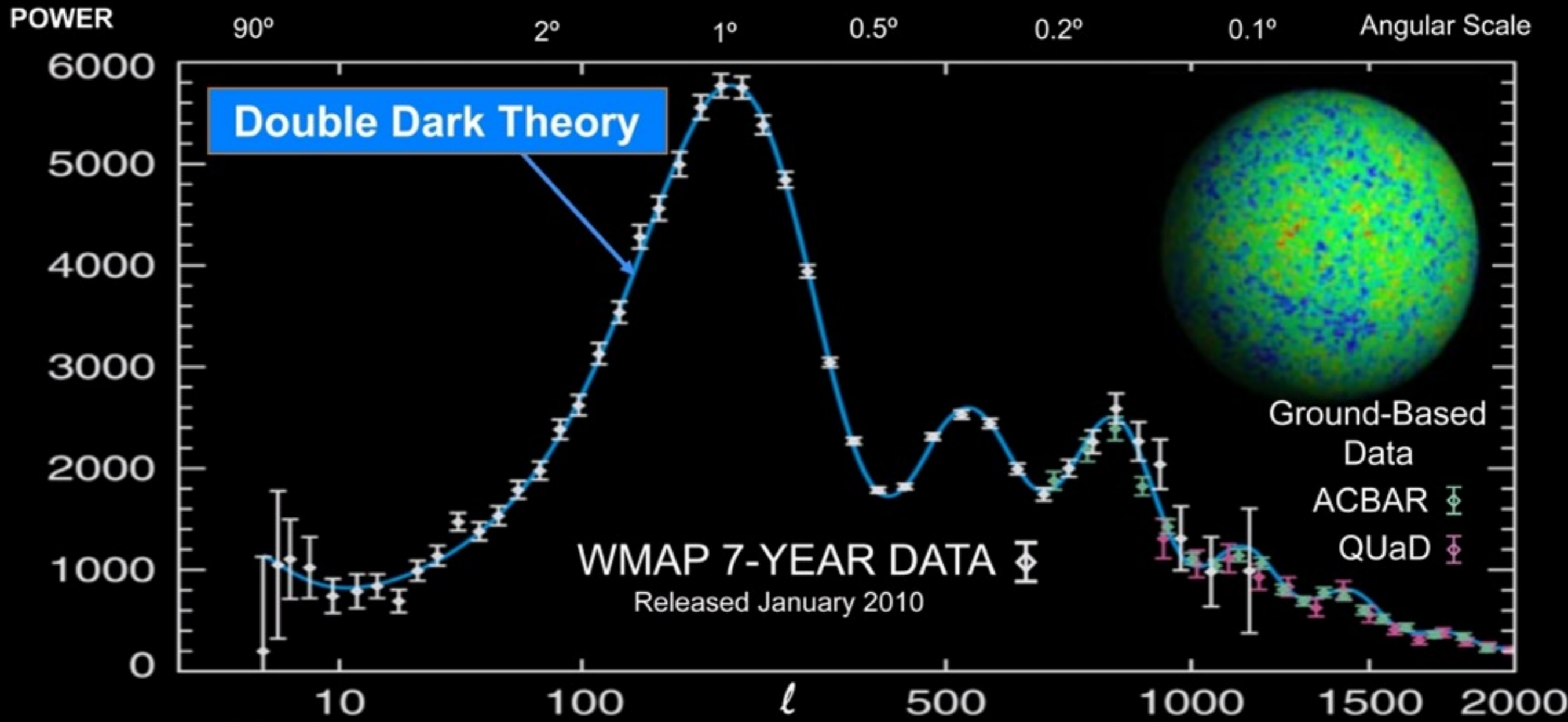
Dark Matter Ships on a Dark Energy Ocean

DARK MATTER
+ DARK ENERGY =
DOUBLE DARK
THEORY

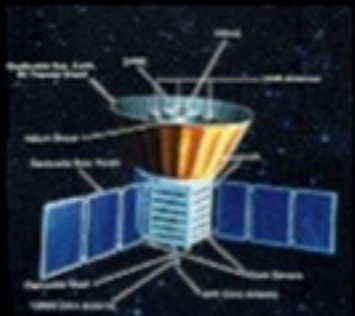
Technical Name:

Lambda Cold Dark Matter (Λ CDM)

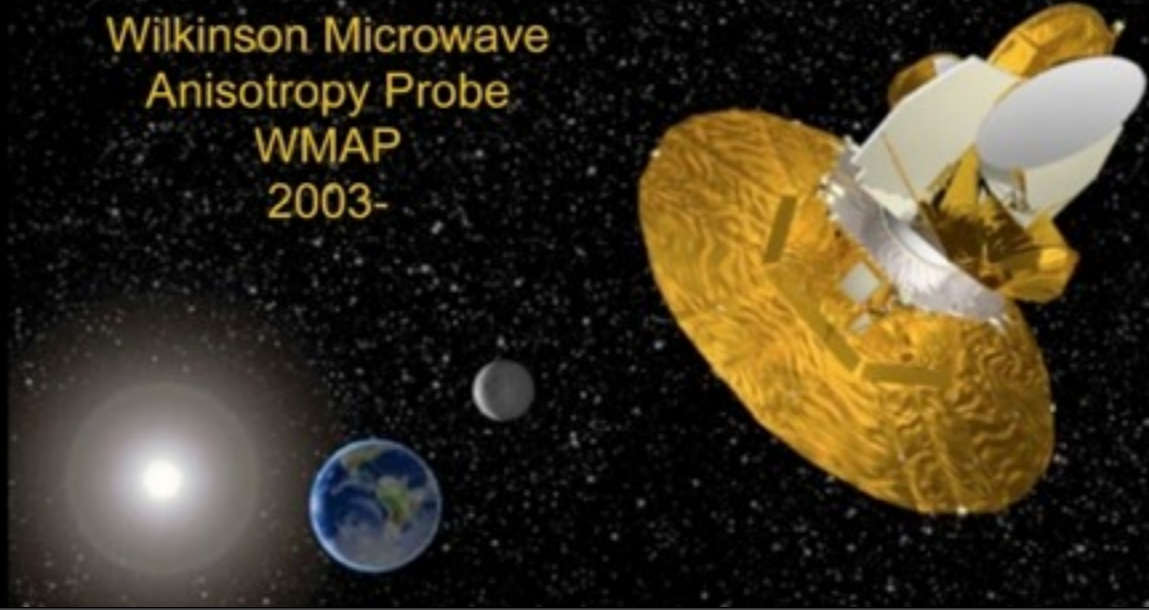
Big Bang Data Agree with Double Dark Theory



Cosmic Background Explorer
COBE
1992

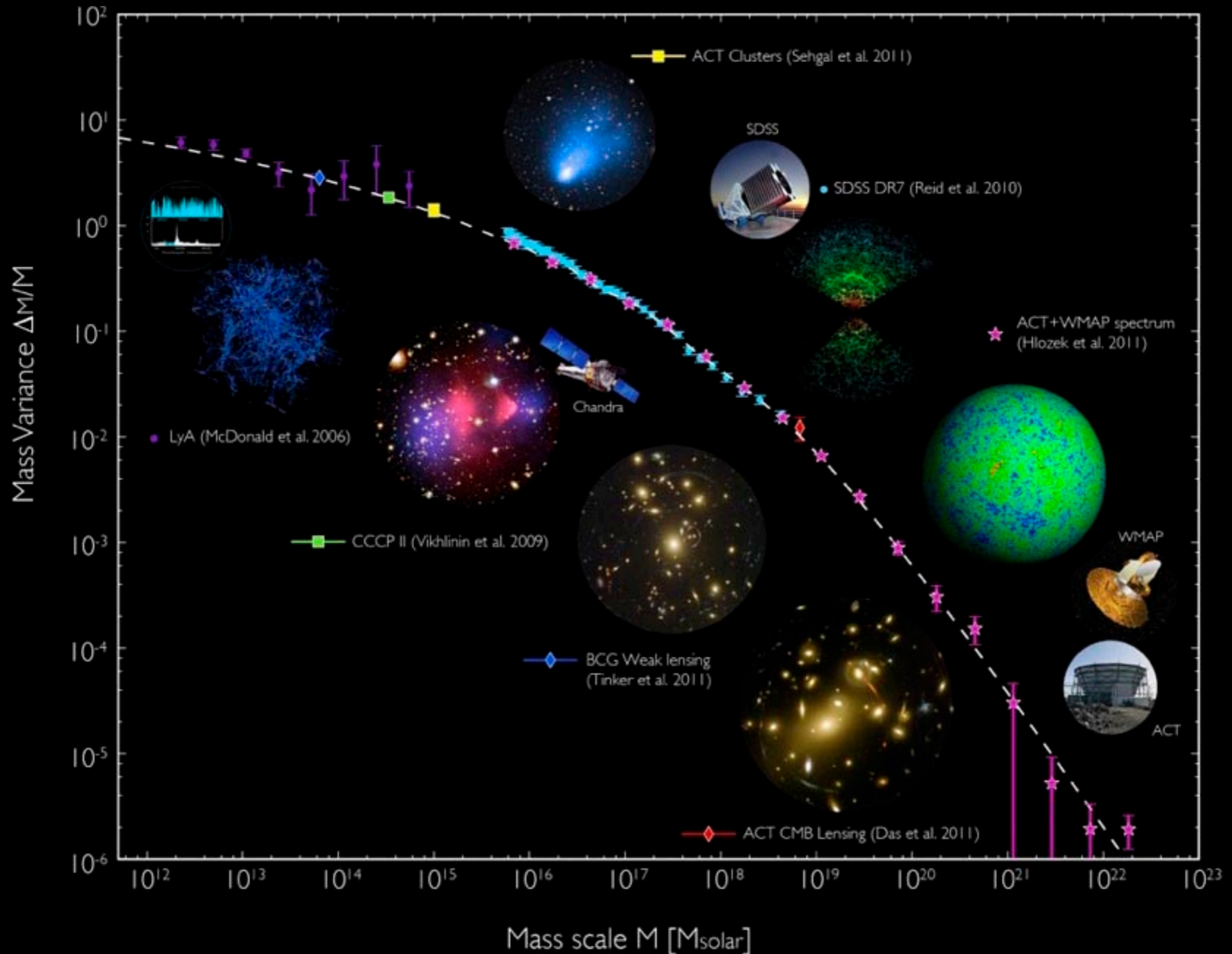


Wilkinson Microwave Anisotropy Probe
WMAP
2003-

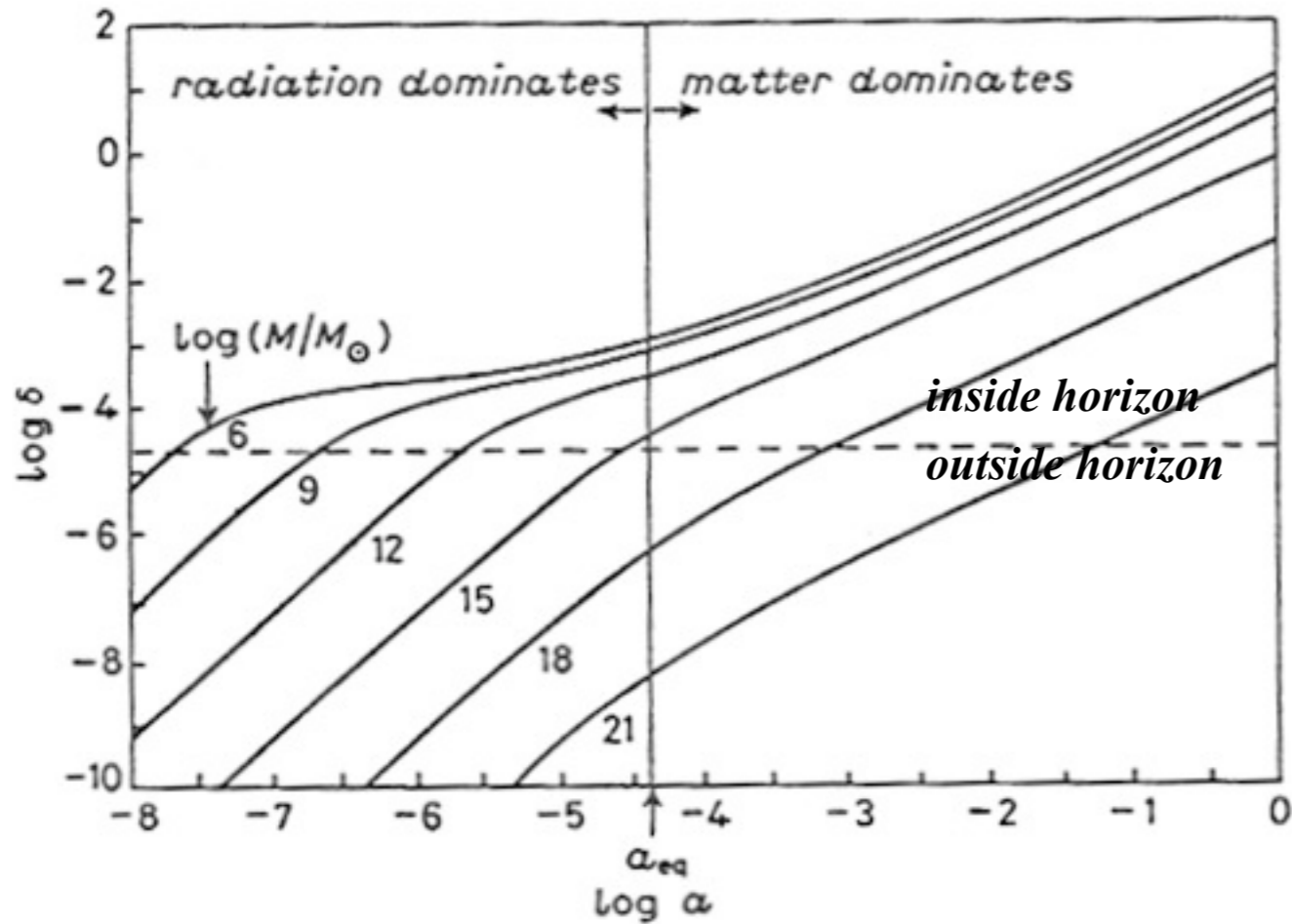


Distribution of Matter

Also Agrees with Double Dark Theory!

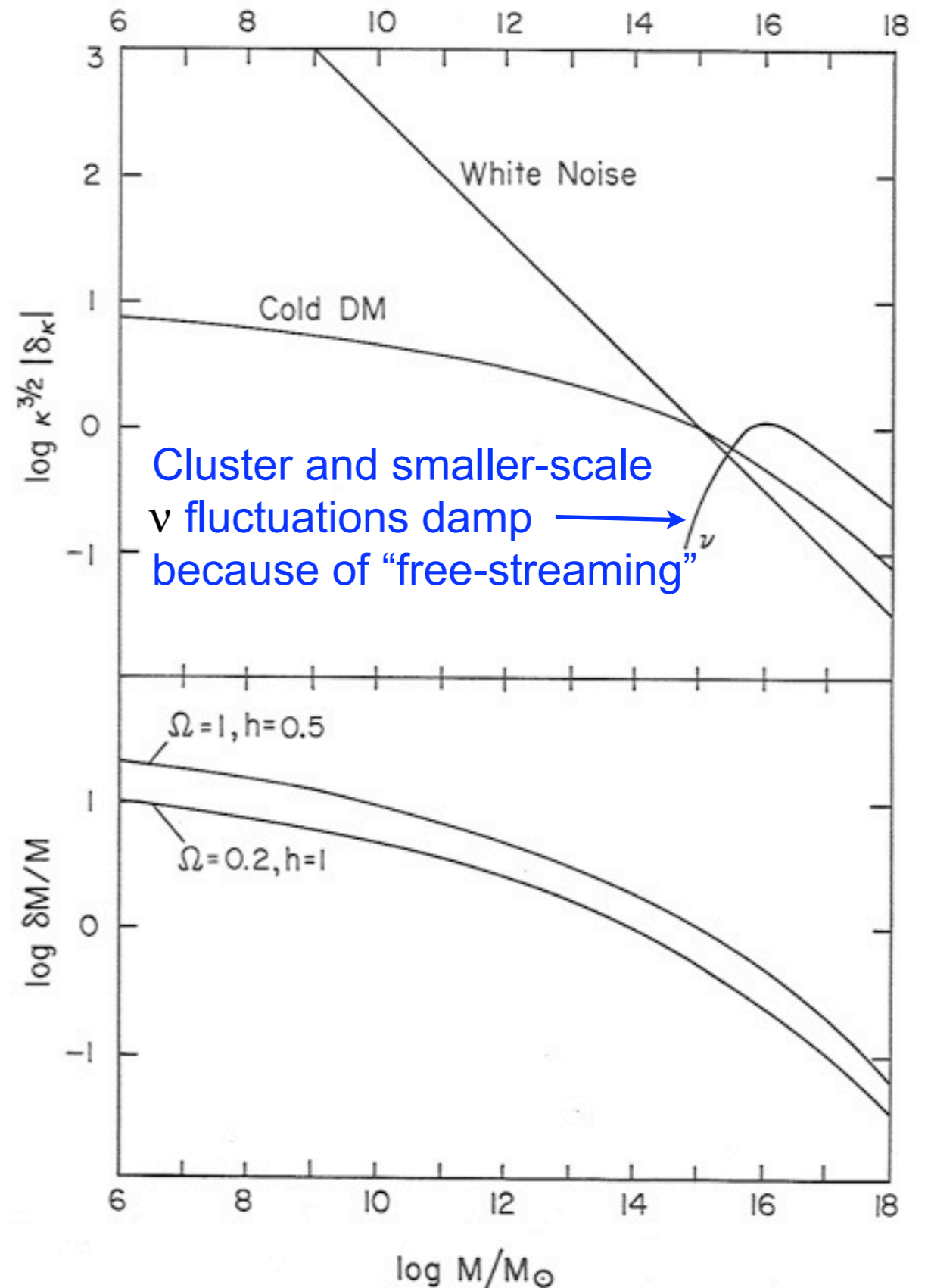


CDM Structure Formation: Linear Theory



Matter fluctuations that enter the horizon during the radiation dominated era, with masses less than about $10^{15} M_{\odot}$ grow only $\propto \log a$, because they are not in the gravitationally dominant component. But matter fluctuations that enter the horizon in the matter-dominated era grow $\propto a$. This explains the characteristic shape of the CDM fluctuation spectrum, with $\delta(k) \propto k^{n/2-2} \log k$

Primack & Blumenthal 1983,
Primack Varenna Lectures 1984



Blumenthal, Faber, Primack, & Rees 1984

Because the Λ CDM **Dark Energy + Cold Dark Matter** (Double Dark) theory of structure formation is now so well confirmed by observations, we study the predictions of this theory for the formation of dark matter structure in the universe and use this to improve our understanding of the visible objects that we can see with our telescopes: galaxies, clusters, and the large-scale structure of the universe.

Cosmological Simulations

Astronomical observations represent snapshots of moments in time. It is the role of astrophysical theory to produce movies -- both metaphorical and actual -- that link these snapshots together into a coherent physical theory.

Cosmological dark matter simulations show large scale structure, growth of structure, and dark matter halo properties

Hydrodynamic galaxy formation simulations: evolution of galaxies, formation of galactic spheroids via mergers, galaxy images in all wavebands including stellar evolution and dust



"QUARKS. NEUTRINOS. MESONS. ALL THOSE DAMN PARTICLES YOU CAN'T SEE. THAT'S WHAT DROVE ME TO DRINK. BUT NOW I CAN SEE THEM!"

Dark Matter Expanding

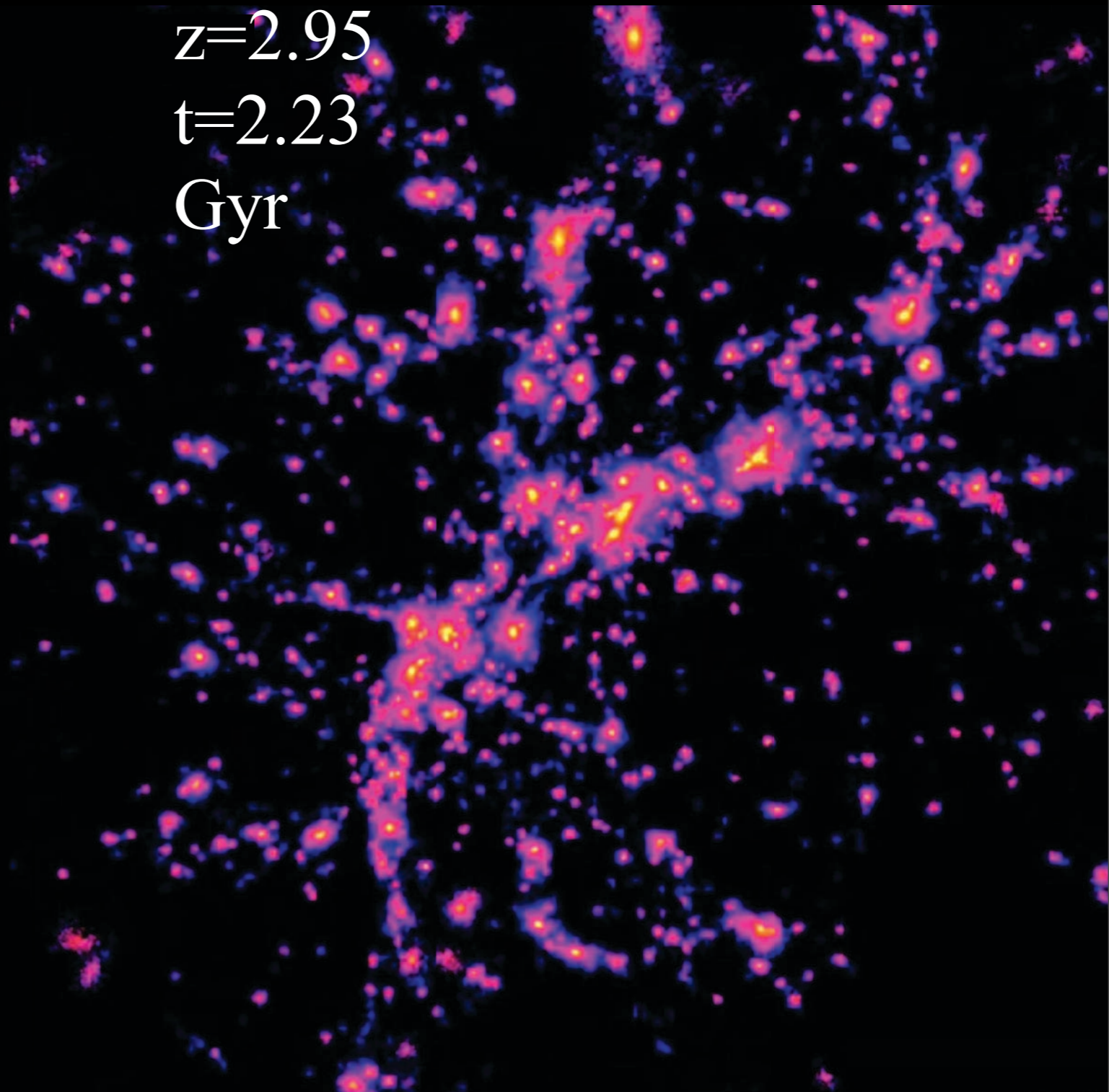
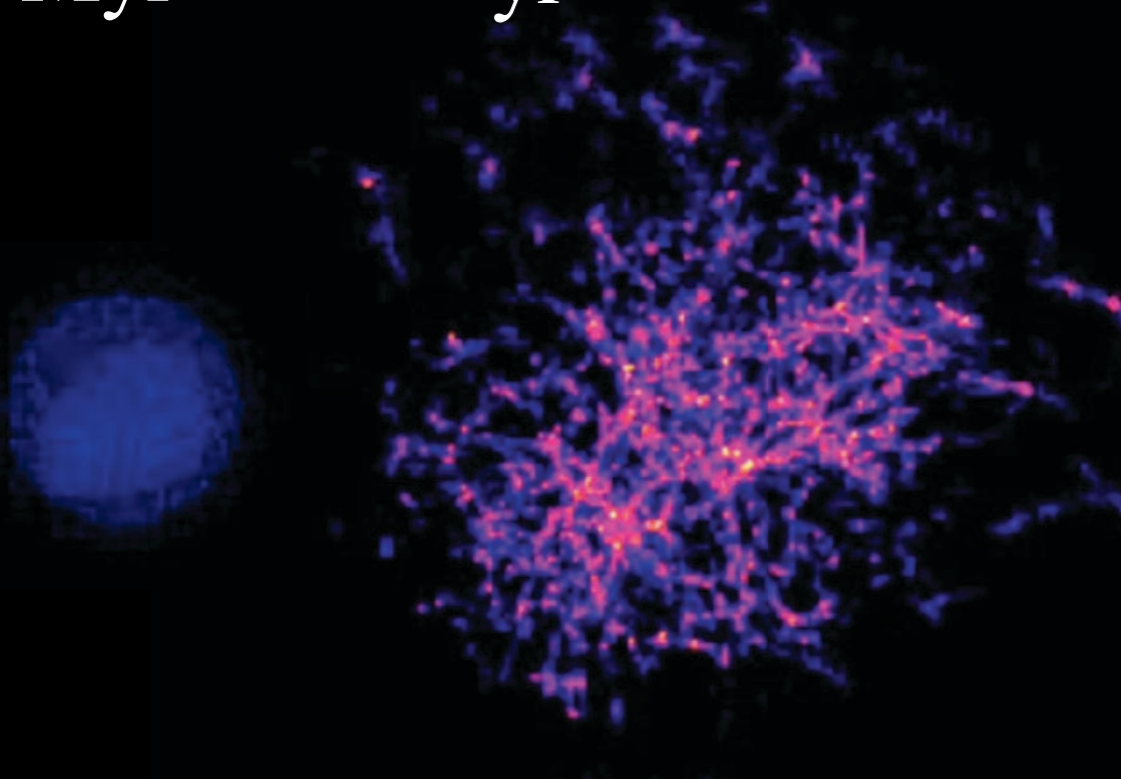


Expansion....

$z=49.00$
 $t=49$
Myr

$z=12.01$
 $t=374\text{M}$
yr

$z=2.95$
 $t=2.23$
Gyr



$z=0.837$ $t=6.66$ Gyr

**End of expansion
for this halo**

$z=0.000$ $t=13.7$ Gyr (today)

**Wild
Space**

**Tame
Space**

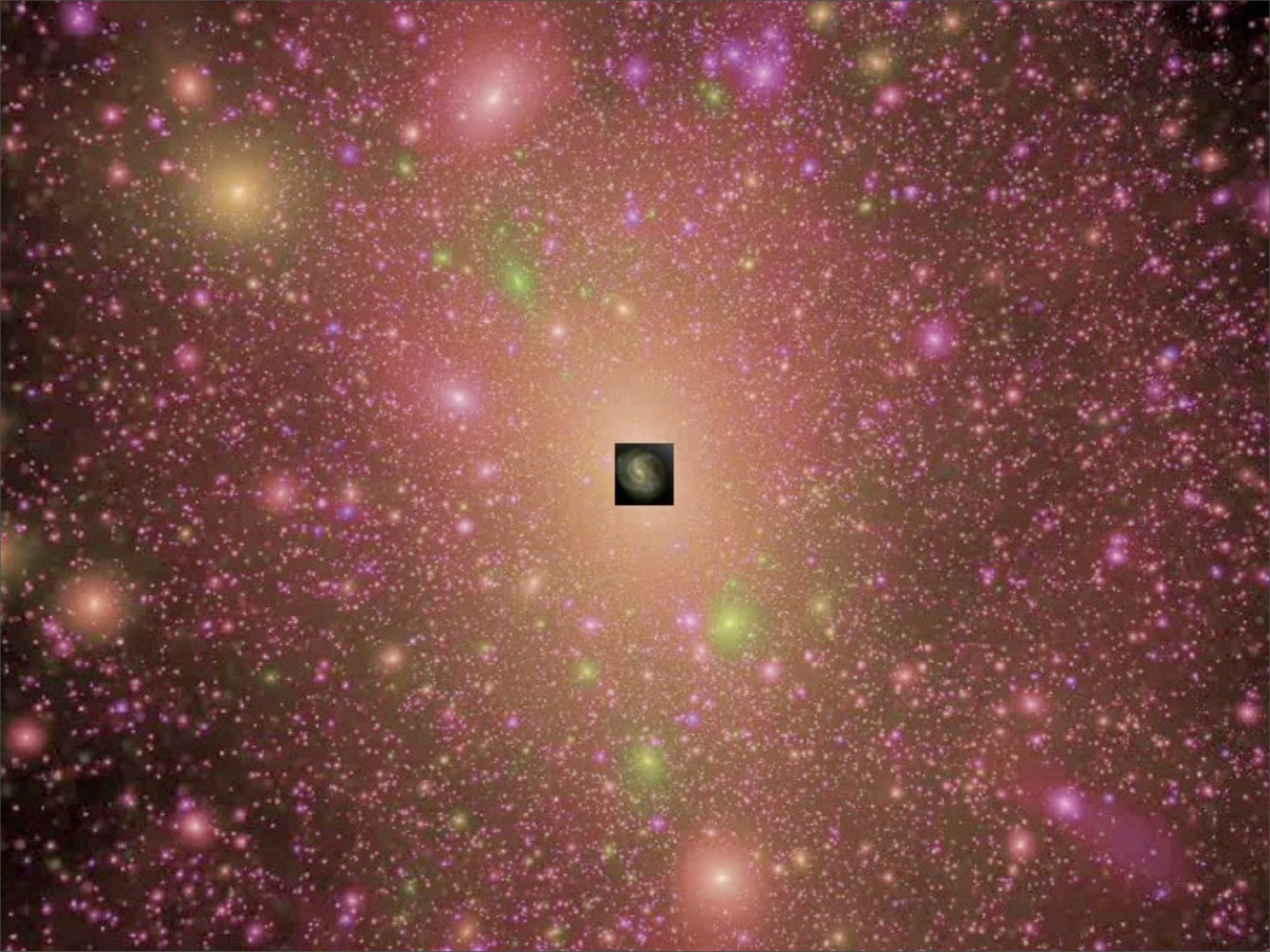
Aquarius Simulation

Milky Way
100,000 Light Years

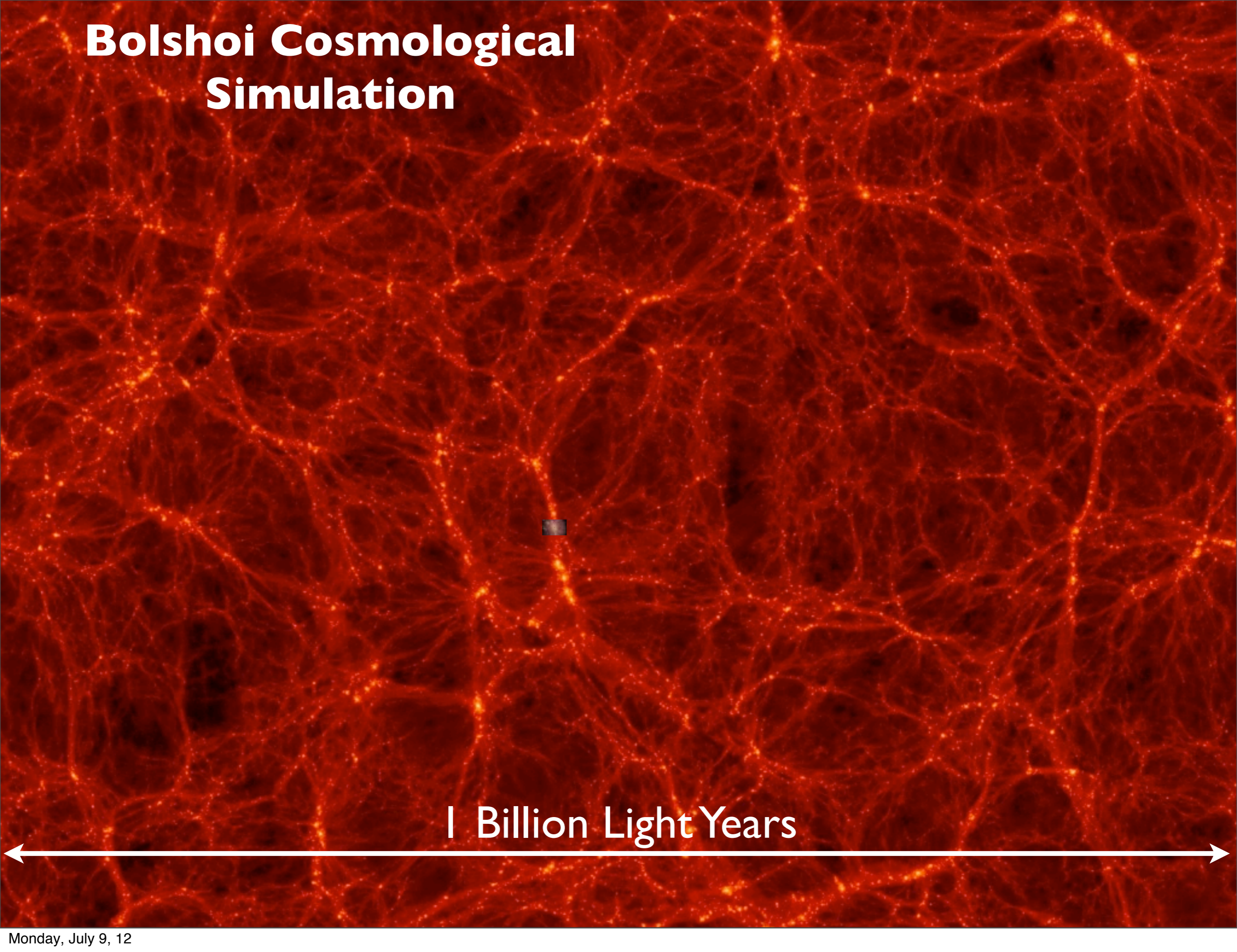


Milky Way Dark Matter Halo
1,500,000 Light Years





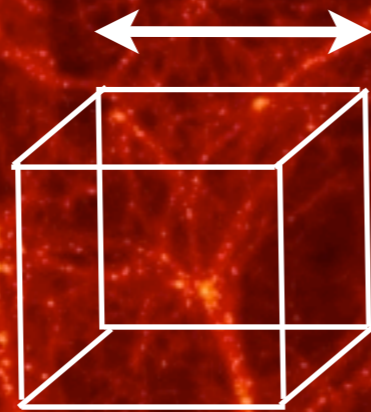
Bolshoi Cosmological Simulation



1 Billion Light Years

Bolshoi Cosmological Simulation

100 Million Light Years



1 Billion Light Years



Bolshoi Cosmological Simulation

100 Million Light Years



Bjork “Dark Matter” *Biophilia*



SKY & TELESCOPE

Dive Deep In
the Lagoon p. 61

JULY 2012

Universe in

From the Big Bang to Now p. 26

a Box



Universe on Fast Forward

Supercomputer modeling is transforming cosmology from a purely observational science into an experimental science.

<https://dl.dropbox.com/u/5495083/Sky%26Telescope%20Bolshoi%20Article.pdf>

EVOLVING UNIVERSE

Facing page, left to right: These frames from the Bolshoi simulation depict the universe at redshifts of 10, 3, 1, and 0, which correspond to cosmic ages of 490 million years, 2.2 billion years, 6 billion years, and 13.7 billion years (today). The bright areas have high densities of dark matter. As the far left frame shows, Bolshoi starts off with only a modest degree of lumpiness in the distribution of matter. But the subsequent frames demonstrate how gravity, acting over billions of years, gathered matter into long filaments that surround immense voids. Galaxies are concentrated along the filaments, clusters at the nodes.

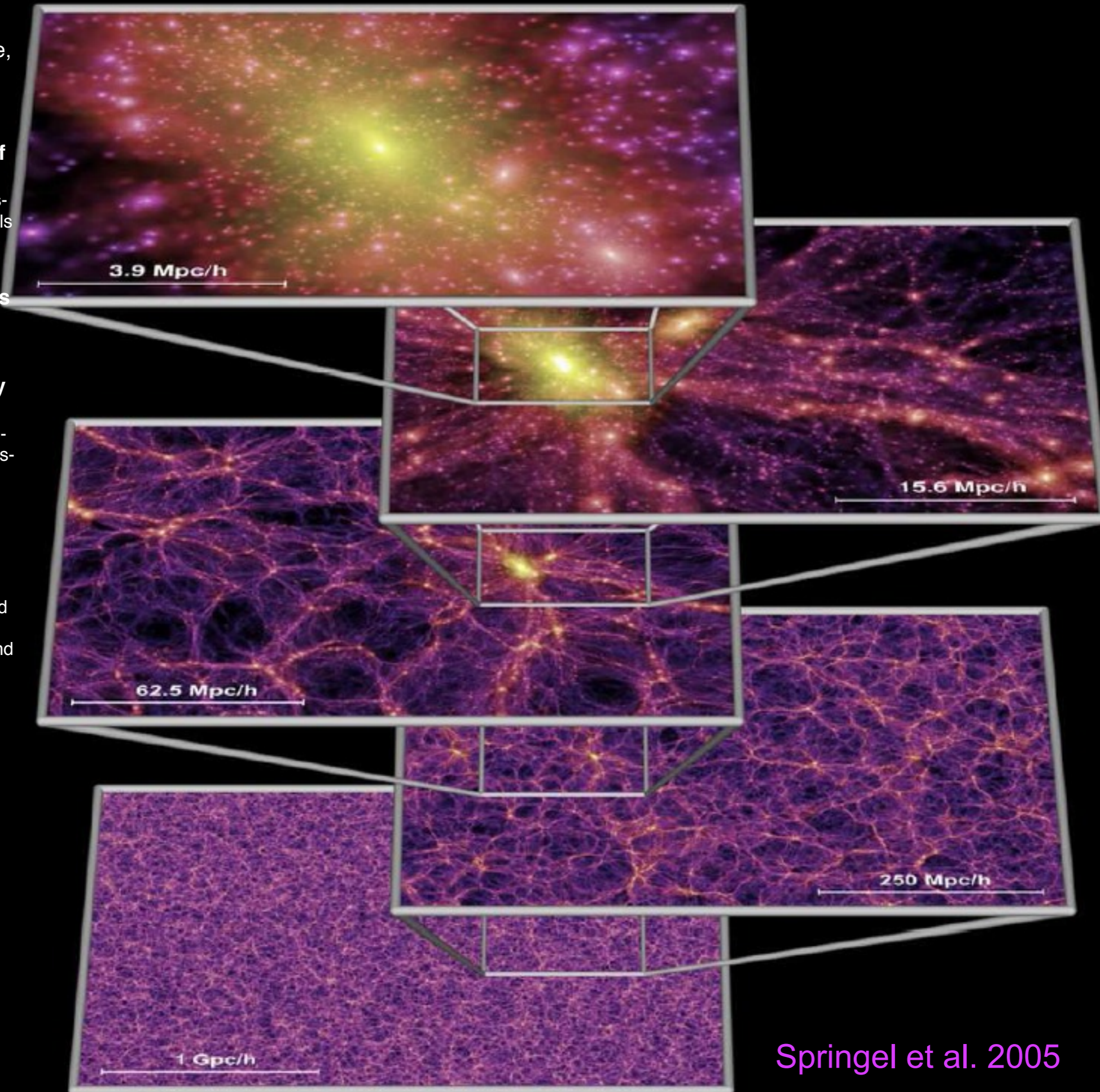


JOEL R. PRIMACK
& TRUDY E. BELL

STEFAN GOTTLÖBER / LEIBNIZ INSTITUT FÜR ASTROPHYSIK POTSDAM

The Millennium Run

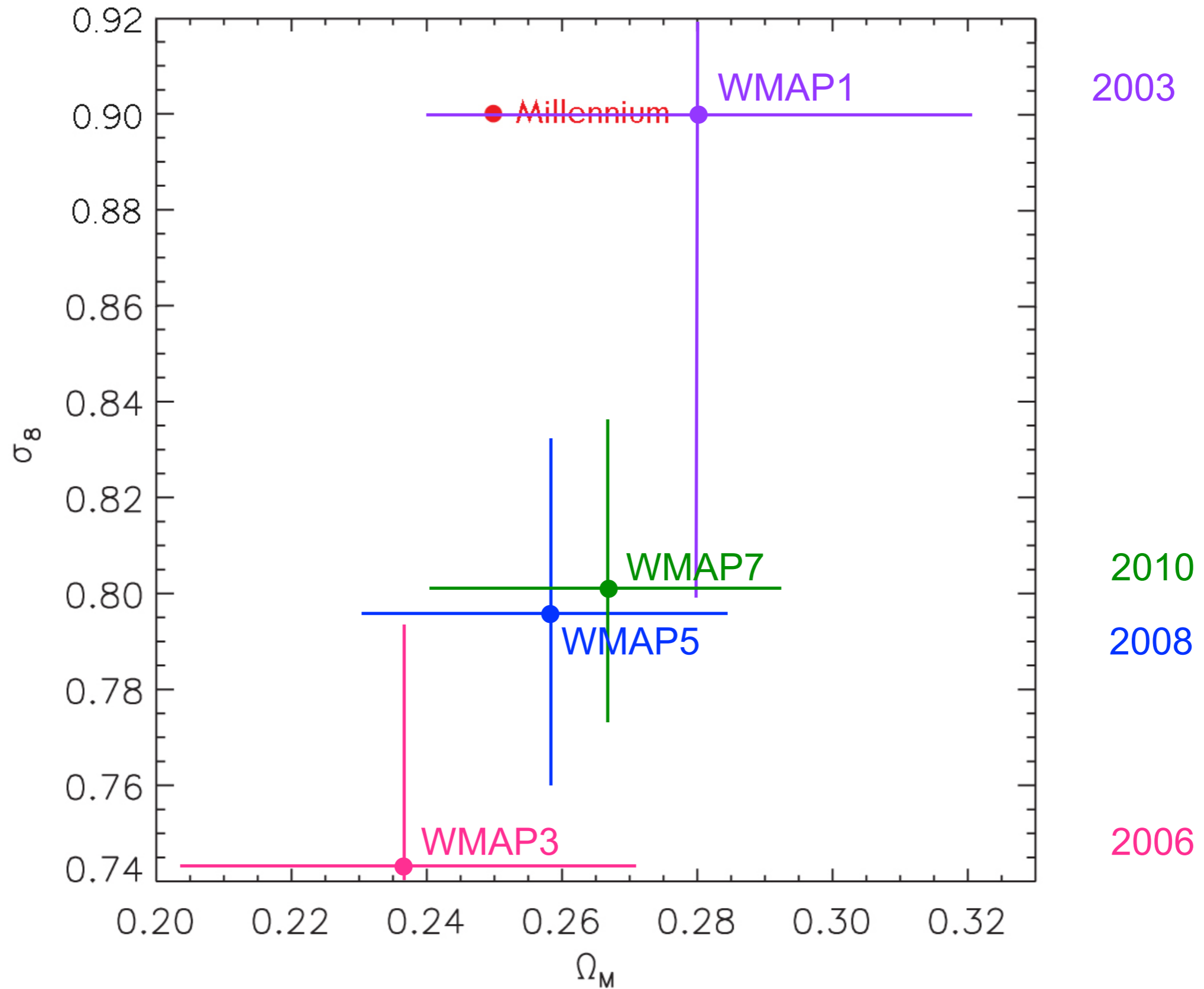
- **properties of halos** (radial profile, concentration, shapes)
- **evolution of the number density of halos**, essential for normalization of Press-Schechter- type models
- **evolution of the distribution and clustering of halos** in real and redshift space, for comparison with observations
- **accretion history of halos**, assembly bias (variation of large-scale clustering with assembly history), and correlation with halo properties including angular momenta and shapes
- **halo statistics** including the mass and velocity functions, angular momentum and shapes, subhalo numbers and distribution, and correlation with environment



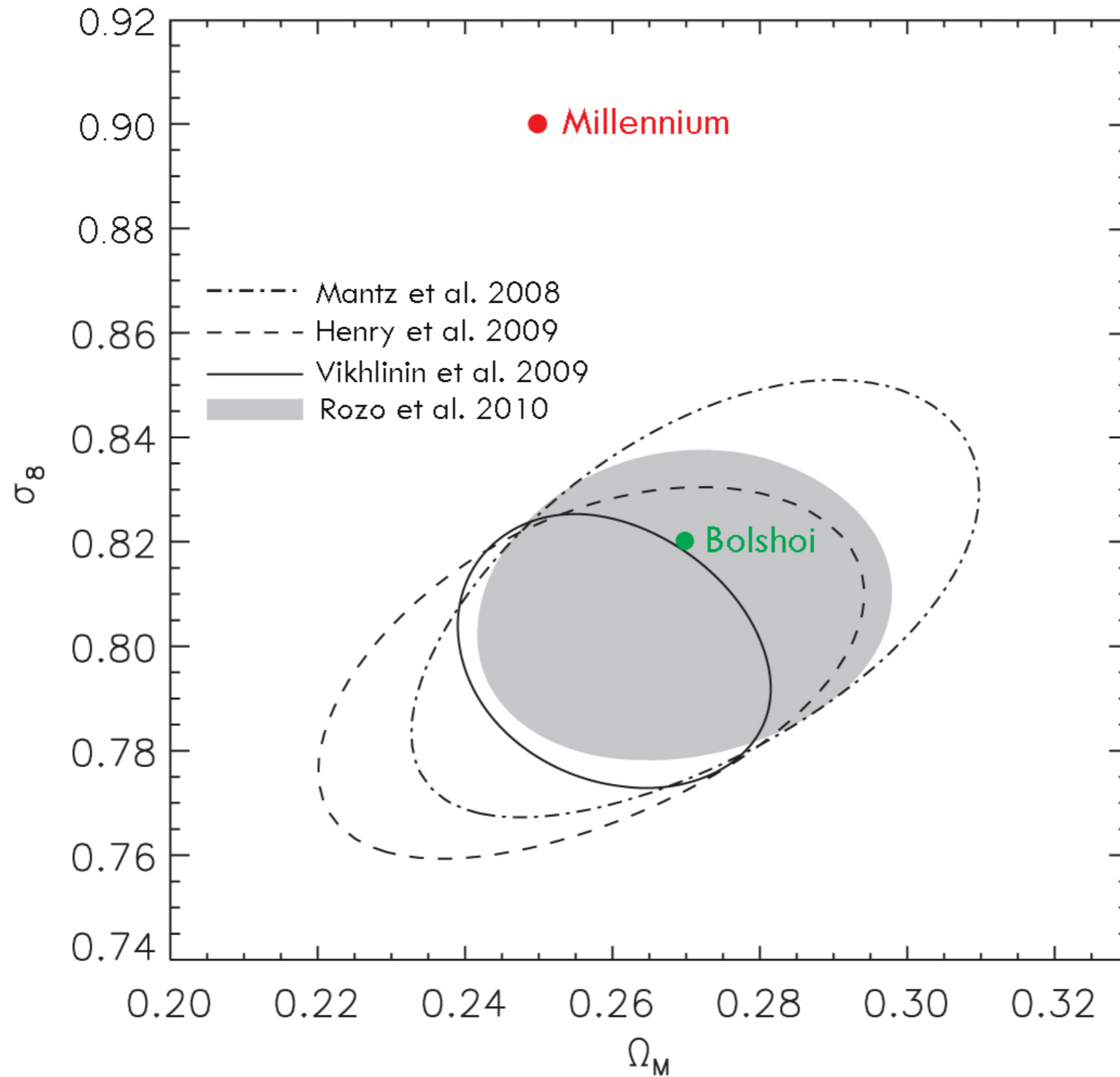
- **void statistics**, including sizes and shapes and their evolution, and the orientation of halo spins around voids
- quantitative descriptions of the evolving **cosmic web**, including applications to weak gravitational lensing
- preparation of **mock catalogs**, essential for analyzing SDSS and other survey data, and for preparing for new large surveys for dark energy etc.
- **merger trees**, essential for **semi-analytic modeling** of the evolving galaxy population, including models for the galaxy merger rate, the history of star formation and galaxy colors and morphology, the evolving AGN luminosity function, stellar and AGN feedback, recycling of gas and metals, etc.

Springel et al. 2005

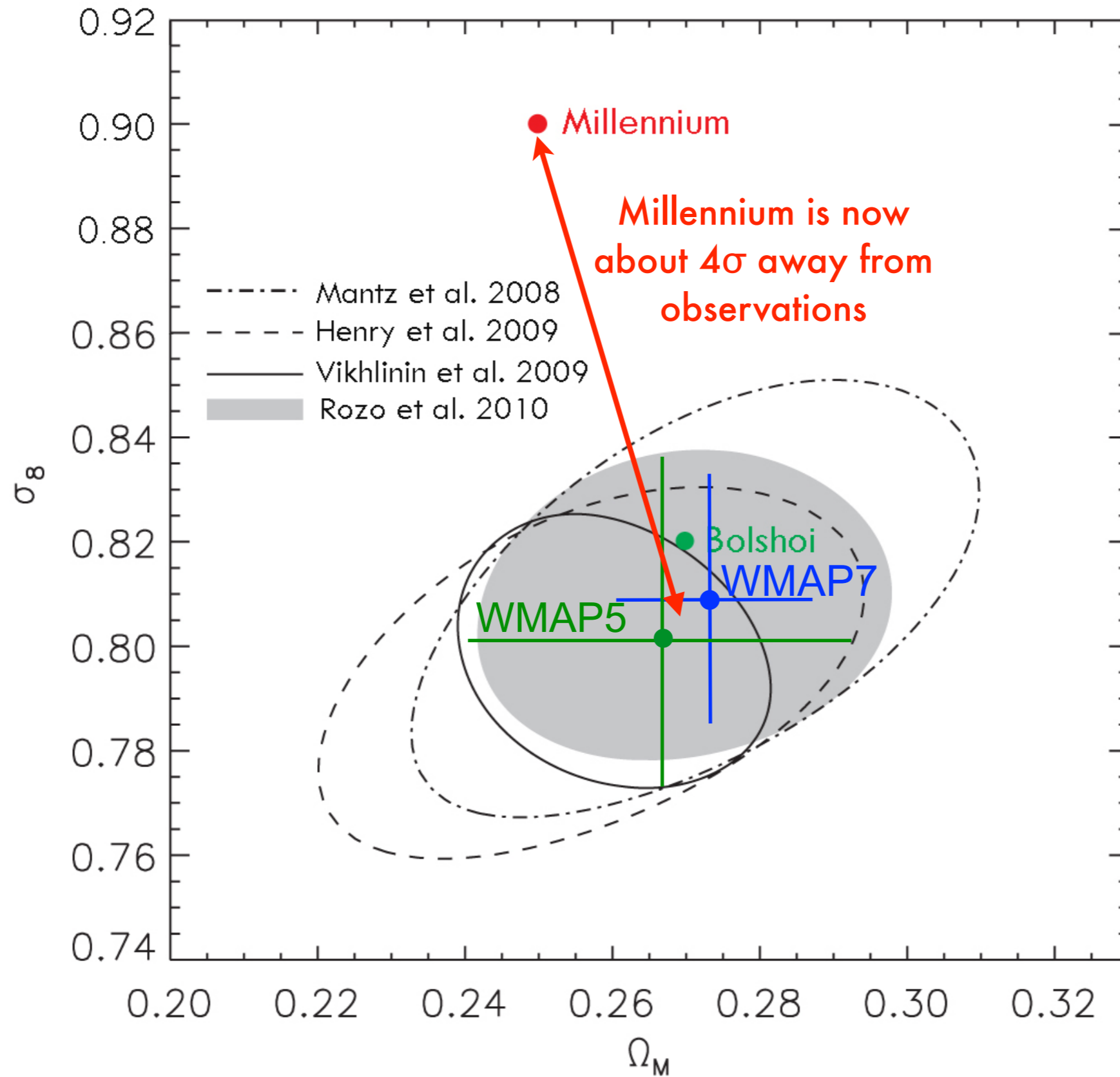
WMAP-only Determination of σ_8 and Ω_M



WMAP+SN+Clusters Determination of σ_8 and Ω_M



WMAP+SN+Clusters Determination of σ_8 and Ω_M



The Bolshoi simulation

ART code

250Mpc/h Box

ΛCDM

$\sigma_8 = 0.82$

$h = 0.70$

8G particles

1kpc/h force resolution

$1e8 M_{\text{sun}}/h$ mass res

dynamical range 262,000

time-steps = 400,000

NASA AMES

supercomputing center

Pleiades computer

13824 cores

12TB RAM

75TB disk storage

6M cpu hrs

18 days wall-clock time

Cosmological parameters are consistent with the latest observations

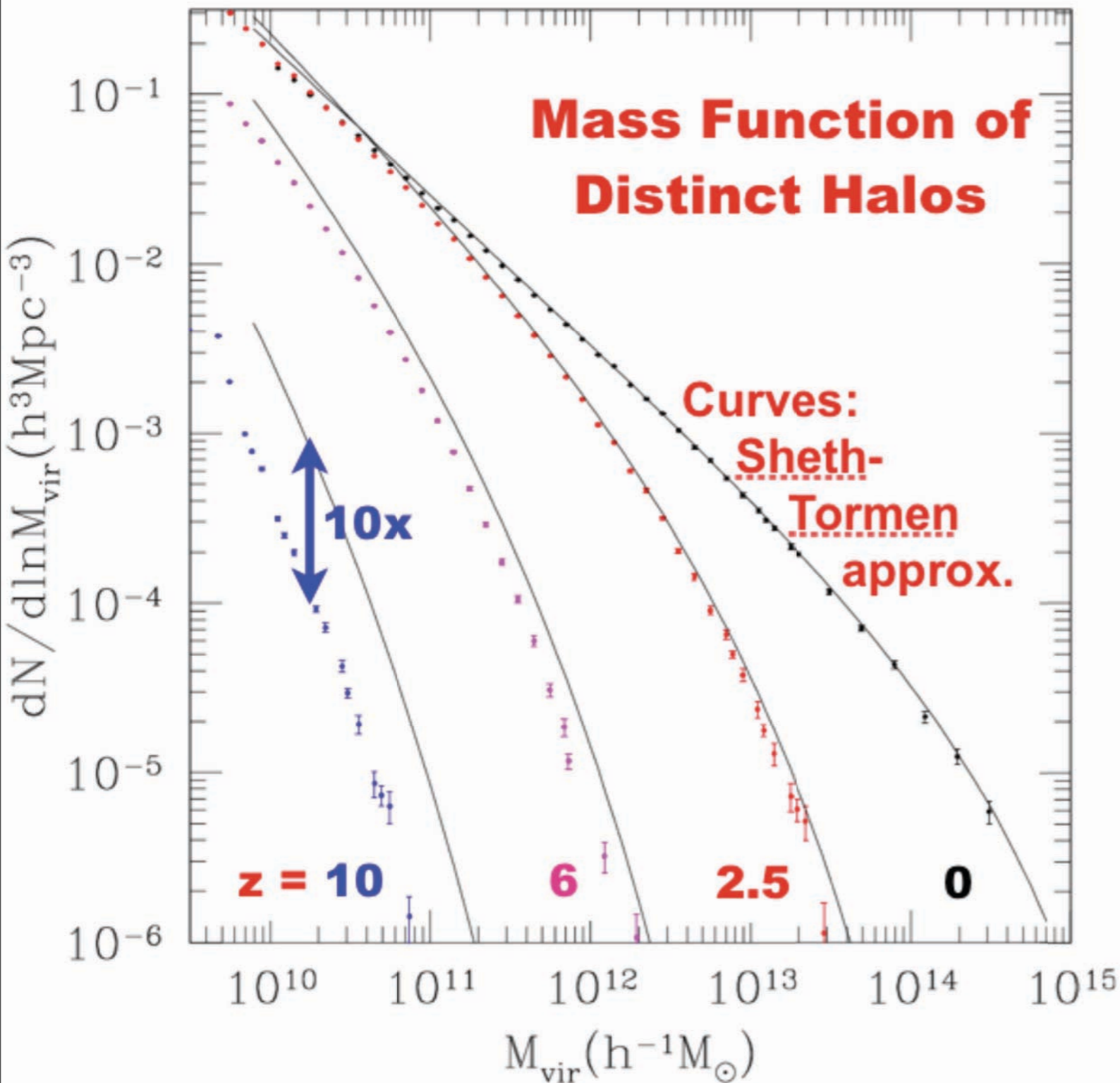
Force and Mass Resolution are nearly an order of magnitude better than Millennium-I

Force resolution is the same as Millennium-II, in a volume 16x larger

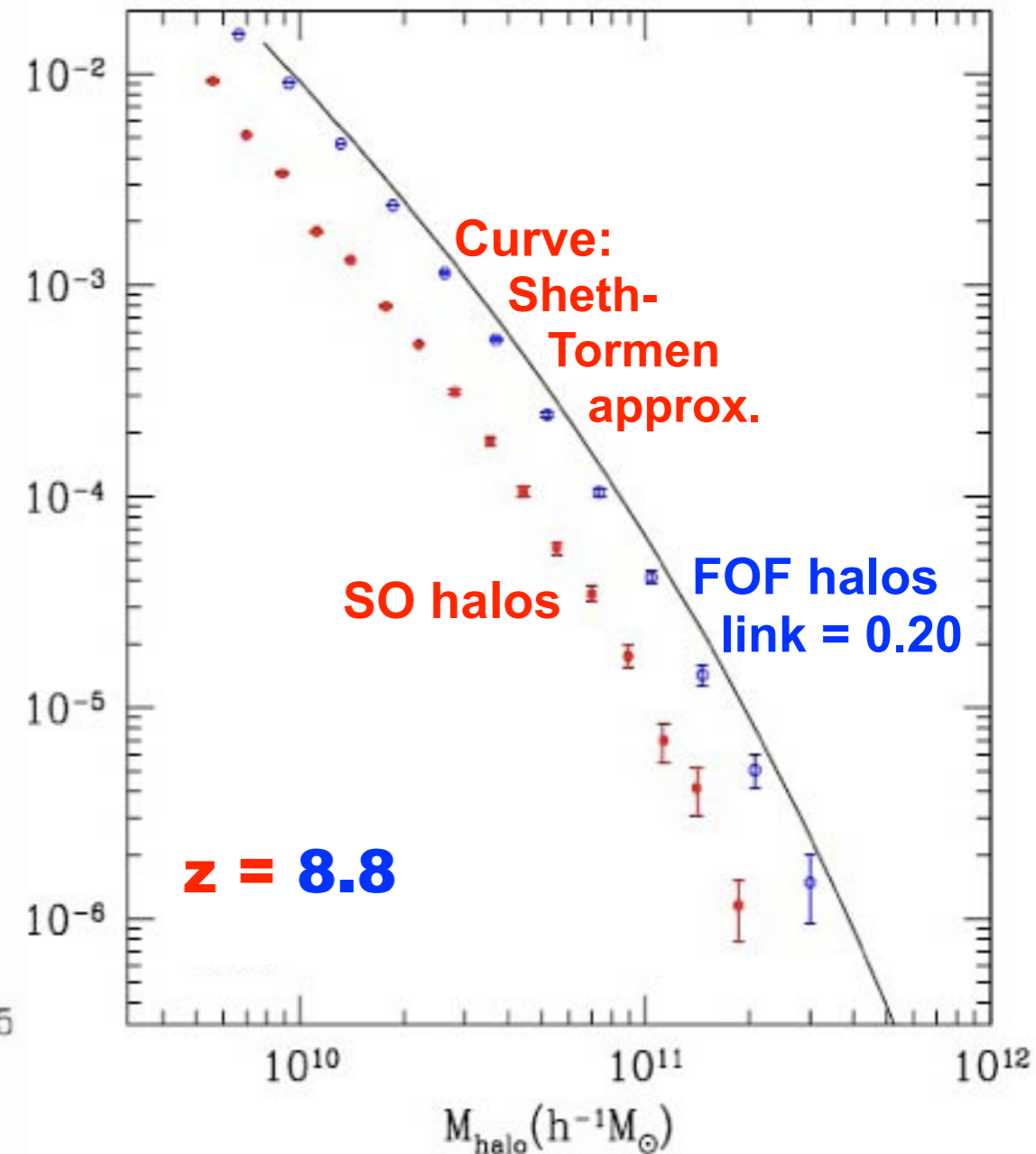
Halo finding is complete to $V_{\text{circ}} > 50$ km/s, using both BDM and ROCKSTAR halo finders

Bolshoi and MultiDark halo catalogs were released in September 2011 at Astro Inst Potsdam; Merger Trees will be available at SDSC.

<http://hipacc.ucsc.edu/Bolshoi/>

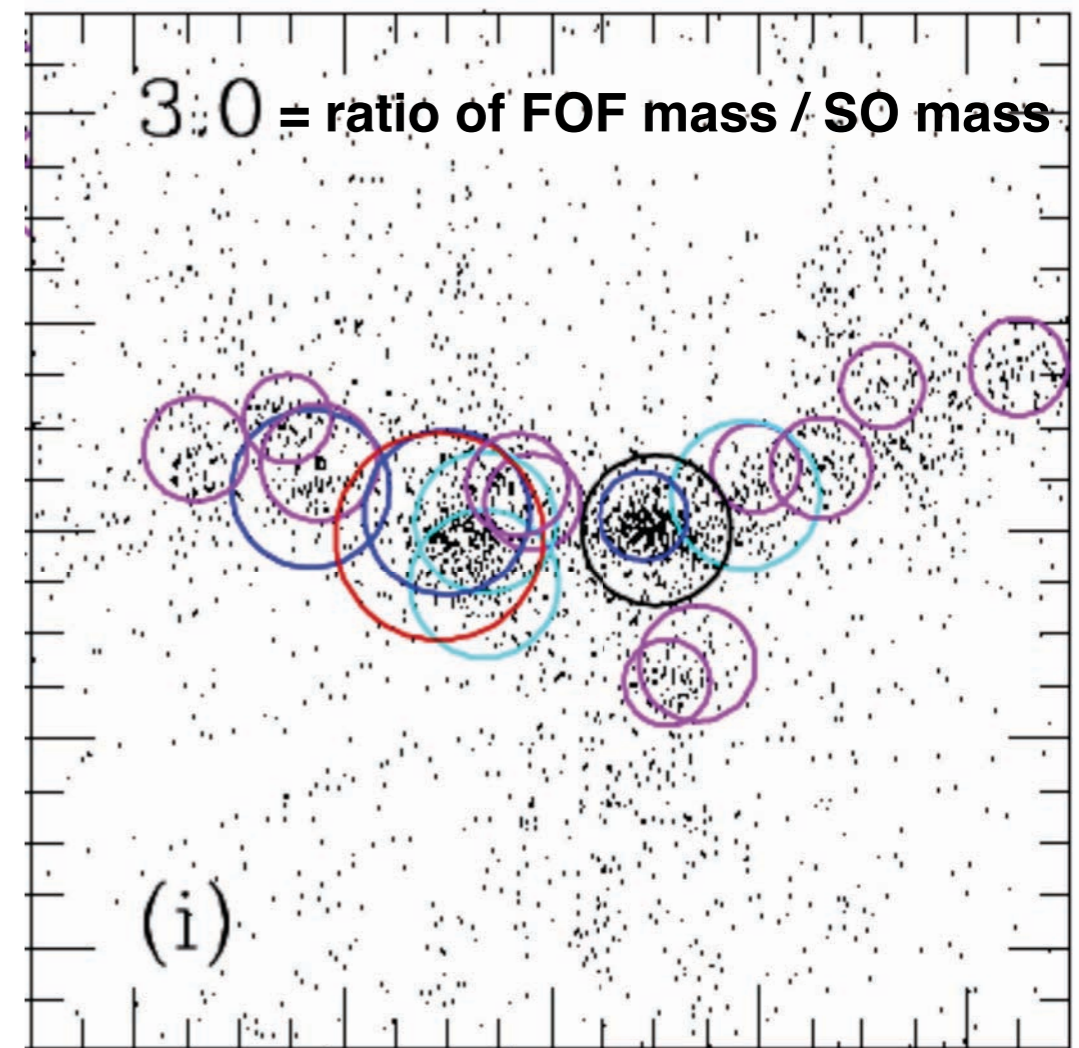
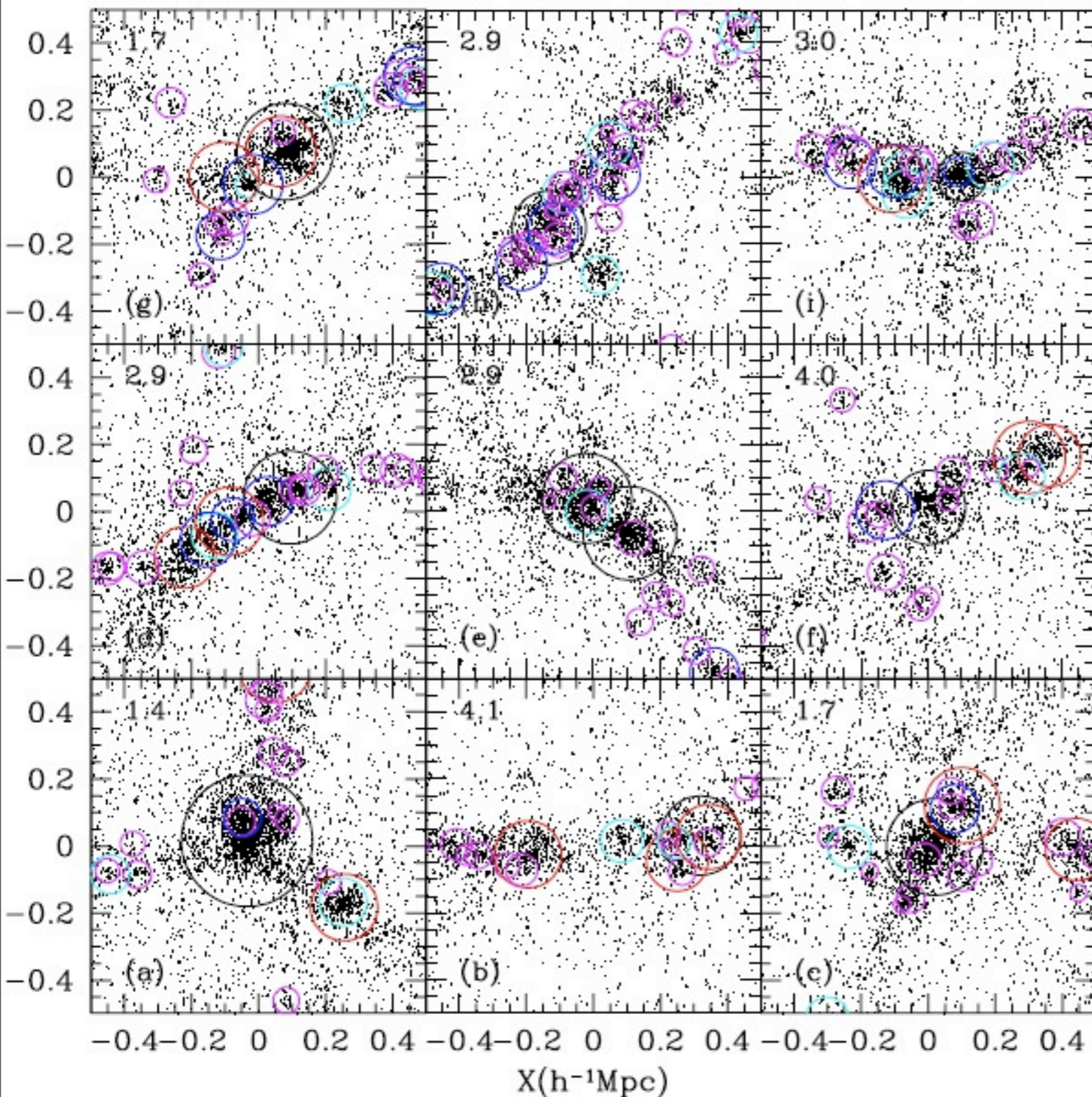


Sheth-Tormen Fails at High Redshifts



The Sheth-Tormen approximation with the same WMAP5 parameters used for the Bolshoi simulation very accurately agrees with abundance of halos at low redshifts, but increasingly overpredicts bound spherical overdensity halo abundance at higher redshifts. ST agrees well with FOF halo abundances, but FOF halos have unrealistically large masses at high z .

Klypin, Trujillo-Gomez, & Primack, 2011 ApJ



FOF linked together a chain of halos that formed in long and dense filaments (also in panels b, d, f, h; e = major merger)

Each panel shows 1/2 of the dark matter particles in cubes of $1 h^{-1}$ Mpc size. The center of each cube is the exact position of the center of mass of the corresponding FOF halo. The effective radius of each FOF halo in the plots is $150 - 200 h^{-1}$ kpc. Circles indicate virial radii of distinct halos and subhalos identified by the spherical overdensity algorithm BDM.

Klypin, Trujillo-Gomez, & Primack, 2011 ApJ

BigBolshoi / MultiDark

Same cosmology as Bolshoi: $h=0.70$, $\sigma_8=0.82$, $n=0.95$, $\Omega_m=0.27$

7 kpc/h resolution, complete to $V_{\text{circ}} > 170$ km/s

Volume 64x larger than Bolshoi

4 Billion Light Years

<http://hipacc.ucsc.edu/Bolshoi/>

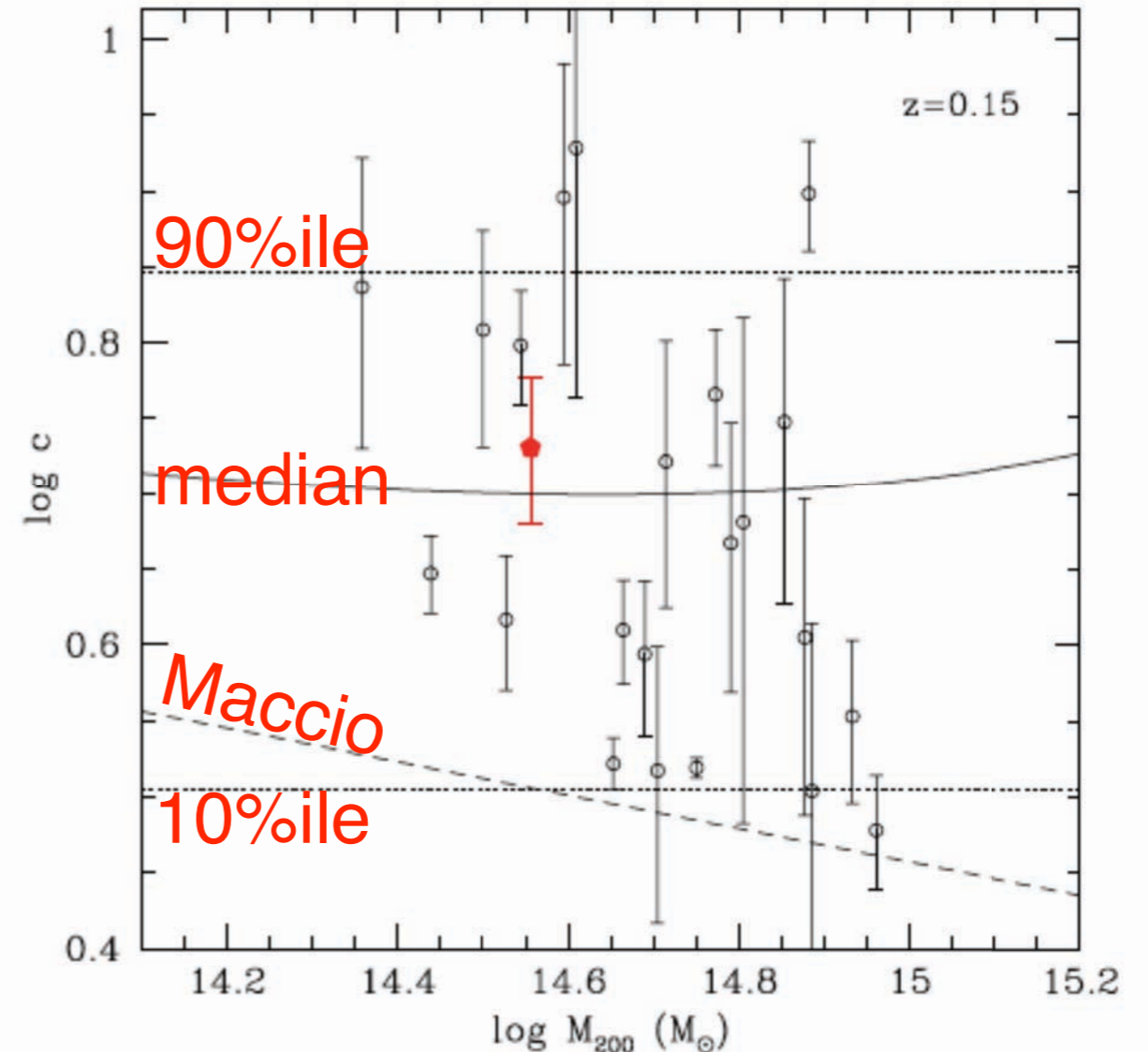
Halo concentrations in the standard CDM cosmology

Francisco Prada, Anatoly A. Klypin, Antonio J. Cuesta, Juan E. Betancort-Rijo, and Joel Primack

ABSTRACT

We study the concentration of dark matter halos and its evolution in N-body simulations of the standard Λ CDM cosmology. The results presented in this paper are based on 4 large N-body simulations with ~ 10 billion particles each: the Millennium-I and II, Bolshoi, and MultiDark simulations. The MultiDark (or BigBolshoi) simulation is introduced in this paper. This suite of simulations with high mass resolution over a large volume allows us to compute with unprecedented accuracy the concentration over a large range of scales (about six orders of magnitude in mass), which constitutes the state-of-the-art of our current knowledge on this basic property of dark matter halos in the Λ CDM cosmology. We find that there is consistency among the different simulation data sets, despite the different codes, numerical algorithms, and halo/subhalo finders used in our analysis. We confirm a novel feature for halo concentrations at high redshifts: a flattening and upturn with increasing mass. The concentration $c(M, z)$ as a function of mass and the redshift and for different cosmological parameters shows a remarkably complex pattern. However, when expressed in terms of the linear rms fluctuation of the density field $\sigma(M, z)$, the halo concentration $c(\sigma)$ shows a nearly-universal simple U-shaped behaviour with a minimum at a well defined scale at $\sigma \sim 0.71$. Yet, some small dependences with redshift and cosmology still remain. At the high-mass end ($\sigma < 1$) the median halo kinematic profiles show large signatures of infall and highly radial orbits. This $c-\sigma(M, z)$ relation can be accurately parametrized and provides an analytical model for the dependence of concentration on halo mass. When applied to galaxy clusters, our estimates of concentrations are substantially larger – by a factor up to 1.5 – than previous results from smaller simulations, and are in much better agreement with results of observations.

Cluster Concentrations



Comparison of observed cluster concentrations (data points with error bars) with the prediction of our model for median halo concentration of cluster-size halos (full curve). Dotted lines show 10% and 90% percentiles. Open circles show results for X-ray luminous galaxy clusters observed with XMMNewton in the redshift range 0.1-0.3 (Ettori et al. 2010). The pentagon presents galaxy kinematic estimate for relaxed clusters by Wojtak & Lokas (2010). The dashed curve shows prediction by Maccio, Dutton, & van den Bosch (2008), which significantly underestimates the concentrations of clusters.

2012 MNRAS

Halo concentrations in the standard Λ CDM cosmology

Francisco Prada^{1,2*}, Anatoly A. Klypin³, Antonio J. Cuesta^{1,4},
Juan E. Betancort-Rijo⁵ and Joel Primack⁶

ABSTRACT

We study the concentration of dark matter halos and its evolution in N-body simulations of the standard Λ CDM cosmology. The results presented in this paper are based on 4 large N-body simulations with ~ 10 billion particles each: the Millennium-I and II, Bolshoi, and MultiDark simulations. The MultiDark (or BigBolshoi) simulation is introduced in this paper. This suite of simulations with high mass resolution over a large volume allows us to compute with unprecedented accuracy the concentration over a large range of scales (about six orders of magnitude in mass), which constitutes the state-of-the-art of our current knowledge on this basic property of dark matter halos in the Λ CDM cosmology. We find that there is consistency among the different simulation data sets, despite the different codes, numerical algorithms, and halo/subhalo finders used in our analysis. We confirm a novel feature for halo concentrations at high redshifts: a flattening and upturn with increasing mass. The concentration $c(M, z)$ as a function of mass and the redshift and for different cosmological parameters shows a remarkably complex pattern. However, when expressed in terms of the linear rms fluctuation of the density field $\sigma(M, z)$, the halo concentration $c(\sigma)$ shows a nearly-universal simple U-shaped behaviour with a minimum at a well defined scale at $\sigma \sim 0.71$. Yet, some small dependences with redshift and cosmology still remain. At the high-mass end ($\sigma < 1$) the median halo kinematic profiles show large signatures of infall and highly radial orbits. This c - $\sigma(M, z)$ relation can be accurately parametrized and provides an analytical model for the dependence of concentration on halo mass. When applied to galaxy clusters, our estimates of concentrations are substantially larger – by a factor up to 1.5 – than previous results from smaller simulations, and are in much better agreement with results of observations.

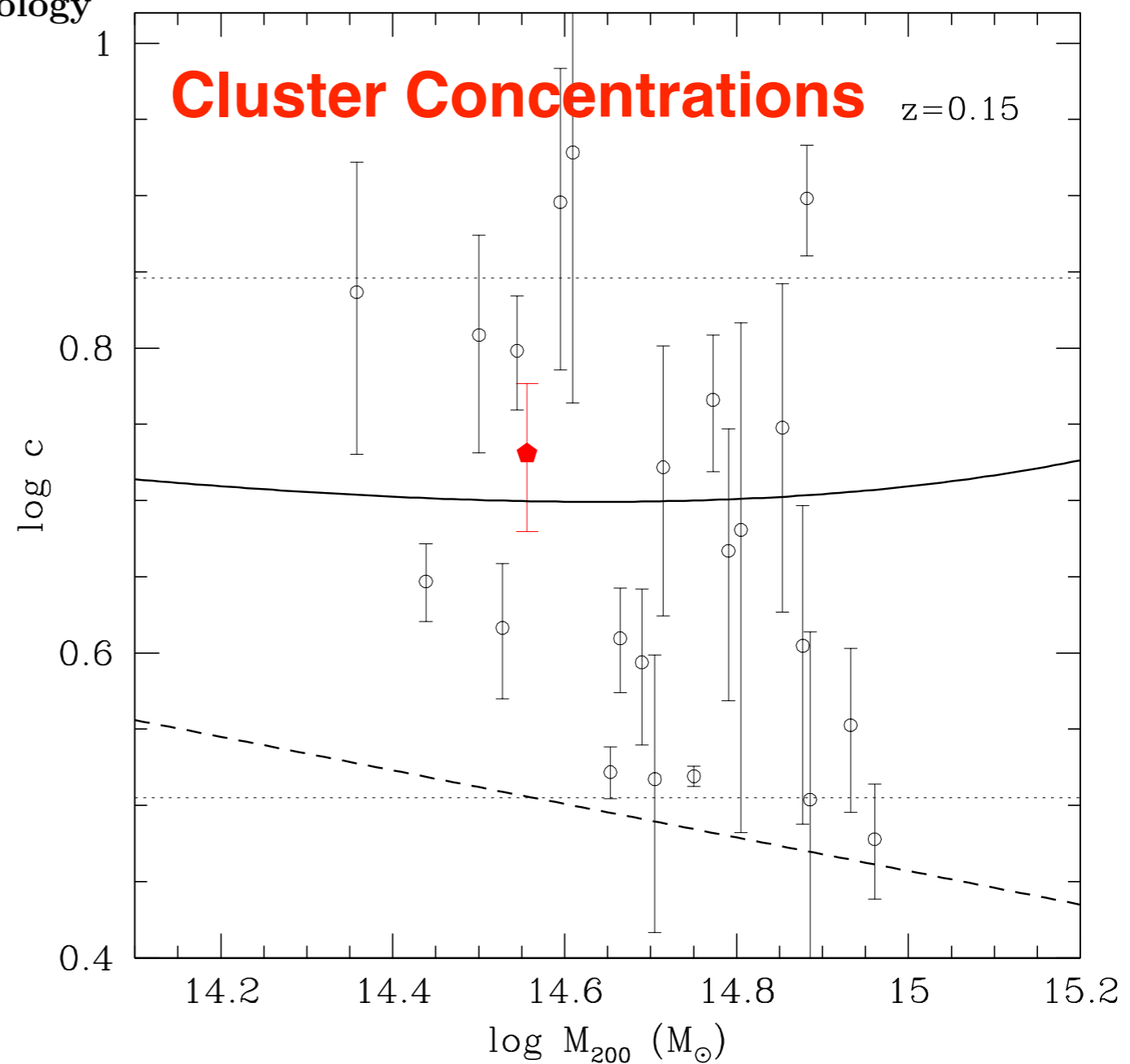
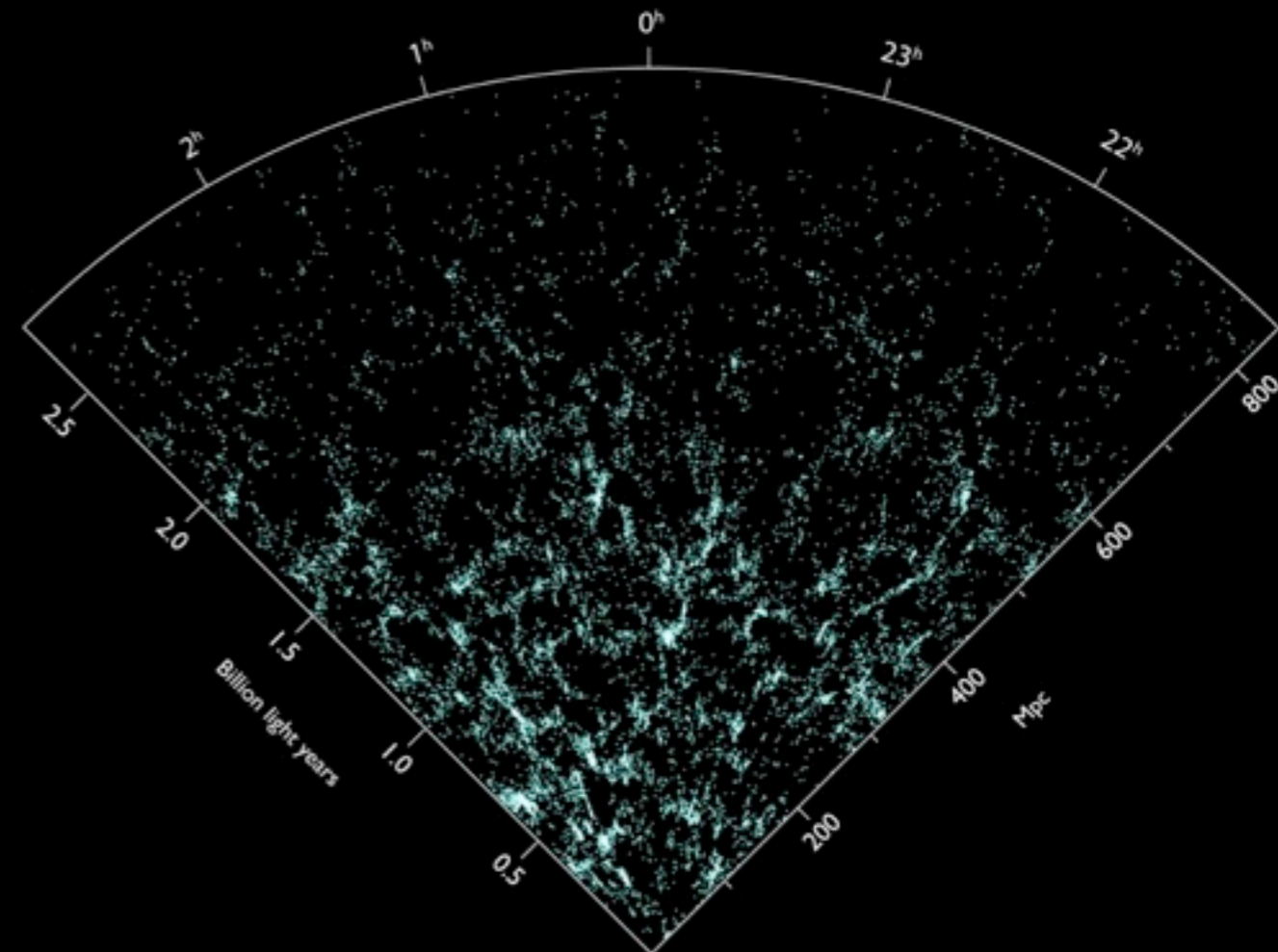
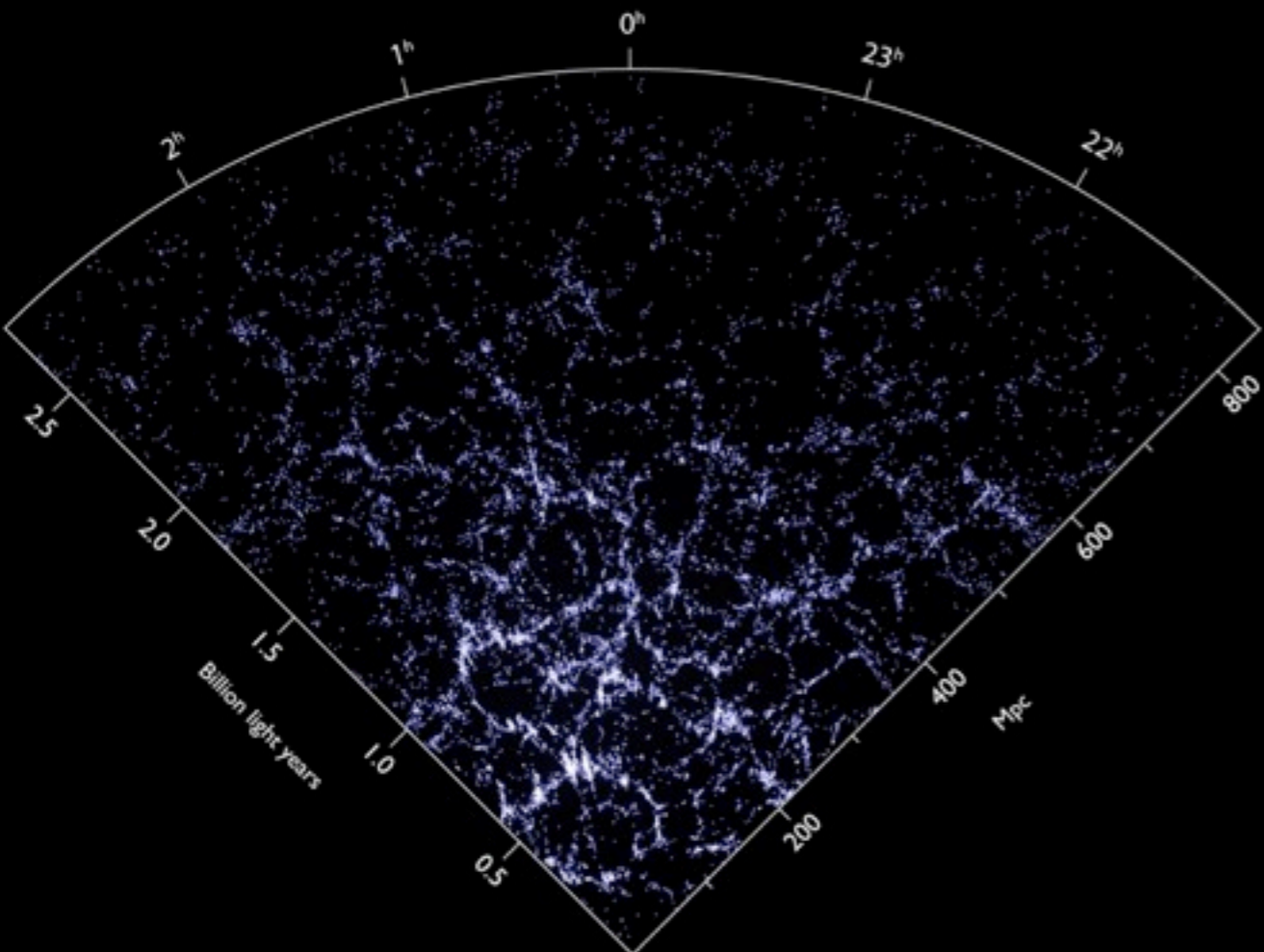


Figure 13. Comparison of observed cluster concentrations (data points with error bars) with the prediction of our model for median halo concentration of cluster-size halos (full curve). Dotted lines show 10% and 90% percentiles. Open circles show results for X-ray luminous galaxy clusters observed with XMM-Newton in the redshift range 0.1-0.3 (Ettori et al. 2010). The pentagon presents galaxy kinematic estimate for relaxed clusters by Wojtak & Łokas (2010). The dashed curve shows prediction by Macciò, Dutton, & van den Bosch (2008), which significantly underestimates the concentrations of clusters.

SDSS

Bolshoi



Risa Wechsler, Ralf Kahler, Nina McCurdy

Bolshoi Merger Tree for the Formation of a Big Cluster Halo

Time: 13664 Myr Ago
Timestep Redshift: 14.083
Radius Mode: Rvir
Focus Distance: 6.1
Aperture: 40.0
World Rotation: (216.7, 0.06, -0.94, -0.34)
Trackball Rotation: (0.0, 0.00, 0.00, 0.00)
Camera Position: (0.0, 0.0, -6.1)

Peter Behroozi

**Bolshoi
Sub-Halo
Abundance
Matching**

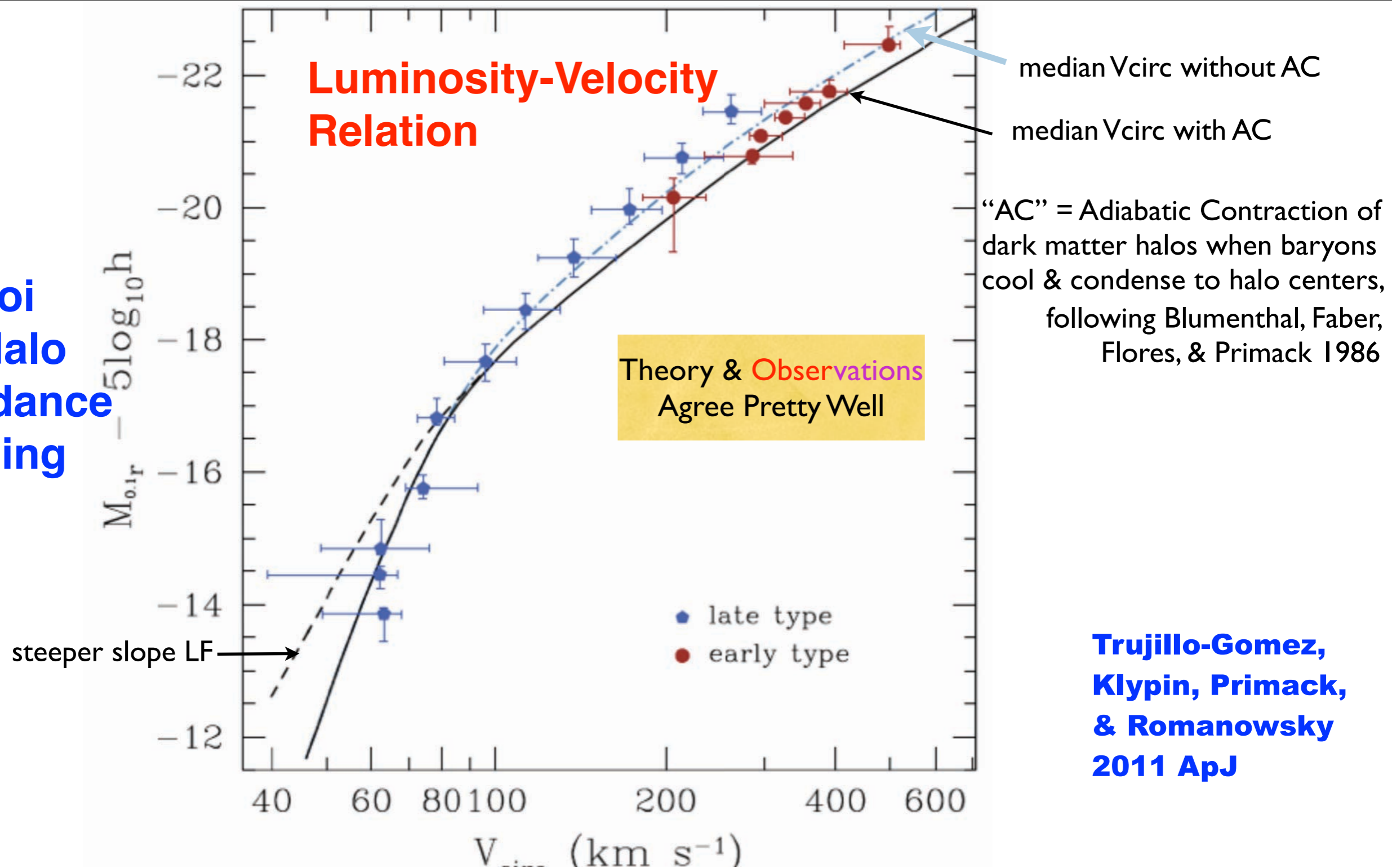


Fig. 4.— Comparison of the observed Luminosity-Velocity relation with the predictions of the Λ CDM model. The solid curve shows the median values of $^{0.1}r$ -band luminosity vs. circular velocity for the model galaxy sample. The circular velocity for each model galaxy is based on the peak circular velocity of its host halo over its entire history, measured at a distance of 10 kpc from the center including the cold baryonic mass and the standard correction due to adiabatic halo contraction. The dashed curve shows results for a steeper ($\alpha = -1.34$) slope of the LF. The dot-dashed curve shows predictions after adding the baryon mass but without adiabatic contraction. Points show representative observational samples.

Bolshoi Sub-Halo Abundance Matching

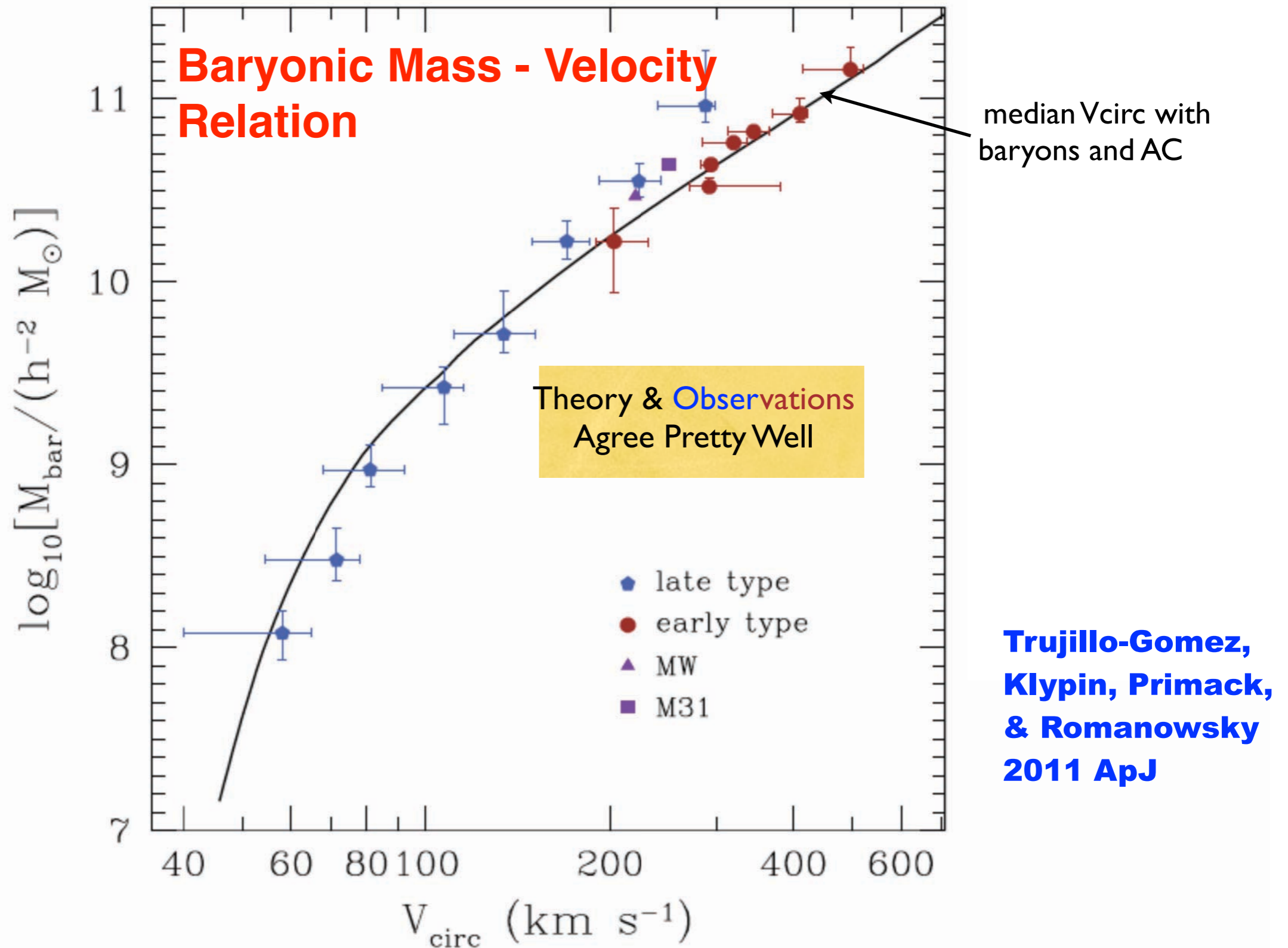
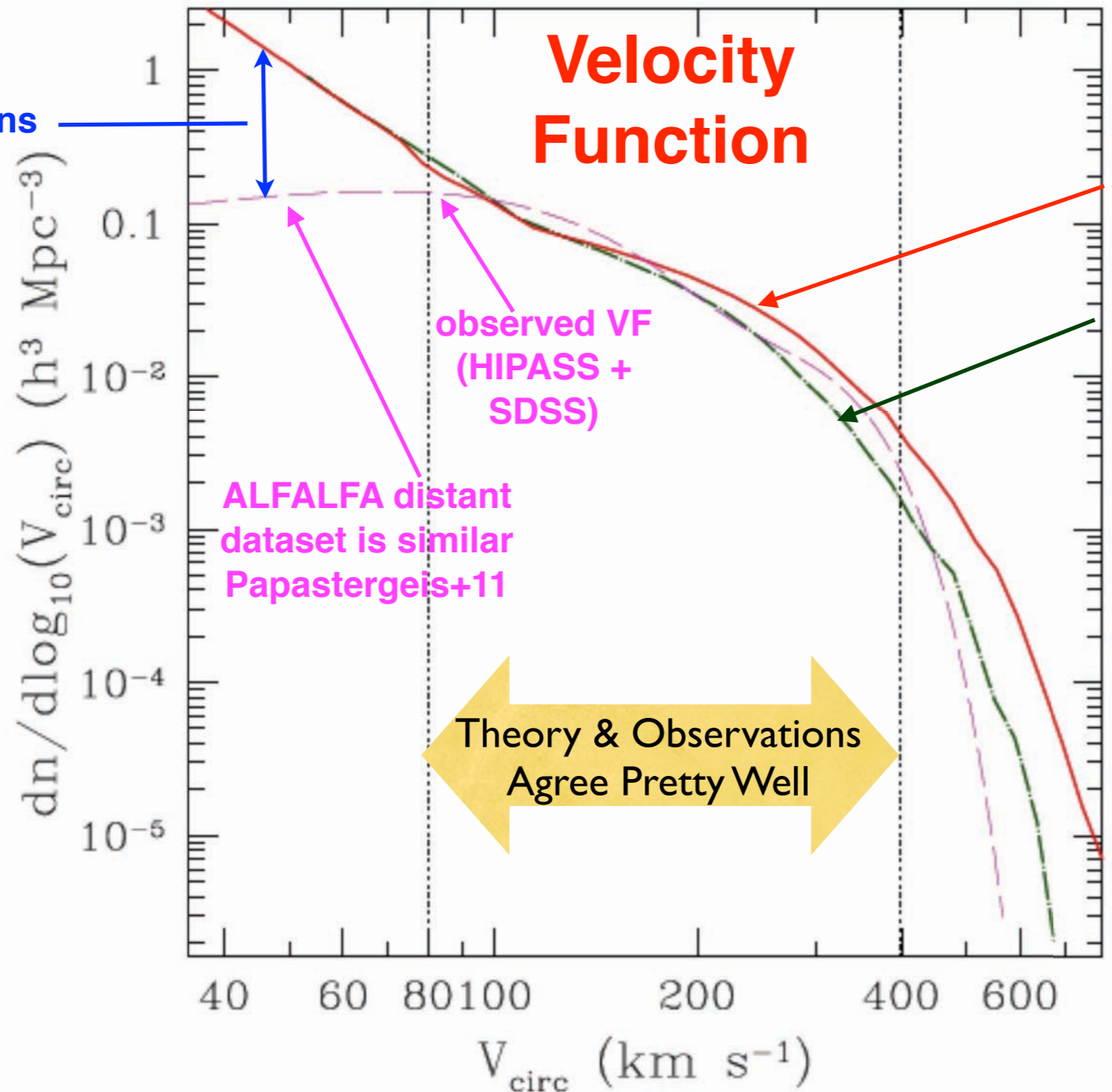


Fig. 10.— Mass in cold baryons as a function of circular velocity. The solid curve shows the median values for the Λ CDM model using halo abundance matching. The cold baryonic mass includes stars and cold gas and the circular velocity is measured at 10 kpc from the center while including the effect of adiabatic contraction. For comparison we show the individual galaxies of several galaxy samples. Intermediate mass galaxies such as the Milky Way and M31 lie very close to our model results.

Discrepancy due to incomplete observations or Λ CDM failure?

Bolshoi Sub-Halo Abundance Matching



theoretical VF with AC
theoretical VF without AC

Theory & Observations Agree Pretty Well

ALFALFA distant dataset is similar Papastergeis+11

Trujillo-Gomez, Klypin, Primack, & Romanowsky 2011 ApJ

Fig. 11.— Comparison of theoretical (dot-dashed and thick solid curves) and observational (dashed curve) circular velocity functions. The dot-dashed line shows the effect of adding the baryons (stellar and cold gas components) to the central region of each DM halo and measuring the circular velocity at 10 kpc. The thick solid line is the distribution obtained when the adiabatic contraction of the DM halos is considered. Because of uncertainties in the AC models, realistic theoretical predictions should lie between the dot-dashed and solid curves. Both the theory and observations are highly uncertain for rare galaxies with $V_{\text{circ}} > 400 \text{ km s}^{-1}$. Two vertical dotted lines divide the VF into three domains: $V_{\text{circ}} > 400 \text{ km s}^{-1}$ with large observational and theoretical uncertainties; $80 \text{ km s}^{-1} < V_{\text{circ}} < 400 \text{ km s}^{-1}$ with a reasonable agreement, and $V_{\text{circ}} < 80 \text{ km s}^{-1}$, where the theory significantly overpredicts the number of dwarfs.

Deeper Local Survey -- better agreement with Λ CDM but still more halos than galaxies below 50 km/s

Local Volume: $D < 10\text{Mpc}$

Total sample: 813 galaxies

Within 10Mpc: 686

$M_B < -13$ N=304

$M_B < -10$ N=611

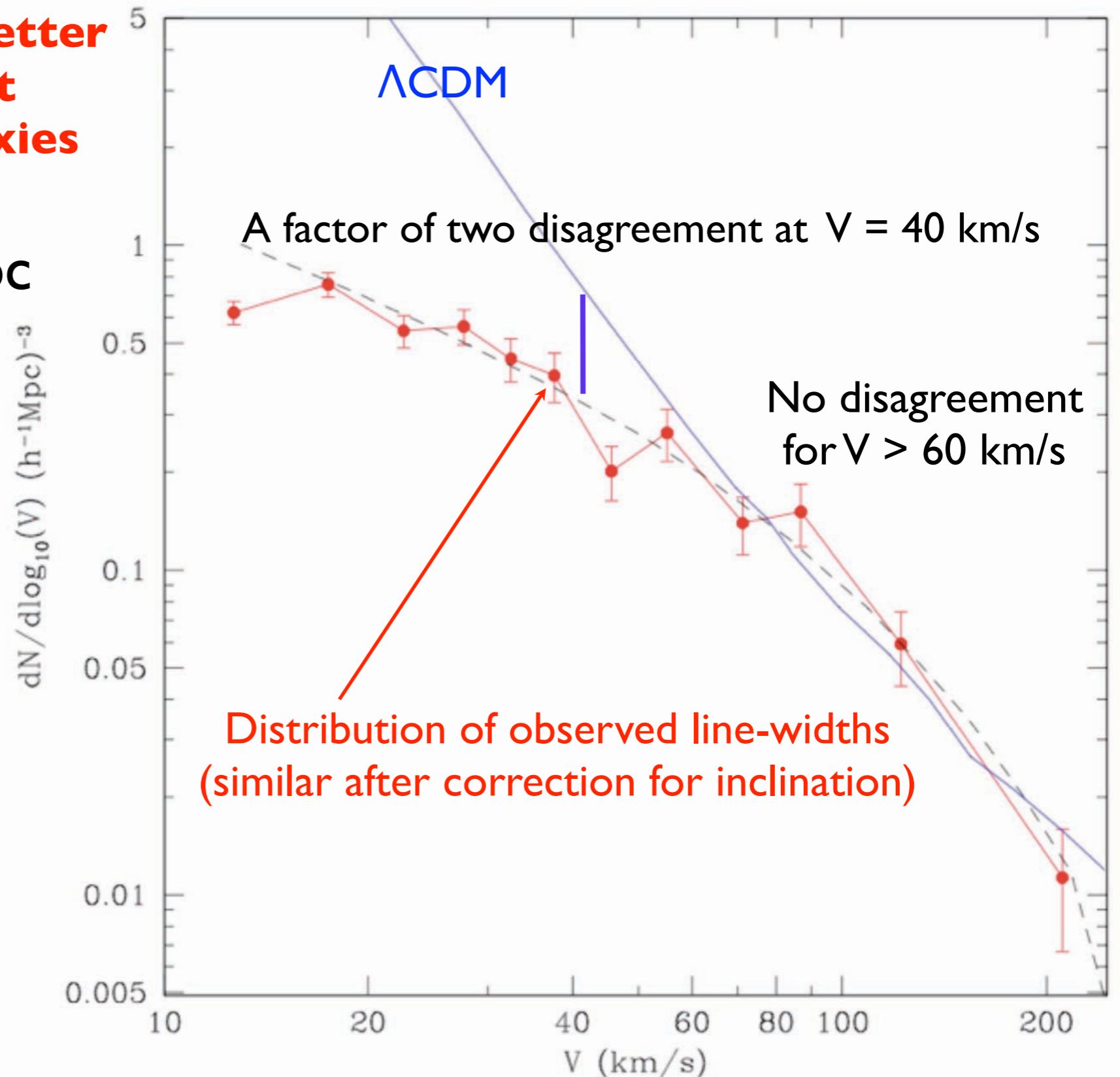
80-90% are spirals or dlrr ($T > 0$)

Accuracy of distances are 8-10%

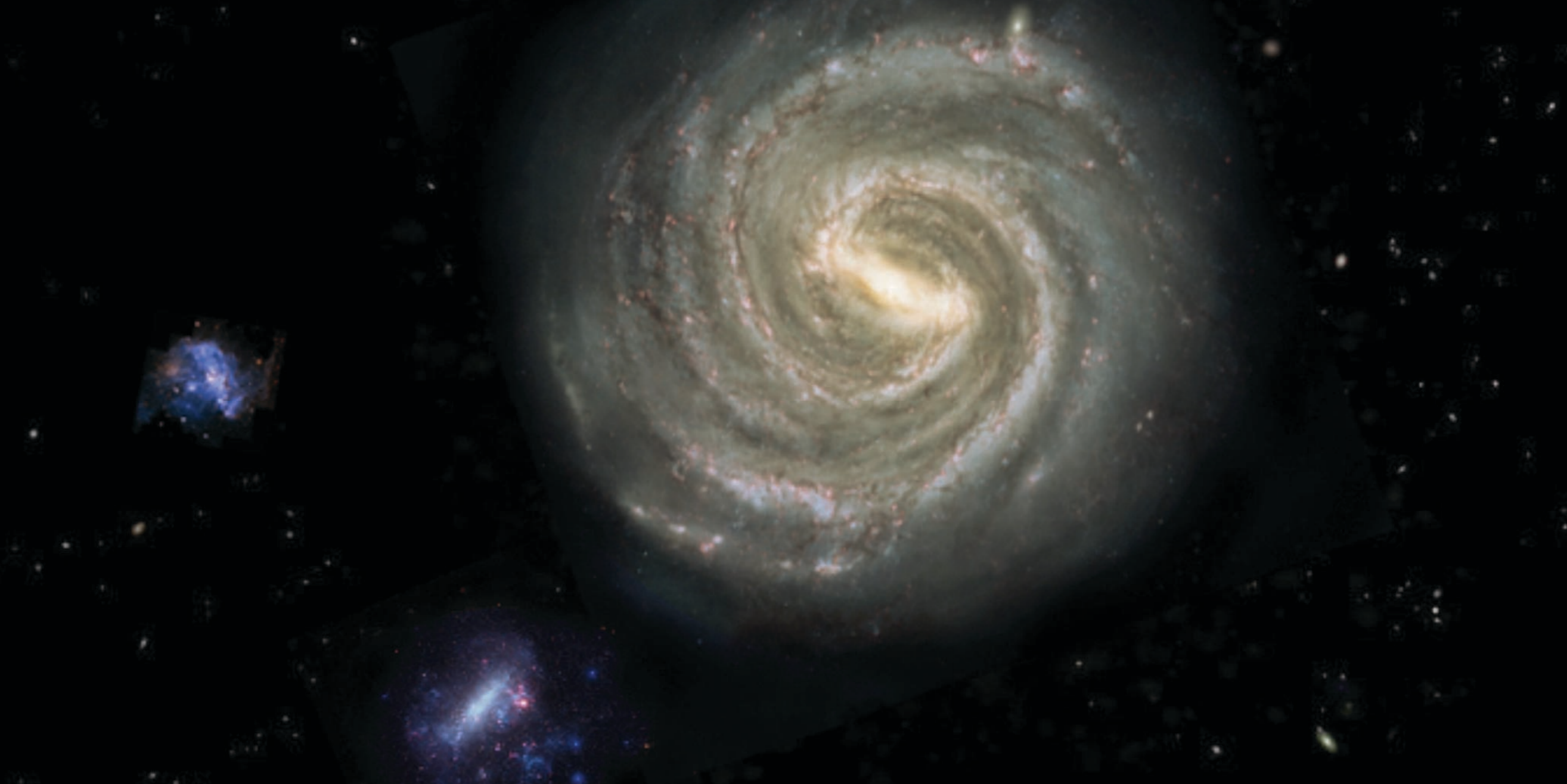
80% with $D < 10\text{Mpc}$ have HI linewidth

$V_{\text{rot}} =$

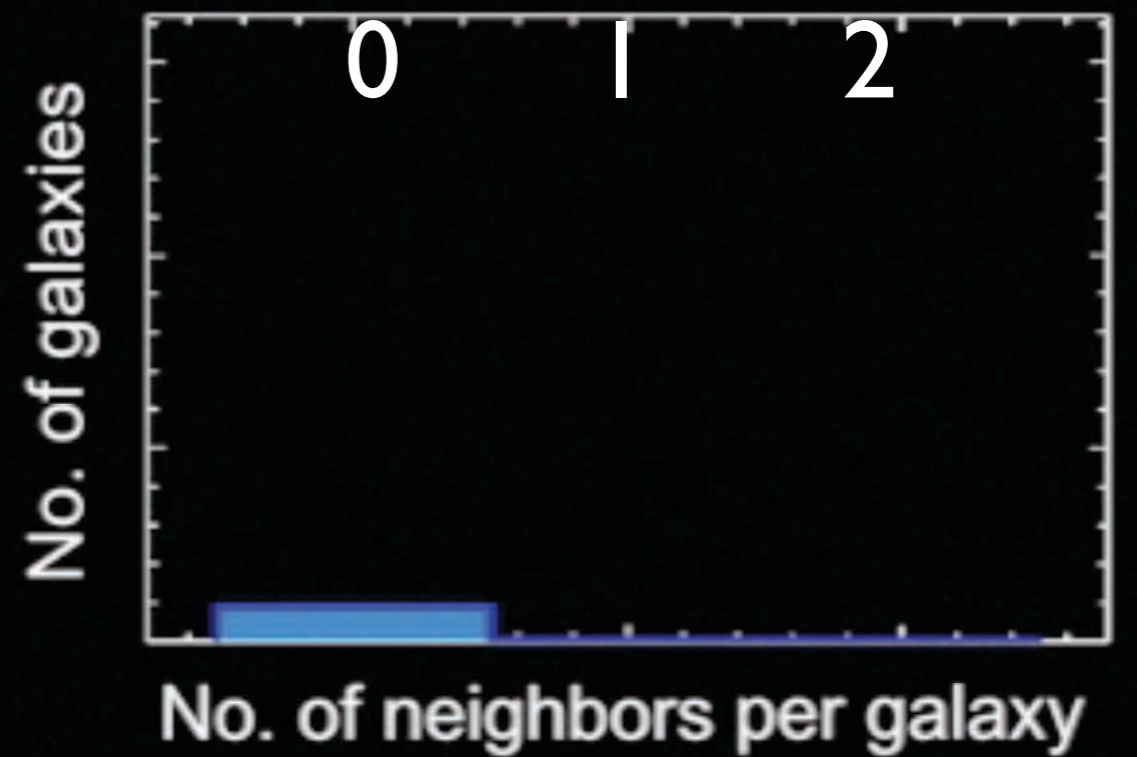
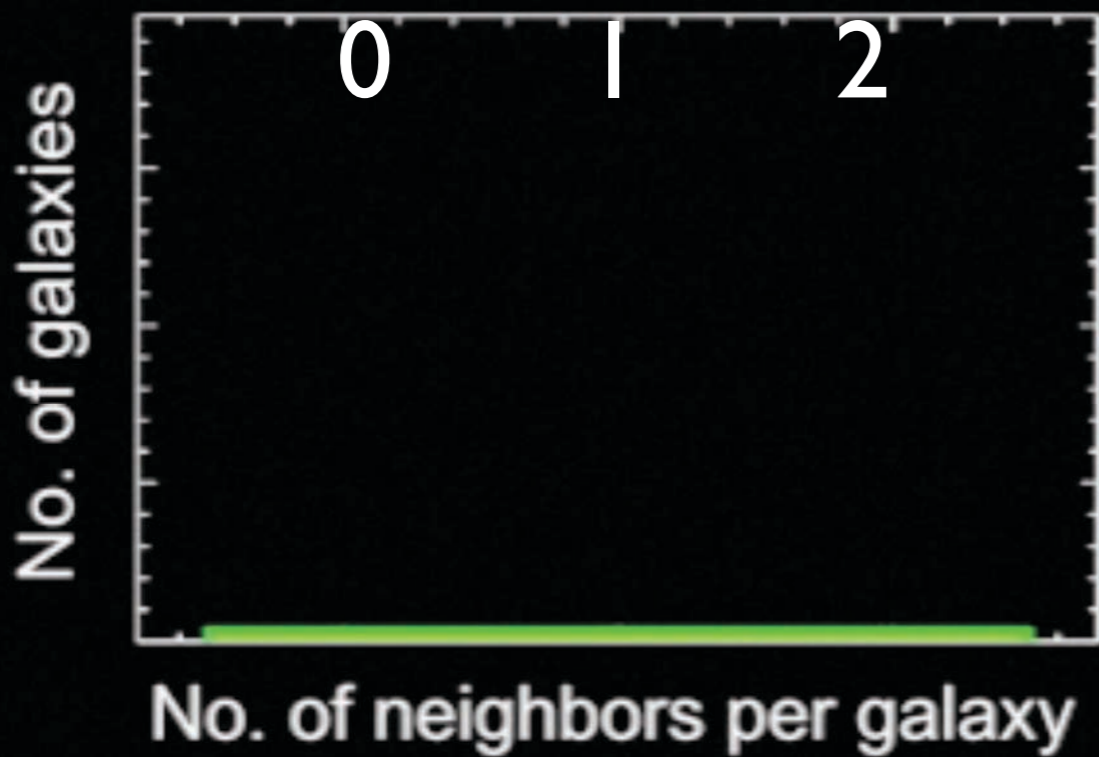
$$150 \times 10^{-(20.5 + M_B)/8.5} \text{ km/s}$$



The Milky Way has two large satellite galaxies,
the small and large Magellanic Clouds



The Bolshoi simulation + halo abundance matching
predicts the likelihood of this



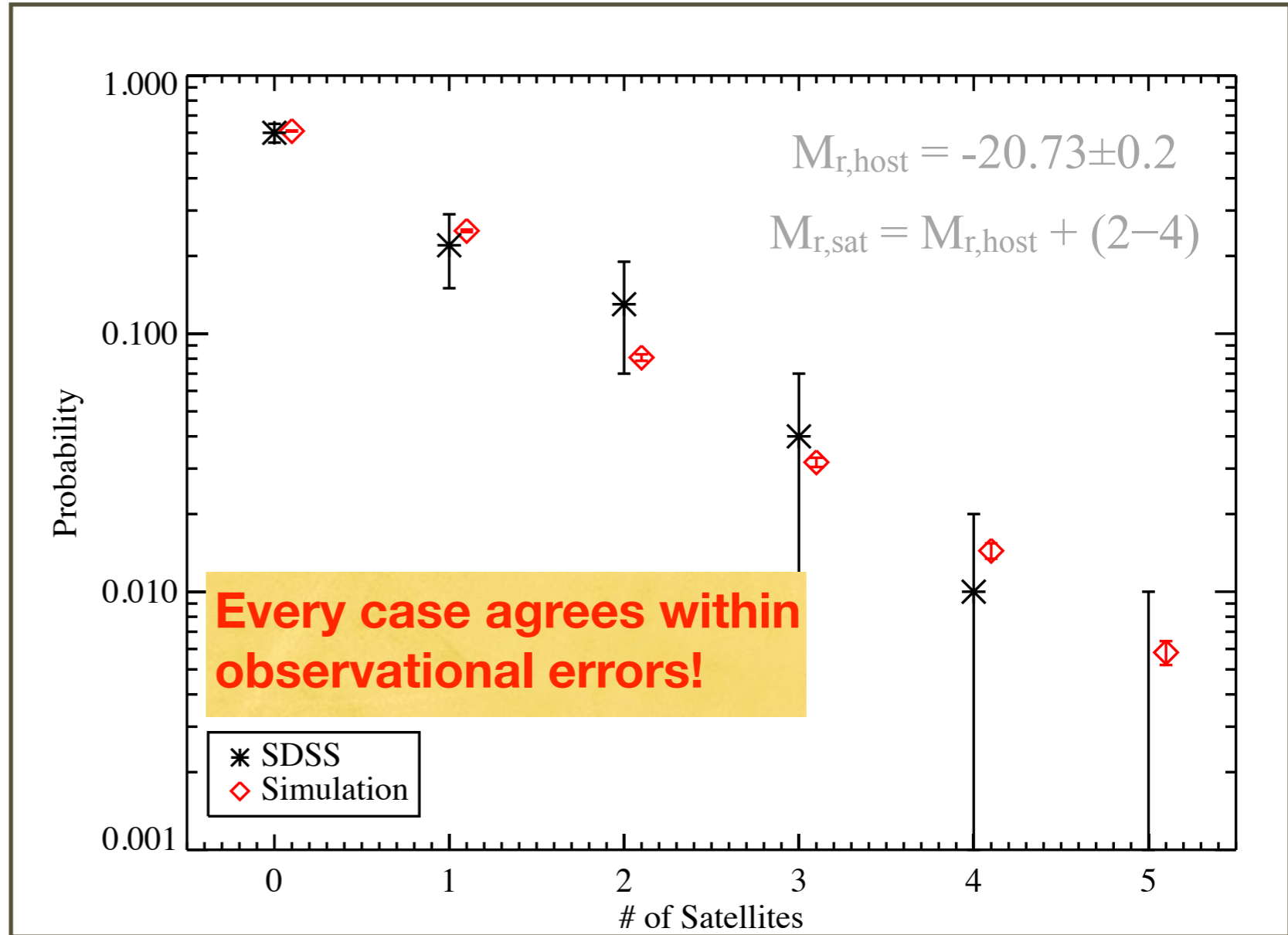
■ Apply the same absolute magnitude and isolation cuts to Bolshoi+SHAM galaxies as to SDSS:

- Identify all objects with absolute $^{0.1}M_r = -20.73 \pm 0.2$ and observed $m_r < 17.6$
- Probe out to $z = 0.15$, a volume of roughly 500 (Mpc/h)^3
- leaves us with 3,200 objects.

■ Comparison of Bolshoi with SDSS observations is in close agreement, well within observed statistical error bars.

# of Subs	Prob (obs)	Prob (sim)
0	60%	61%
1	22%	25%
2	13%	8.1%
3	4%	3.2%
4	1%	1.4%
5	0%	0.58%

Statistics of MW bright satellites: SDSS data vs. Bolshoi simulation



Busha et al. 2011 ApJ
Liu et al. 2011 ApJ

Risa Wechsler

Similarly good agreement with SDSS for brighter satellites with spectroscopic redshifts compared with Millennium-II using abundance matching -- Tollerud, Boylan-Kolchin, et al. 2011 ApJ

Similarly good agreement with SDSS for brighter satellites with spectroscopic redshifts compared with Millennium-II using abundance matching.

We use a volume-limited spectroscopic sample of isolated galaxies in the Sloan Digital Sky Survey (SDSS) to investigate the frequency and radial distribution of luminous ($M_r \lesssim -18.3$) satellites like the Large Magellanic Cloud (LMC) around $\sim L_*$ Milky Way analogs and compare our results object-by-object to Λ CDM predictions based on abundance matching in simulations. We show that 12% of Milky Way-like galaxies host an LMC-like satellite within 75 kpc (projected), and 42% within 250 kpc (projected). This implies $\sim 10\%$ have a satellite within the distance of the LMC, and $\sim 40\%$ of L_* galaxies host a bright satellite within the virialized extent of their dark matter halos. Remarkably, the simulation reproduces the observed frequency, radial dependence, velocity distribution, and luminosity function of observed secondaries exceptionally well, suggesting that Λ CDM provides an accurate reproduction of the observed Universe to galaxies as faint as $L \sim 10^9 L_\odot$ on ~ 50 kpc scales. When stacked, the observed projected pairwise velocity dispersion of these satellites is $\sigma \simeq 160 \text{ km s}^{-1}$, in agreement with abundance-matching expectations for their host halo masses. Finally, bright satellites around L_* primaries are significantly *redder* than typical galaxies in their luminosity range, indicating that environmental quenching is operating within galaxy-size dark matter halos that typically contain only a single bright satellite. This redness trend is in stark contrast to the Milky Way's LMC, which is unusually blue even for a field galaxy. We suggest that the LMC's discrepant color might be further evidence that it is undergoing a triggered star-formation event upon first infall.

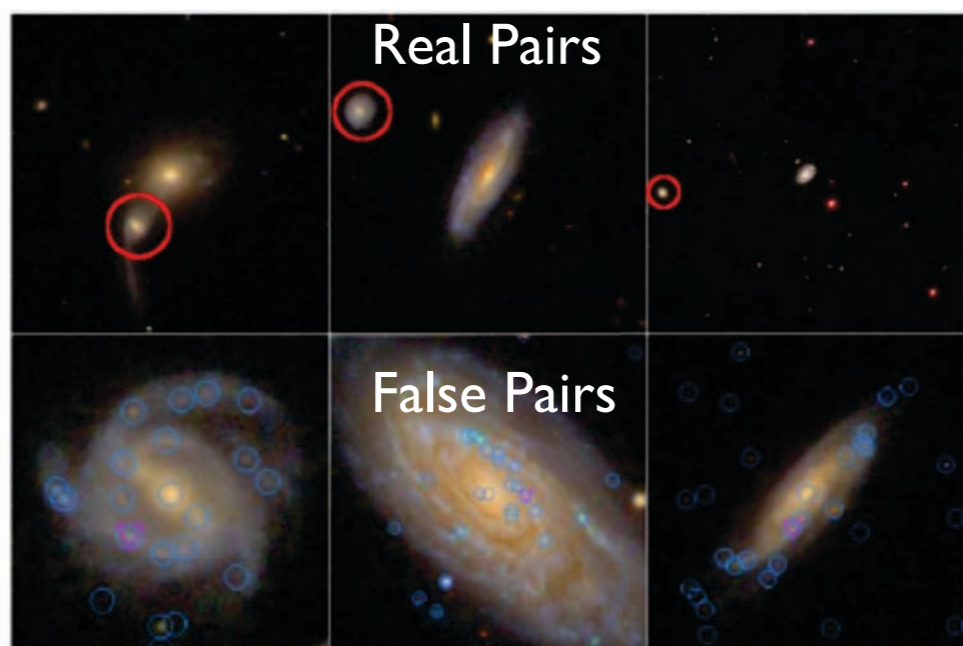


FIG. 1.— Examples of SDSS primary/secondary pairs in the clean sample (upper) and false pairs (lower). Secondaries identified by our criteria (see text) are marked with red circles (upper panels) or magenta triangles (lower panels). The upper three are all in the clean sample (have redshifts close to the primary) and span a range of projected separations. For the lower three images, blue circles are SDSS pipeline photometric objects, clearly showing the identification of HII regions as photometric objects. For these same lower three, the secondaries are clearly HII regions in the primary (or satellites that are indistinguishable from HII regions). We visually identify and remove all pairs of this kind from our sample.

Good agreement between simulated and observed pairwise velocities

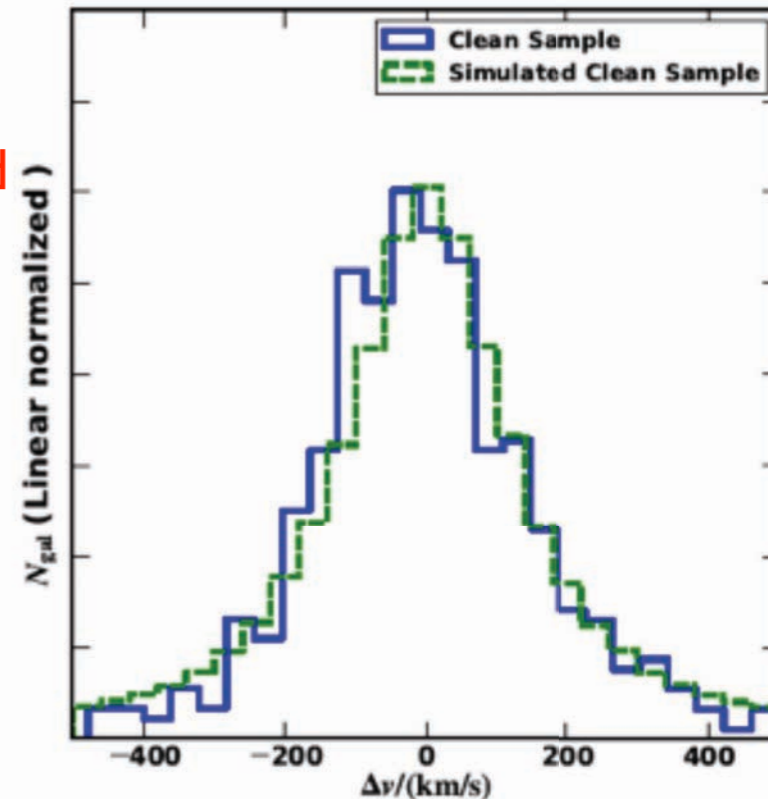
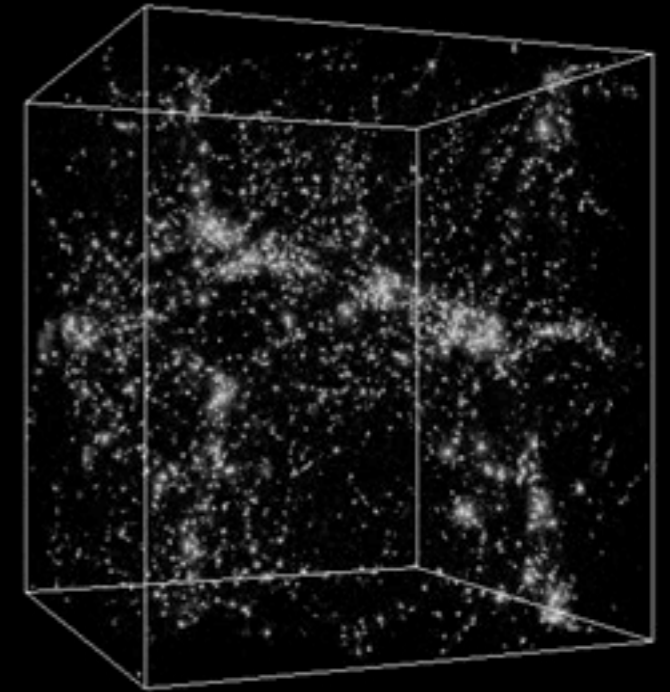
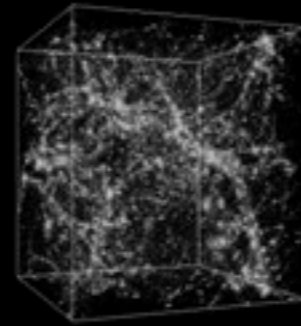
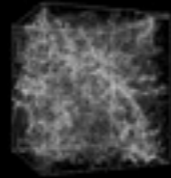
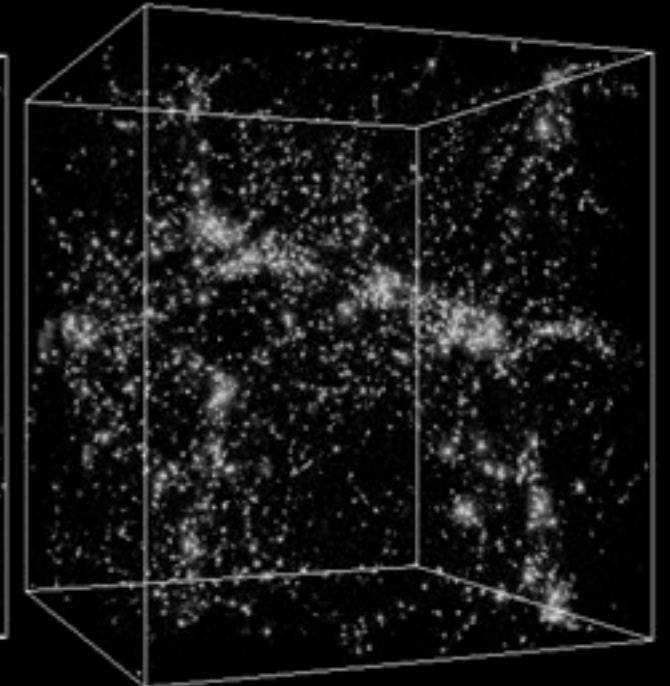
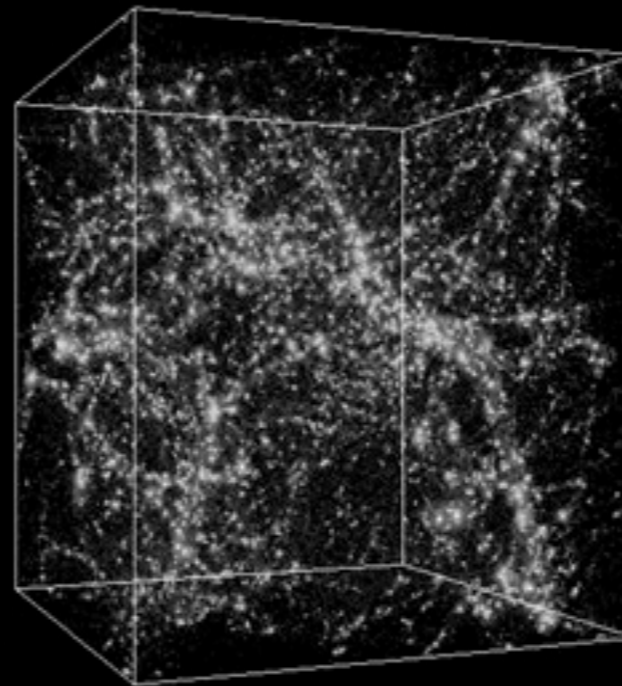
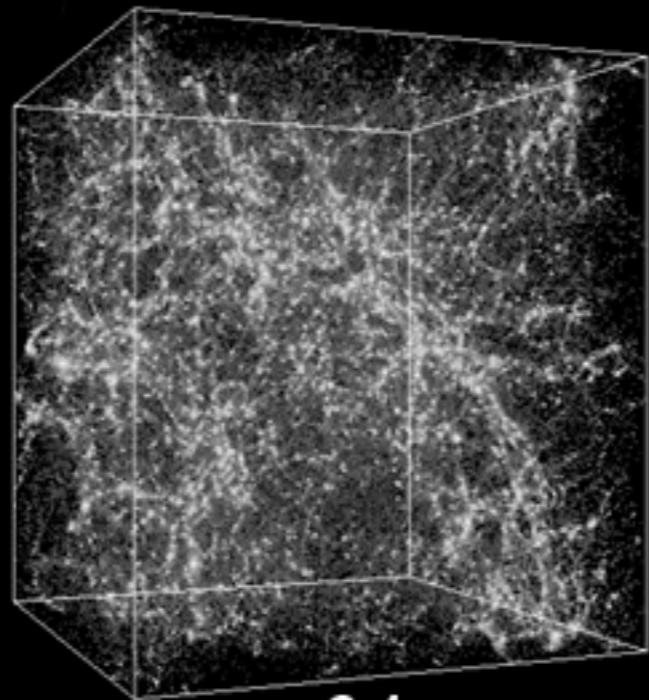
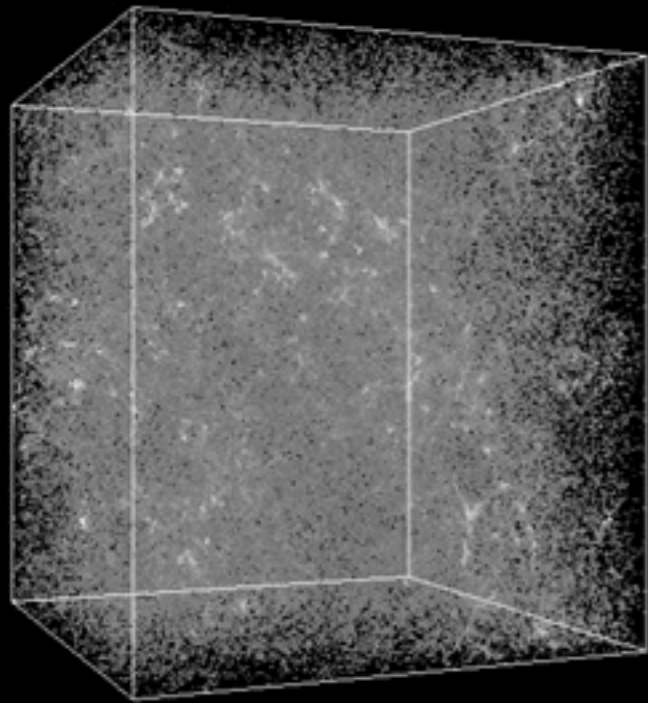


FIG. 6.— Distribution of $\Delta v \equiv c(z_{\text{pri}} - z_{\text{sec}})$ for the clean sample (solid blue histogram), the clean-like sample from MS-II (dashed green). The KS test yields $p_{\text{KS}} = 33\%$. The pairwise velocity dispersion in the observed sample is $\sigma = 161 \text{ km s}^{-1}$.

dark matter simulation - expanding with the universe



same simulation - not showing expansion



0.5

2.1

5.7

13.5

Billions of years after the Big Bang

Evolution of CLUES, a Constrained Local Universe Simulation

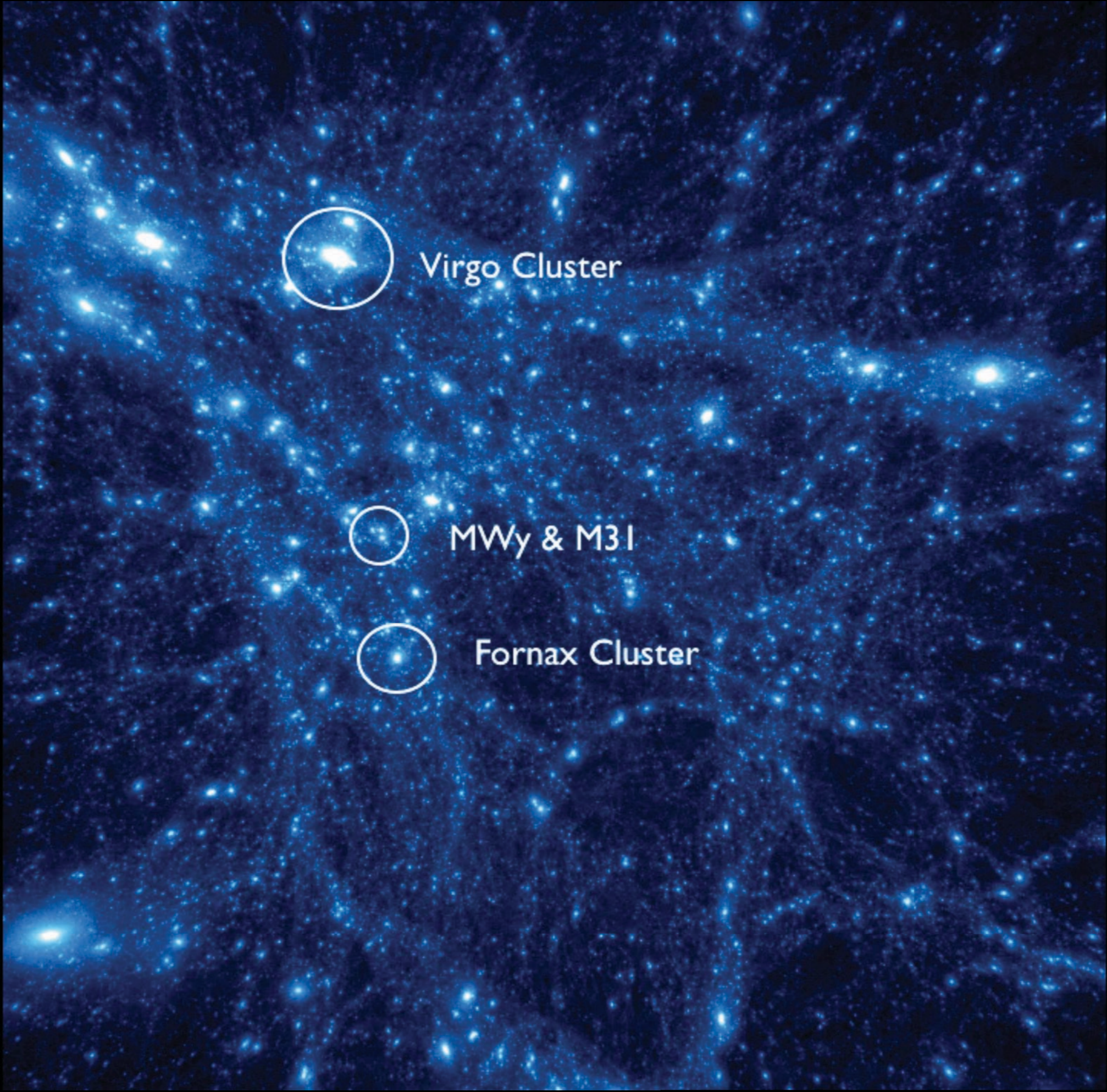
Two different observational data sets were used to set up the initial conditions. The first is made of radial velocities of galaxies drawn from the MARK III, SBF, and Karachentsev catalogs. Peculiar velocities are less affected by non-linear effects and are used as constraints as if they were linear quantities. The other constraints are obtained from the ROSAT all-sky catalog of nearby X-ray selected clusters of galaxies. These data constrain the simulations on scales larger than $\sim 5h^{-1}$ Mpc. The main features that characterise the local universe, such as the Local Supercluster, Virgo cluster, Coma cluster, and Great attractor, are all reproduced by the simulations.

Since these data only constrain scales larger than a few Mpc, a series of different realizations were performed to obtain one that contain an Local Group candidate with the correct properties (e.g., two halos with proper position relative to each-other, mass, negative radial velocity, etc.). Low resolution 256^3 -particle simulations were searched, and the ones with the most suitable Local Group-like objects were chosen for follow-up higher resolution resimulations. More than 200 resimulations were evolved from $z = 50$ to $z = 0$ using GADGET2. We then searched for an object which closely resembles the Local Group and is in the right direction and distance to Virgo.

CONSTRAINED LOCAL UNIVERSE SIMULATION

300 Million Light Years

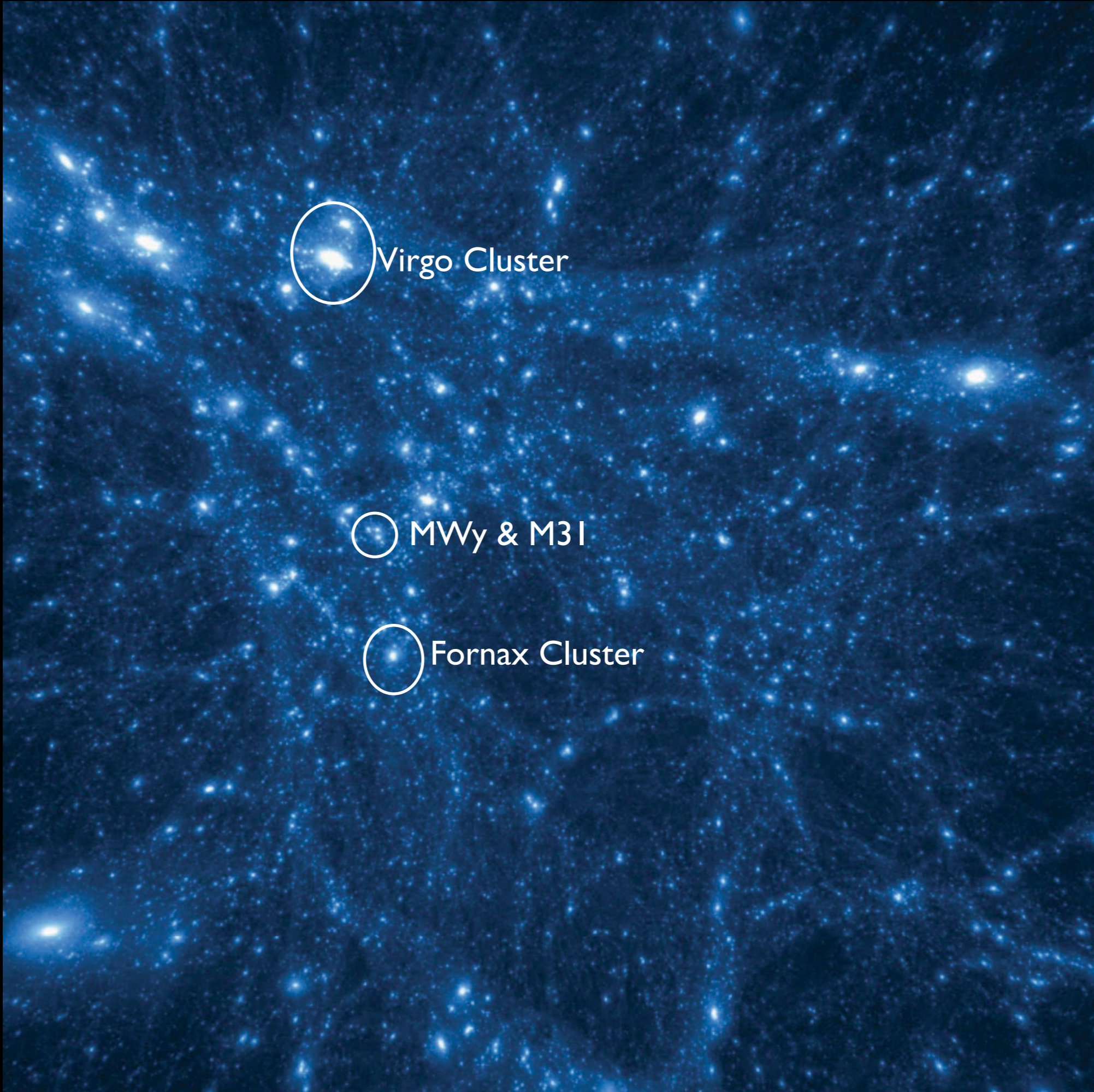




Virgo Cluster

MWy & M31

Fornax Cluster



Virgo Cluster

MWy & M31

Fornax Cluster

Λ CDM vs. Downsizing

Λ CDM:

hierarchical formation
(small things form first)

small structures



large structures

early

late

“Downsizing”:

massive galaxies are old, star
formation moves to smaller galaxies

large galaxies



small galaxies

Λ CDM vs. Downsizing

Λ CDM:

hierarchical formation
(small things form first)

=

mass assembly
simulations (DM)



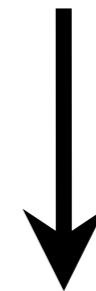
present-day structure

“Downsizing”:

massive galaxies are old, star
formation moves to smaller galaxies

=

star formation history
semi-analytic models



current stellar population

How are these
processes related?

Formation of galaxies and large-scale structure with cold dark matter

Blumenthal, Faber, Primack, & Rees -- Nature 311, 517 (1984)

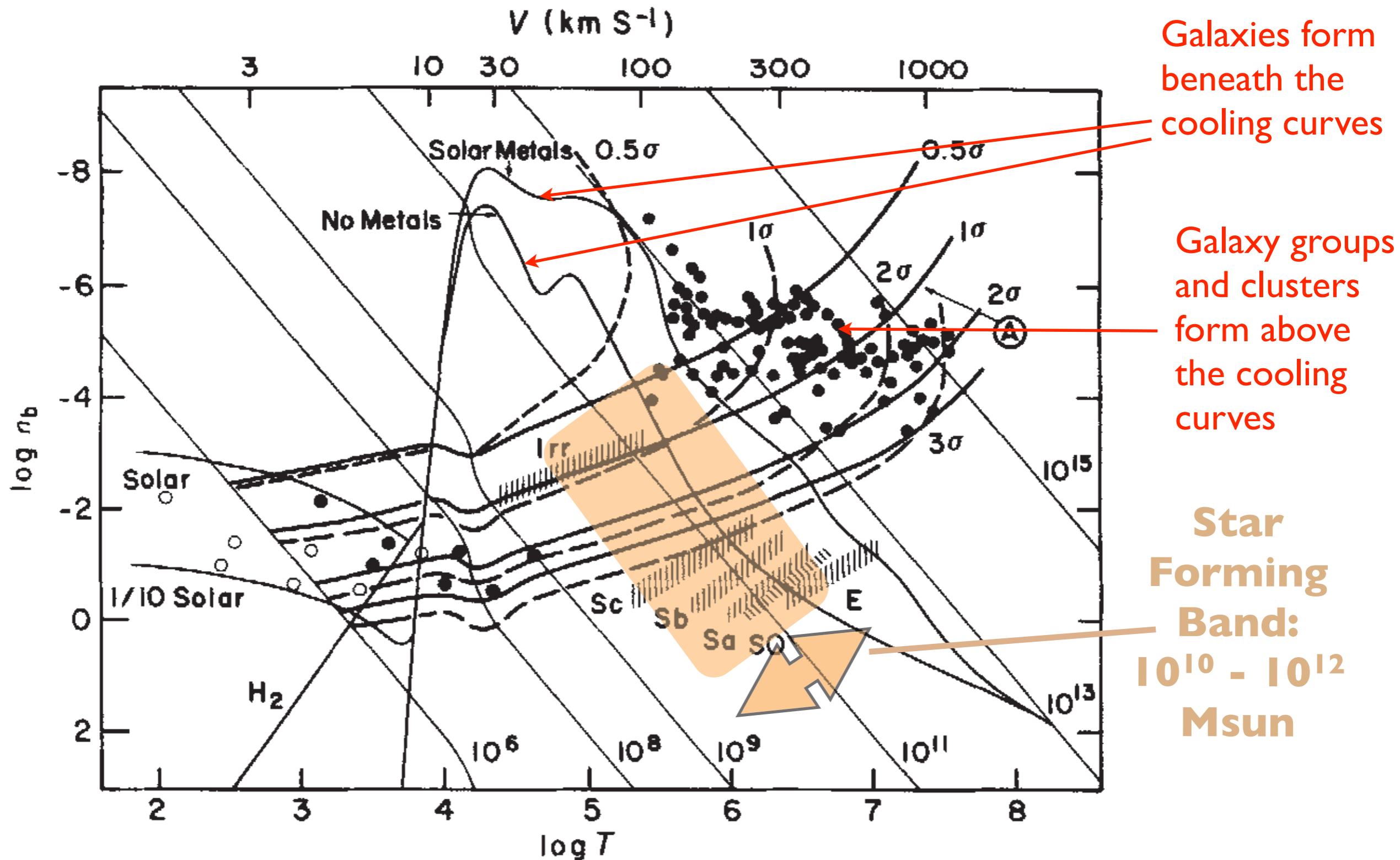
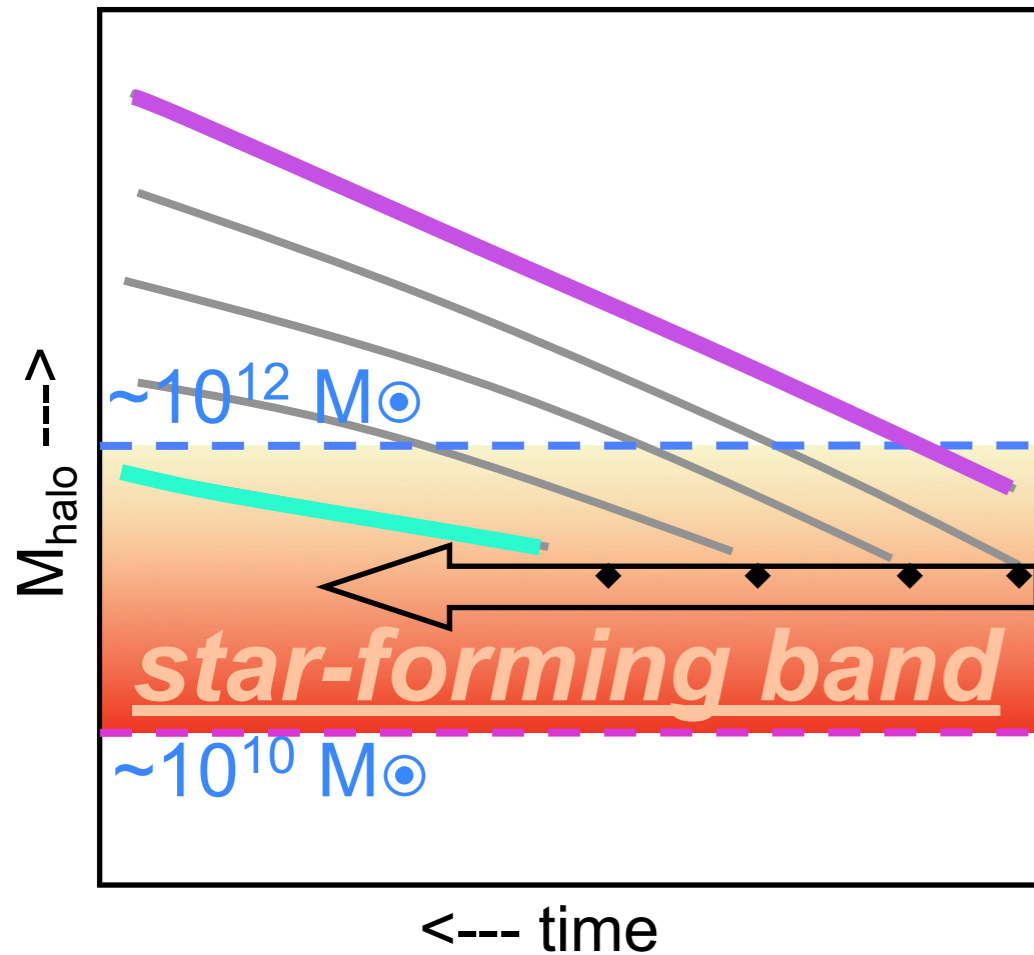


Fig. 3 Baryon density n_b versus three-dimensional, r.m.s. velocity dispersion V and virial temperature T for structures of various size in the Universe. The quantity T is $\mu V^2/3k$, where μ is mean molecular weight (≈ 0.6 for ionized, primordial H+He) and k is Boltzmann's constant.

Implications of the Star-Forming Band Model



Massive galaxies:

- Started forming stars early.
- Shut down early.
- Are red today.
- Populate dark halos that are much more massive than their stellar mass.

Small galaxies:

- Started forming stars late.
- Are still making stars today.
- Are blue today.
- Populate dark halos that match their stellar mass.

“Downsizing”

Star formation is a wave that started in the largest galaxies and swept down to smaller masses later (Cowie et al. 1996).

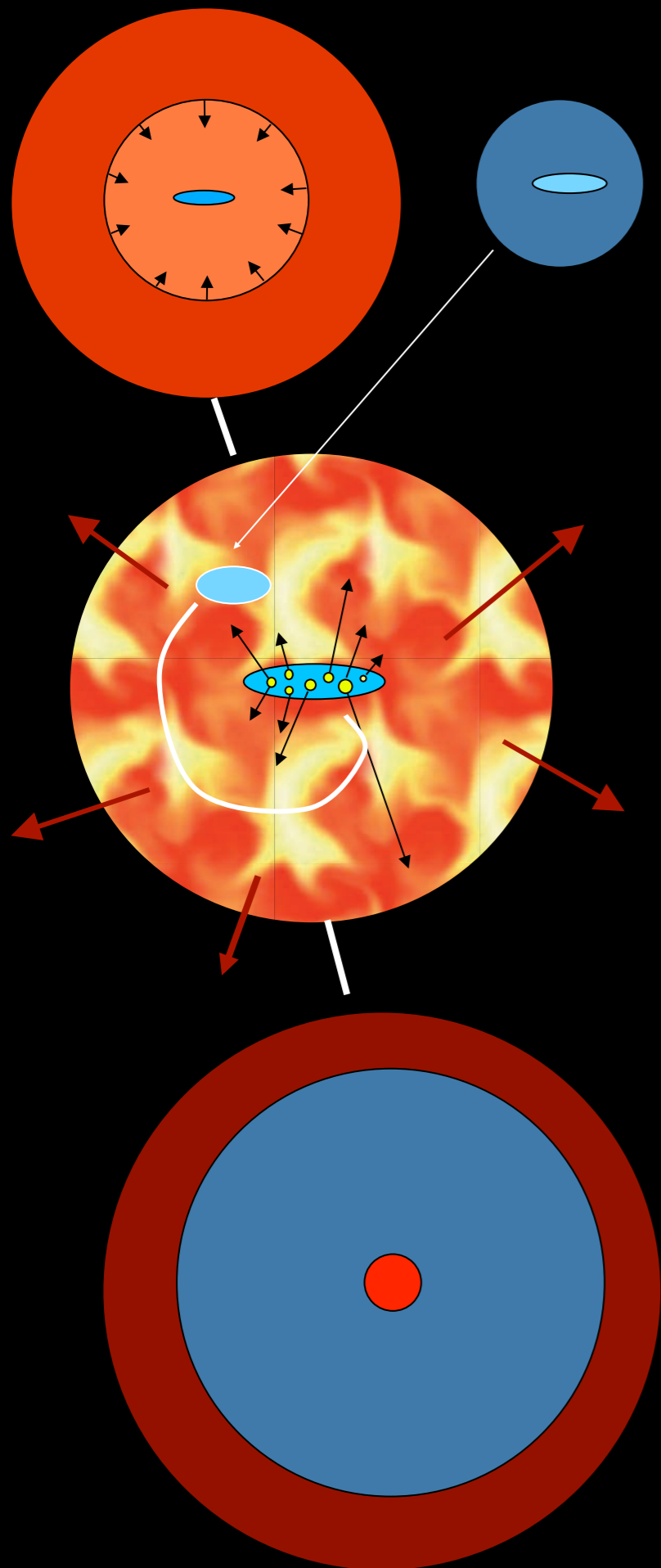
Sandy Faber

Galaxy Formation - Introduction

The details of the origin of the **star-forming band** are still being worked out. Back in 1984, we argued that cooling would be inefficient for masses greater than about $10^{12} M_{\odot}$ because the density would be too low, and inefficient for masses less than about $10^8 M_{\odot}$ because the gas would not be heated enough by falling into these small potential wells.

Now we know that reionization, supernovae, and other energy input additionally impedes star formation for halo masses below about $10^{10} M_{\odot}$, that gas efficiently streams down filaments into halos up to about $10^{12} M_{\odot}$, and that feedback from active galactic nuclei (AGN) impedes star formation for halo masses above about $10^{12} M_{\odot}$. All of these processes and more are included in **semi-analytic models (SAMs)** of the evolution of galaxy populations.

Galaxy Formation via SAMs



- gas is collisionally heated when perturbations ‘turn around’ and collapse to form gravitationally bound structures
- gas in halos cools via atomic line transitions (depends on density, temperature, and metallicity)
- cooled gas collapses to form a rotationally supported disk
- cold gas forms stars, with efficiency a function of gas density (e.g. Schmidt-Kennicutt Law, metallicity effects?)
- massive stars and SNe reheat (and in small halos expel) cold gas and some metals
- galaxy mergers trigger bursts of star formation; ‘major’ mergers transform disks into spheroids and fuel AGN
- AGN feedback cuts off star formation
- including effects of dissipation in gas-rich galaxy mergers leads to observed elliptical size-mass relation
- including spheroid formation by disk instability is essential to reproduce the observed elliptical luminosity function

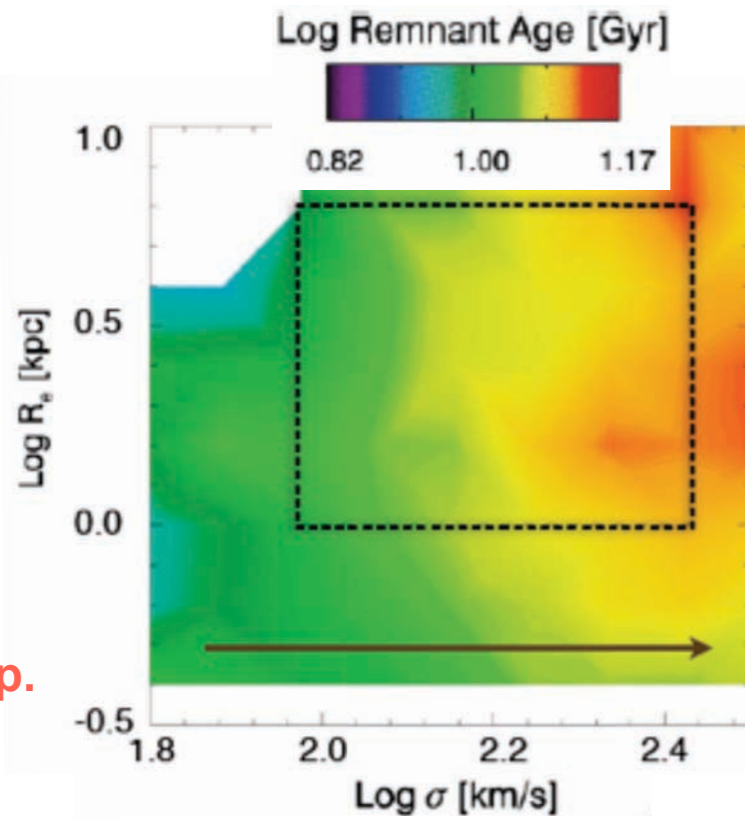
White & Frenk 91; Kauffmann+93; Cole+94; Somerville & Primack 99; Cole+00; Somerville, Primack, & Faber 01; Croton et al. 2006; Somerville +08; Fanidakis+09; Covington et al. 10, 11; Somerville, Gilmore, Primack, & Dominguez 11; Porter et al.

SAM Predictions vs. SDSS Observations

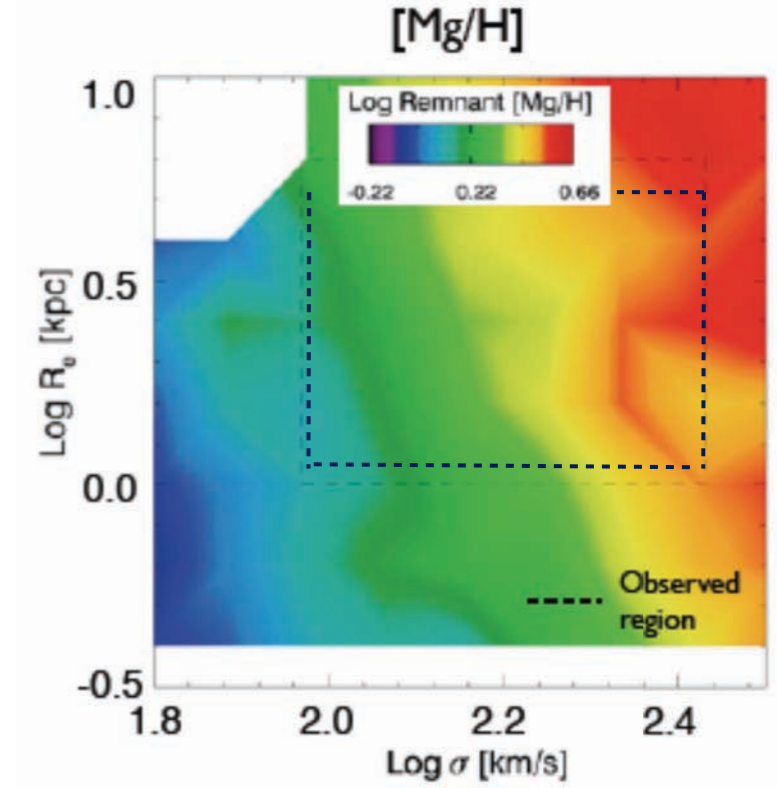
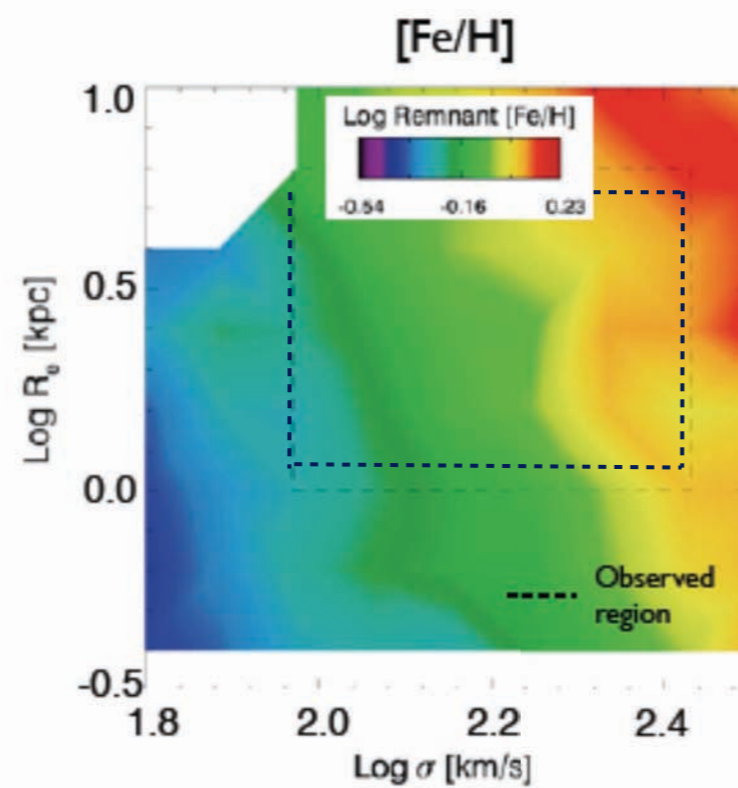
Galaxy Age

Galaxy Metallicity

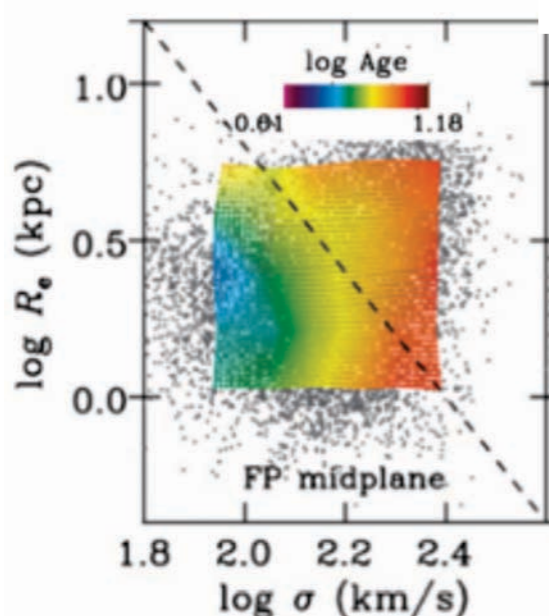
SAM



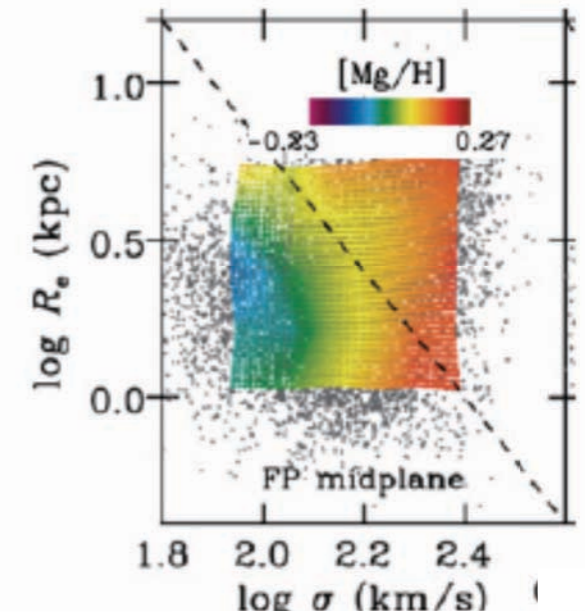
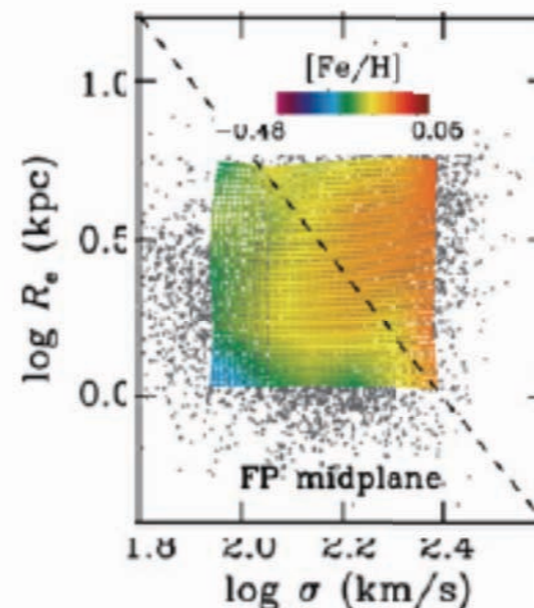
Lauren Porter et al. in prep.



SDSS



Jenny Graves et al. 2009



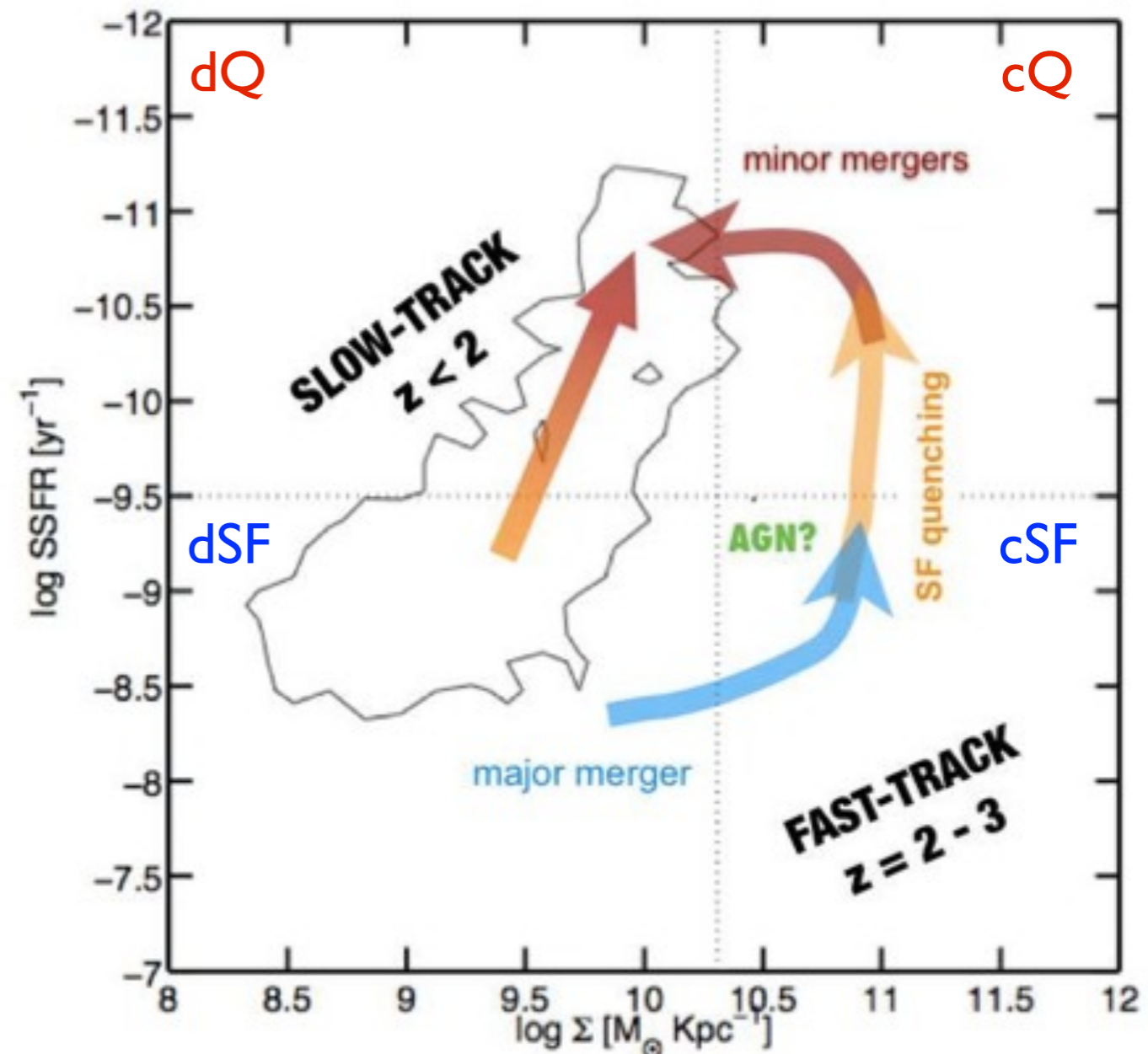
CANDELS: THE PROGENITORS OF COMPACT QUIESCENT GALAXIES AT $Z \sim 2$

GUILLERMO BARRO¹, S. M. FABER¹, PABLO G. PÉREZ-GONZÁLEZ^{2,3}, DAVID C. KOO¹, CHRISTINA C. WILLIAMS⁴, DALE D. KOCEVSKI¹, JONATHAN R. TRUMP¹, MARK MOZENA¹, ELIZABETH McGRATH¹, ARJEN VAN DER WEL⁵, STIJN WUYTS⁶, ERIC F. BELL⁷, DARREN J. CROTON⁸, AVISHAI DEKEL⁹, M. L. N. ASHBY¹⁰, HENRY C. FERGUSON¹¹, ADRIANO FONTANA¹², MAURO GIAVALISCO⁴, NORMAN A. GROGIN¹¹, YICHENG GUO⁴, NIMISH P. HATHI¹³, PHILIP F. HOPKINS¹⁴, KUANG-HAN HUANG¹¹, ANTON M. KOEKEMOER¹¹, JEYHAN S. KARTALTEPE¹⁵, KYOUNG-SOO LEE¹⁶, JEFFREY A. NEWMAN¹⁷, LAUREN A. PORTER¹, JOEL R. PRIMACK¹, RUSSELL E. RYAN¹¹, DAVID ROSARIO⁶, RACHEL S. SOMERVILLE¹⁸

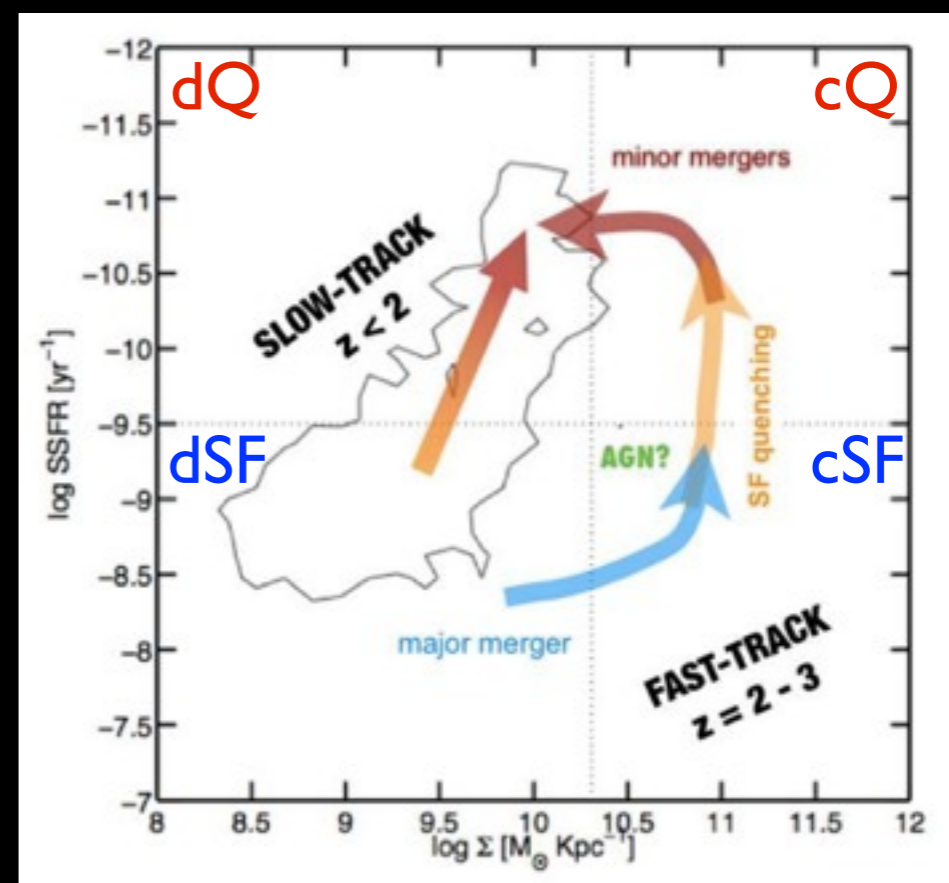
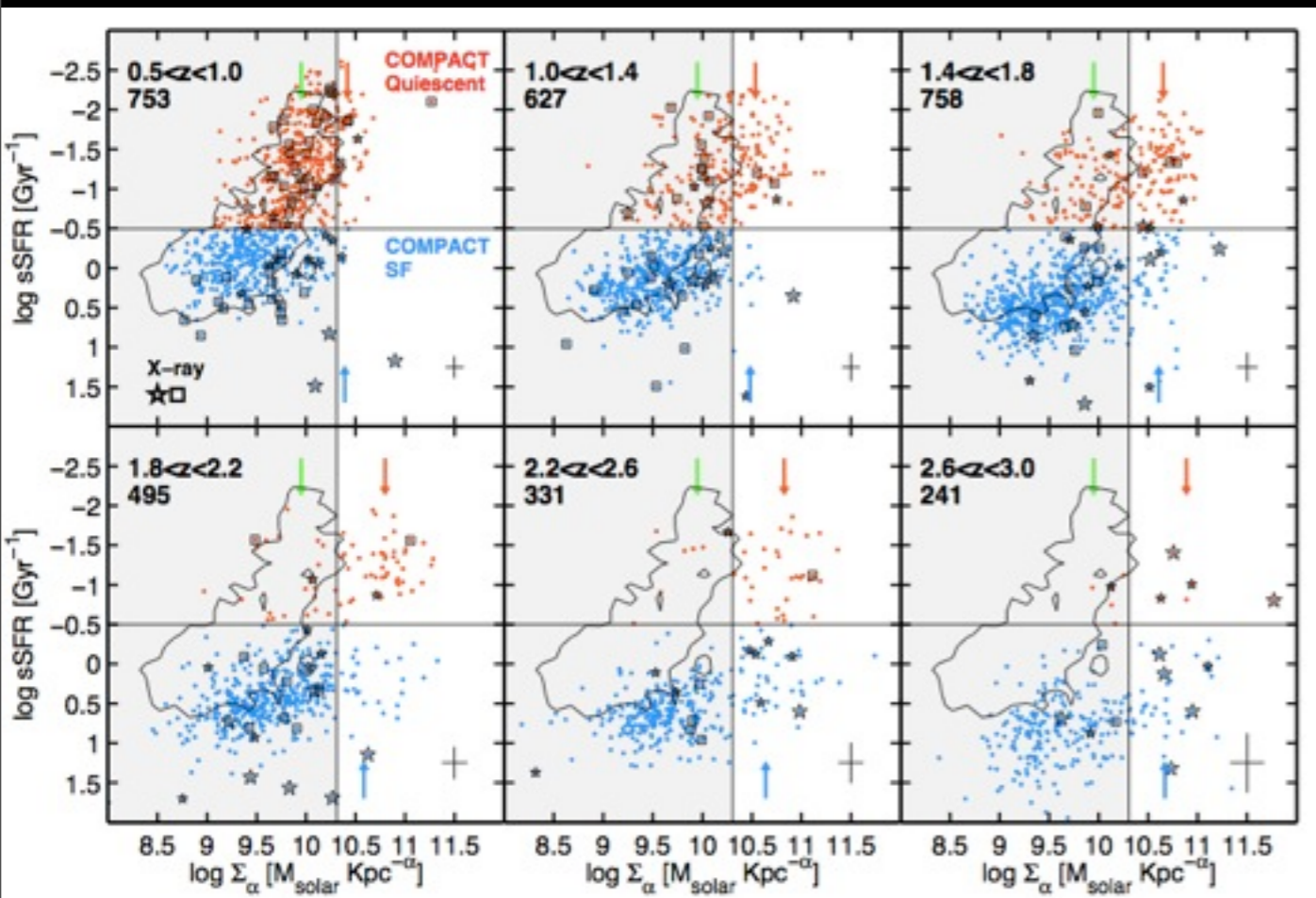
Submitted to the Astrophysical Journal Letters

arXiv:1206.5000v1

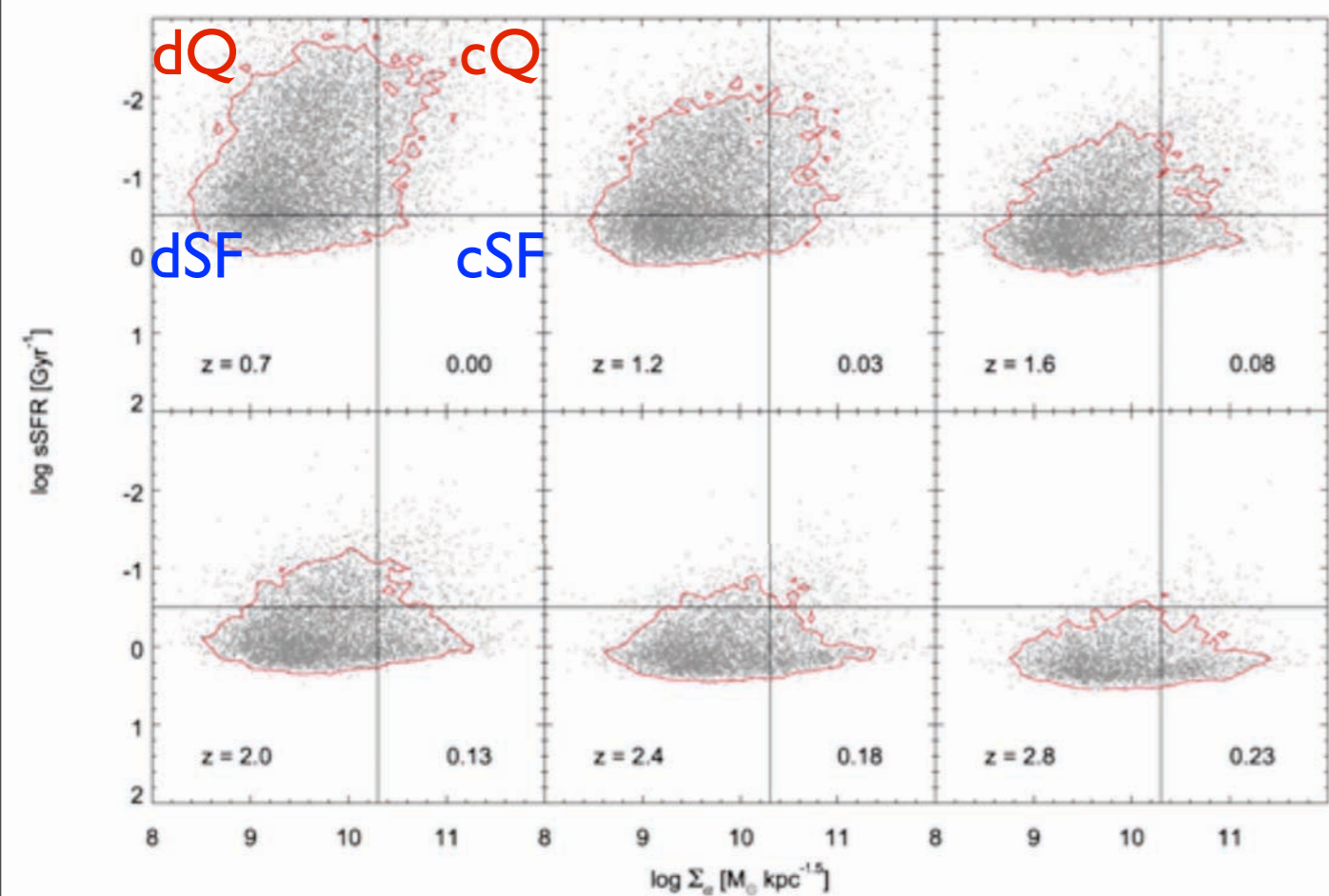
ABSTRACT We combine high-resolution HST/WFC3 images with multi-wavelength photometry to track the evolution of structure and activity of massive ($M_\star > 10^{10} M_\odot$) galaxies at redshifts $z = 1.4 - 3$ in two fields of the Cosmic Assembly Near-infrared Deep Extragalactic Legacy Survey (CANDELS). We detect compact, star-forming galaxies (cSFGs) whose number densities, masses, sizes, and star formation rates qualify them as likely progenitors of compact, quiescent, massive galaxies (cQGs) at $z = 1.5 - 3$. At $z > 2$, most cSFGs have specific star-formation rates half that of typical massive SFGs, and host X-ray luminous AGNs 30 times more frequently. These properties suggest that cSFGs are formed by gas-rich processes (mergers or disk-instabilities) that induce a compact starburst and feed an AGN, which, in turn, quenches the star formation on dynamical timescales (few 10^8 yr). The cSFGs are continuously being formed at $z = 2 - 3$ and fade to cQGs down to $z \sim 1.5$. After this epoch, cSFGs are rare, thereby truncating the formation of new cQGs. In summary, we propose two evolutionary tracks of QG formation: an early ($z > 2$), fast-formation path of rapidly-quenched cSFGs fading into cQGs that later enlarge within the quiescent phase, and a slow, late-arrival ($z < 2$) path in which larger SFGs form extended QGs without passing through a compact state.



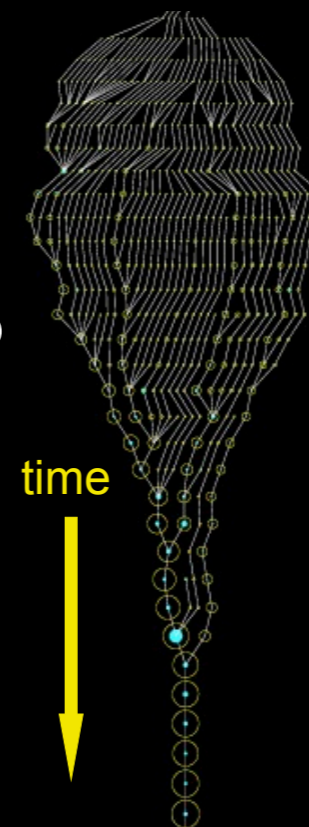
Evolution of Galaxies: Observations vs. Theory



Barro et al. (2012 - Hubble Observations)



Bolshoi
DM Halo
Merger
Tree

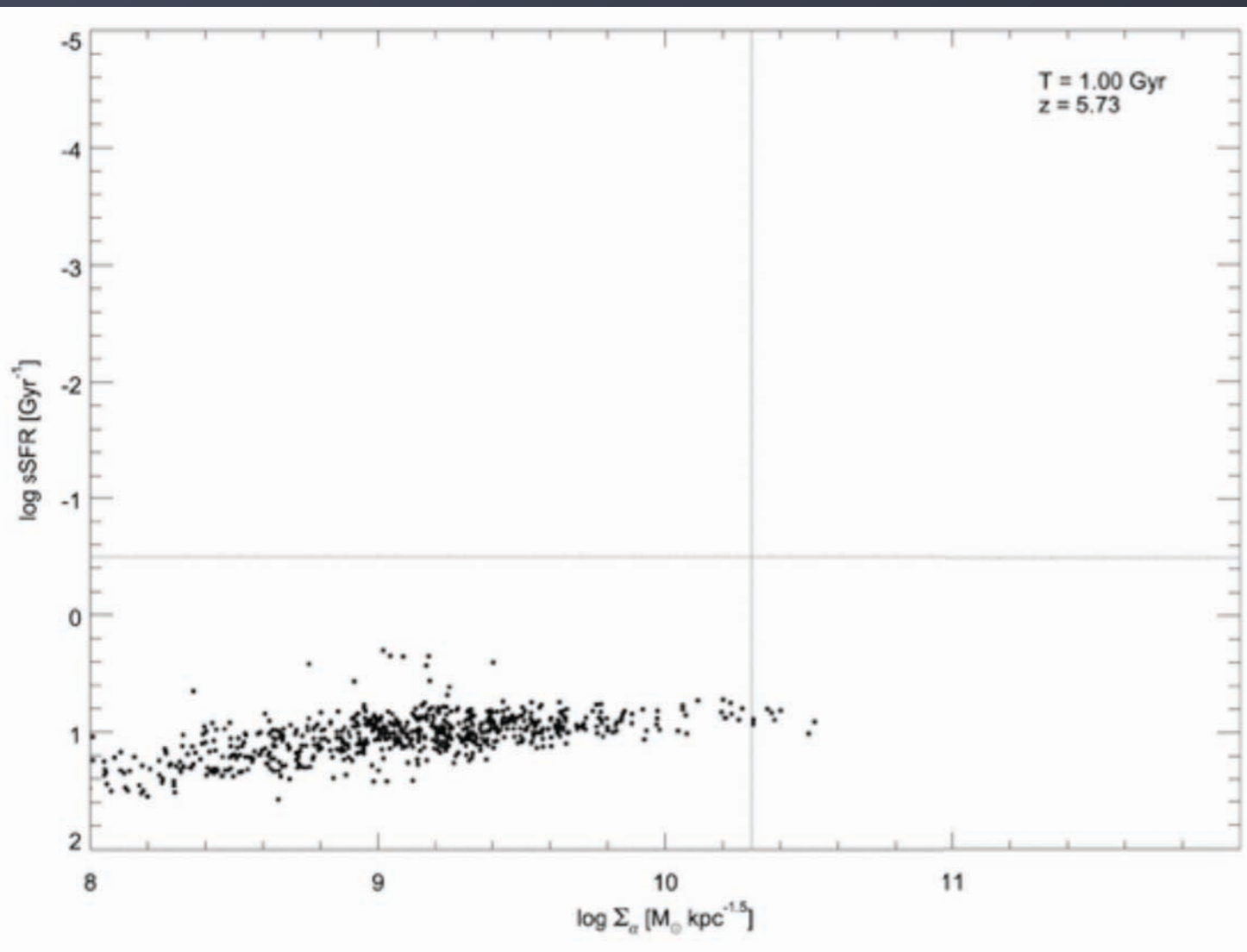


Astrophysical
processes modeled:

- shock heating & radiative cooling
- photoionization squelching
- merging
- star formation (quiescent & burst)
- SN heating & SN-driven winds
- AGN accretion and feedback
- chemical evolution
- stellar populations & dust

Porter et al. (in prep.) - Bolshoi SAM

Evolution of Compact Star-Forming Galaxies According to Bolshoi-based Semi-Analytic Model



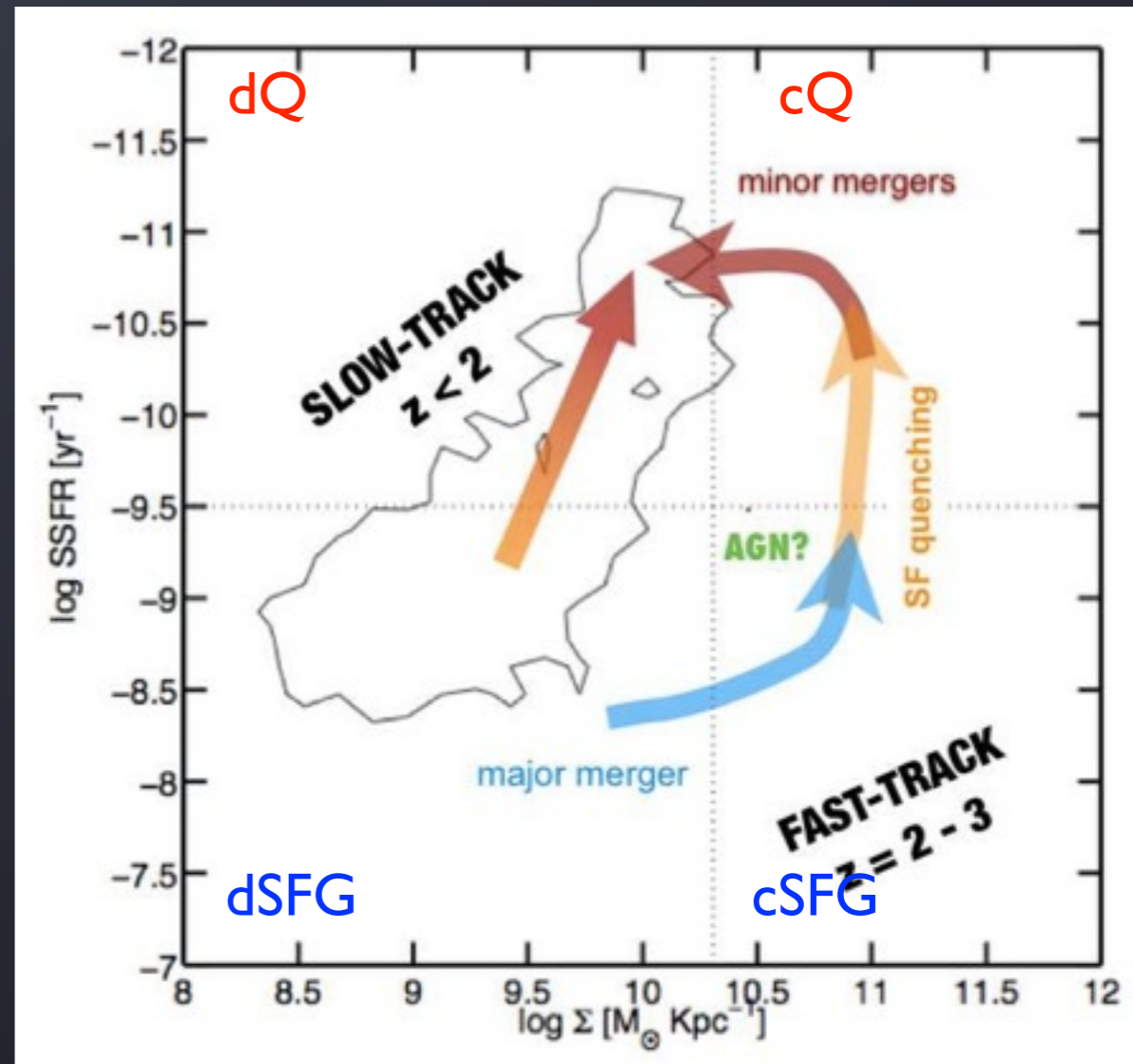
Gas-rich merger in past Gyr

Gas-poor merger in past Gyr

cSFG at z = 2.4

Porter et al. (in prep.) - Bolshoi SAM

Observed Evolution of Galaxies from Latest Hubble Telescope Data



Barro et al. (2012 - Hubble Observations)

Cosmological Simulations

Astronomical observations represent snapshots of moments in time. It is the role of astrophysical theory to produce movies -- both metaphorical and actual -- that link these snapshots together into a coherent physical theory.

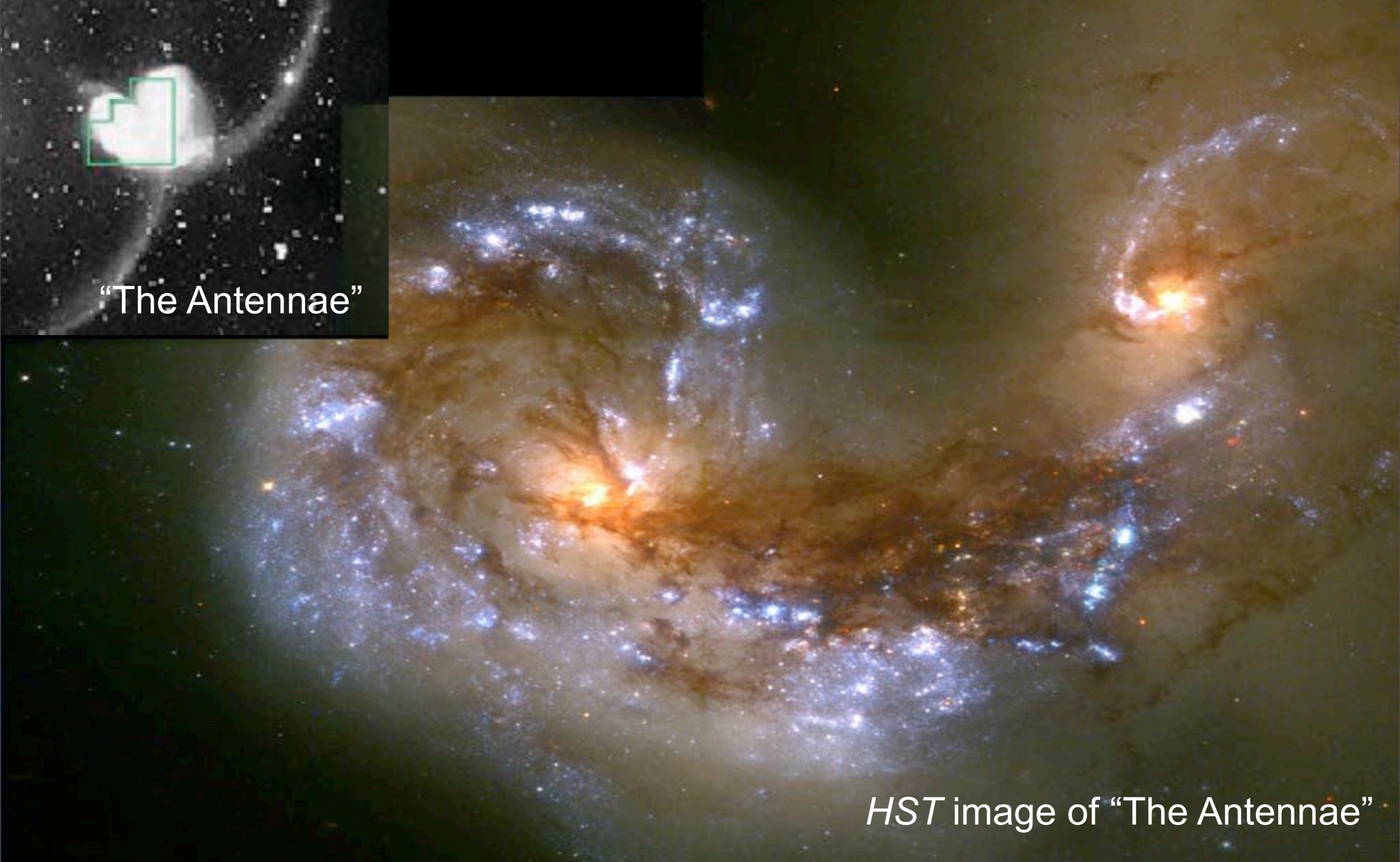
Cosmological dark matter simulations show large scale structure, growth of structure, and dark matter halo properties

Hydrodynamic galaxy formation simulations: evolution of galaxies, formation of galactic spheroids via mergers, galaxy images in all wavebands including stellar evolution and dust

Simulations of Galaxies Including Stellar Evolution and Dust



“The Antennae”

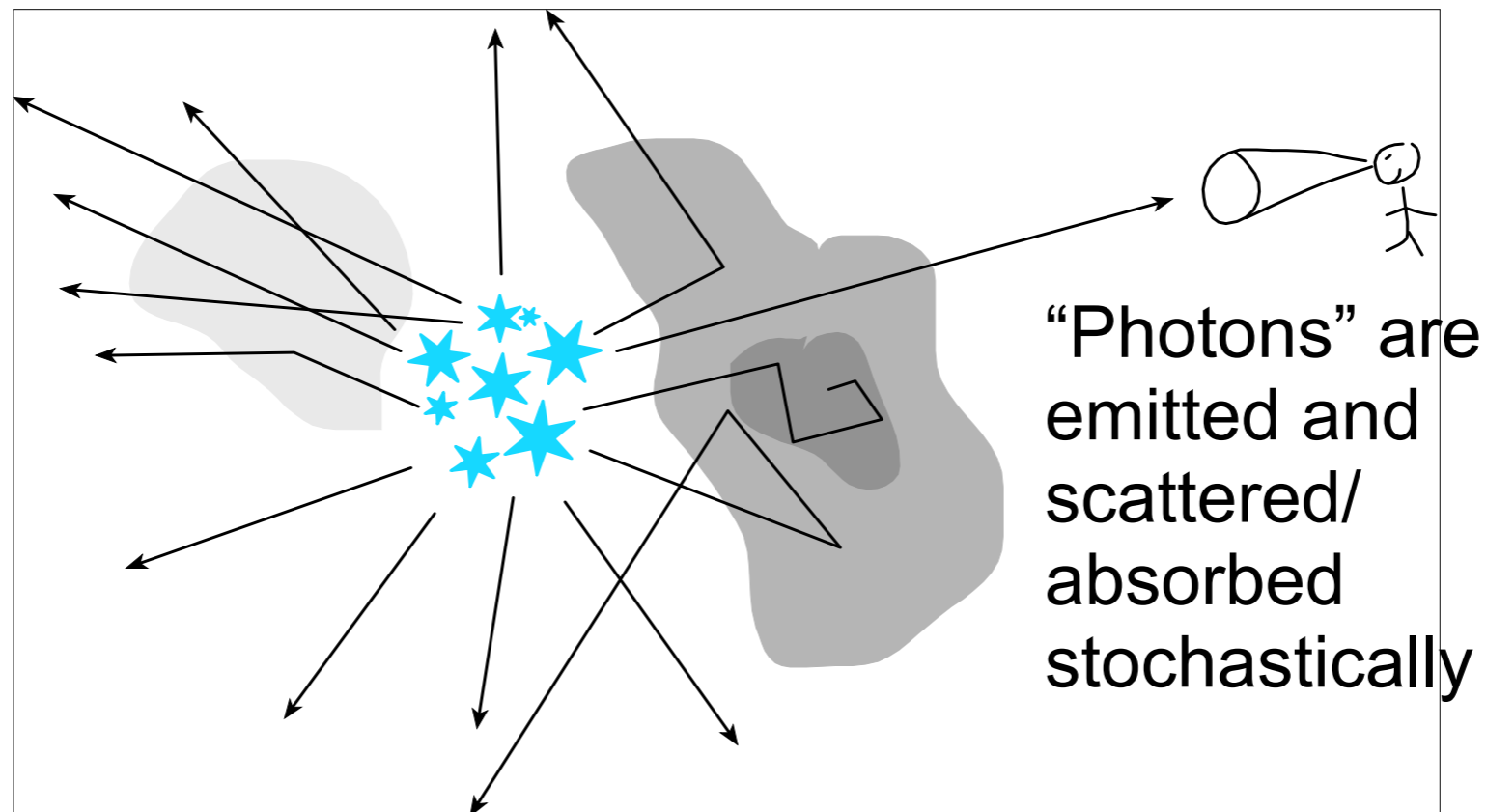


HST image of “The Antennae”

Sunrise Radiative Transfer Code

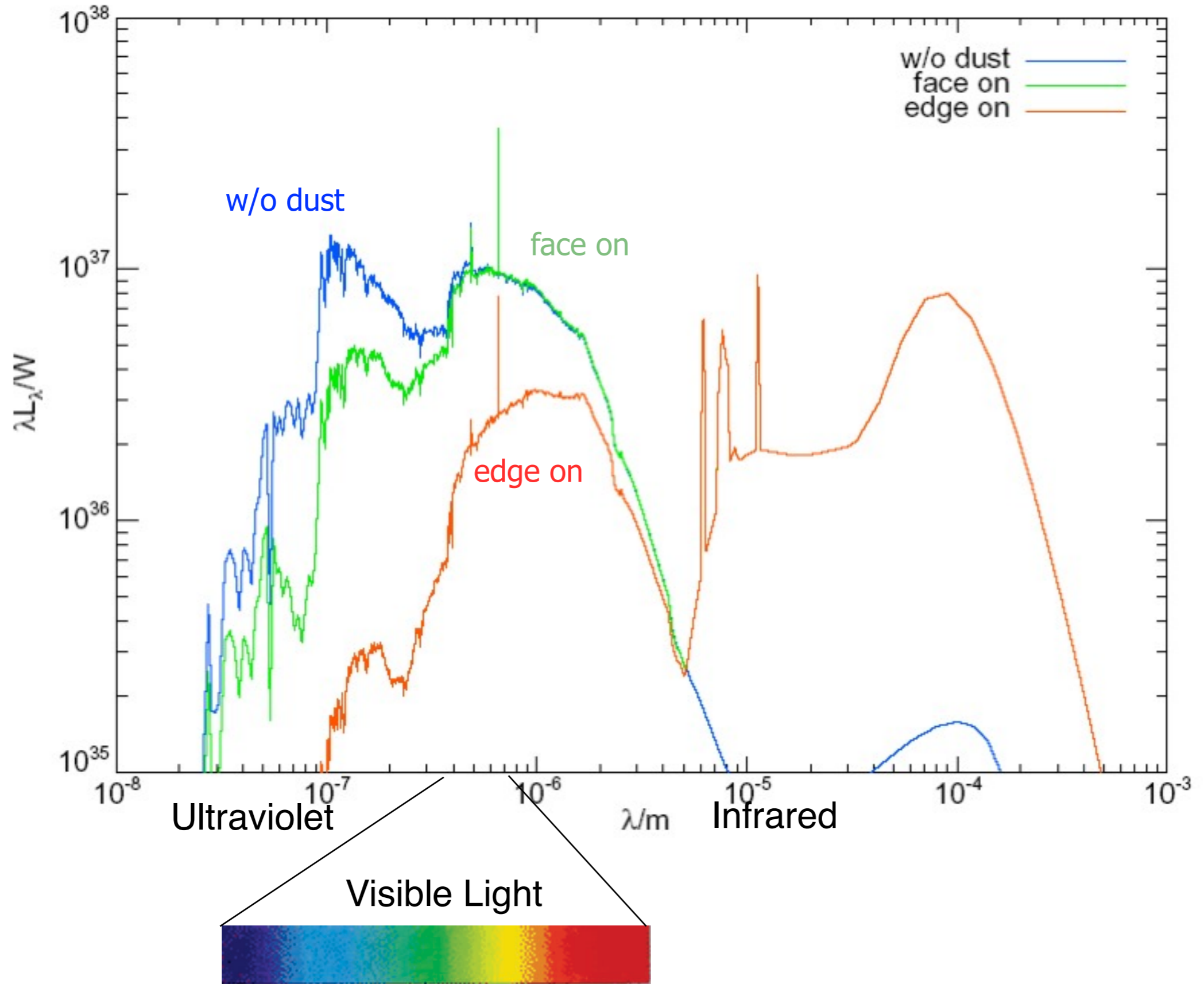
For every simulation snapshot:

- Evolving stellar spectra calculation
- Adaptive grid construction
- Monte Carlo radiative transfer
- “Polychromatic” rays save 100x CPU time
- Graphic Processor Units give 10x speedup




Patrik Jonsson

Spectral Energy Distribution



Galaxy Merger Simulation



A merger between galaxies like the Milky Way and the Andromeda galaxy. Galaxy mergers like this one trigger gigantic "starbursts" forming many millions of new stars (which look blue in these images). But dust (orange in the video) absorbs ~90% of the light, and reradiates the energy in invisible long wavelengths.



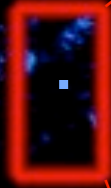
When the universe is twice its present age, the distant galaxies will have disappeared over the cosmic horizon.



Milky Andromeda will eventually become all that's visible.

The Double Dark Future of the Universe

now



in 40 billion years



in 80 billion years

**Milky
Andromeda
becomes
isolated**

Mike Busha

Accelerating Dust Temperature Calculations with Graphics Processing Units

Patrik Jonsson, Joel R. Primack

[New Astronomy 15, 509 \(2010\) \(arXiv:0907.3768\)](#)

When calculating the infrared spectral energy distributions (SEDs) of galaxies in radiation-transfer models, the calculation of dust grain temperatures is generally the most time-consuming part of the calculation. Because of its highly parallel nature, this calculation is perfectly suited for massively parallel general-purpose Graphics Processing Units (GPUs). This paper presents an implementation of the calculation of dust grain equilibrium temperatures on GPUs in the Monte-Carlo radiation transfer code Sunrise, using the CUDA API. The Nvidia Tesla GPU can perform this calculation 55 times faster than the 8 CPU cores, showing great potential for accelerating calculations of galaxy SEDs.

On 64 special NAS Pleiades nodes with 2 Westmere chips (12 cores) and an Nvidia 2090 GPU, using the GPU makes the calculation run 12x faster.

Dust Attenuation in Hydrodynamic Simulations of Spiral Galaxies

Rocha, Jonsson, Primack, & Cox 2008 MN

Right hand side:
Xilouris et al. 1999
metallicity gradient

Sbc - no dust



Sbc - Xilouris
metallicity gradient



Sbc - constant
metallicity gradient



50 Kpc



50 Kpc

Sbc



G3



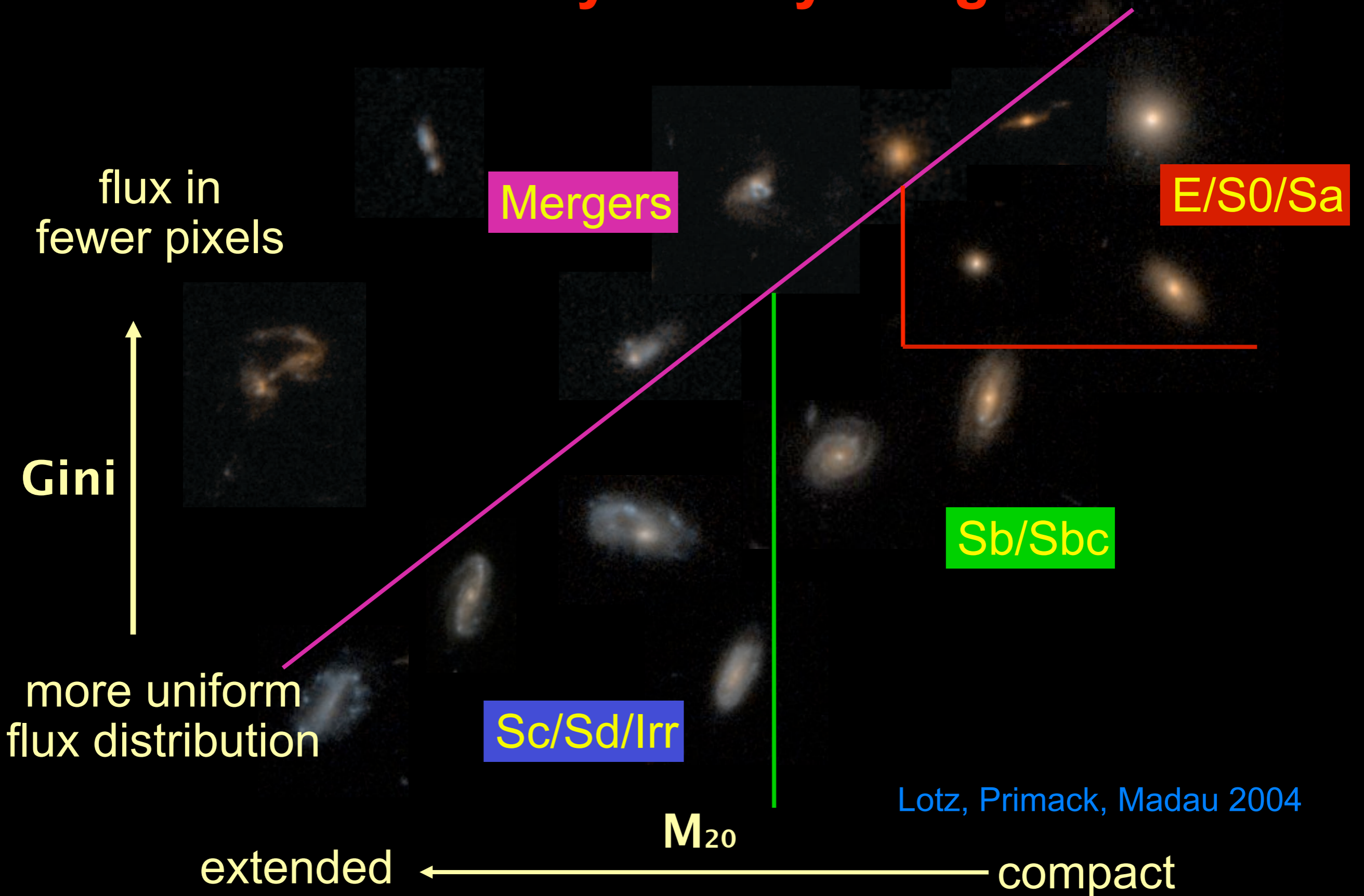
G2



G1



G-M₂₀ Nonparametric Morphology Measures Can Identify Galaxy Mergers

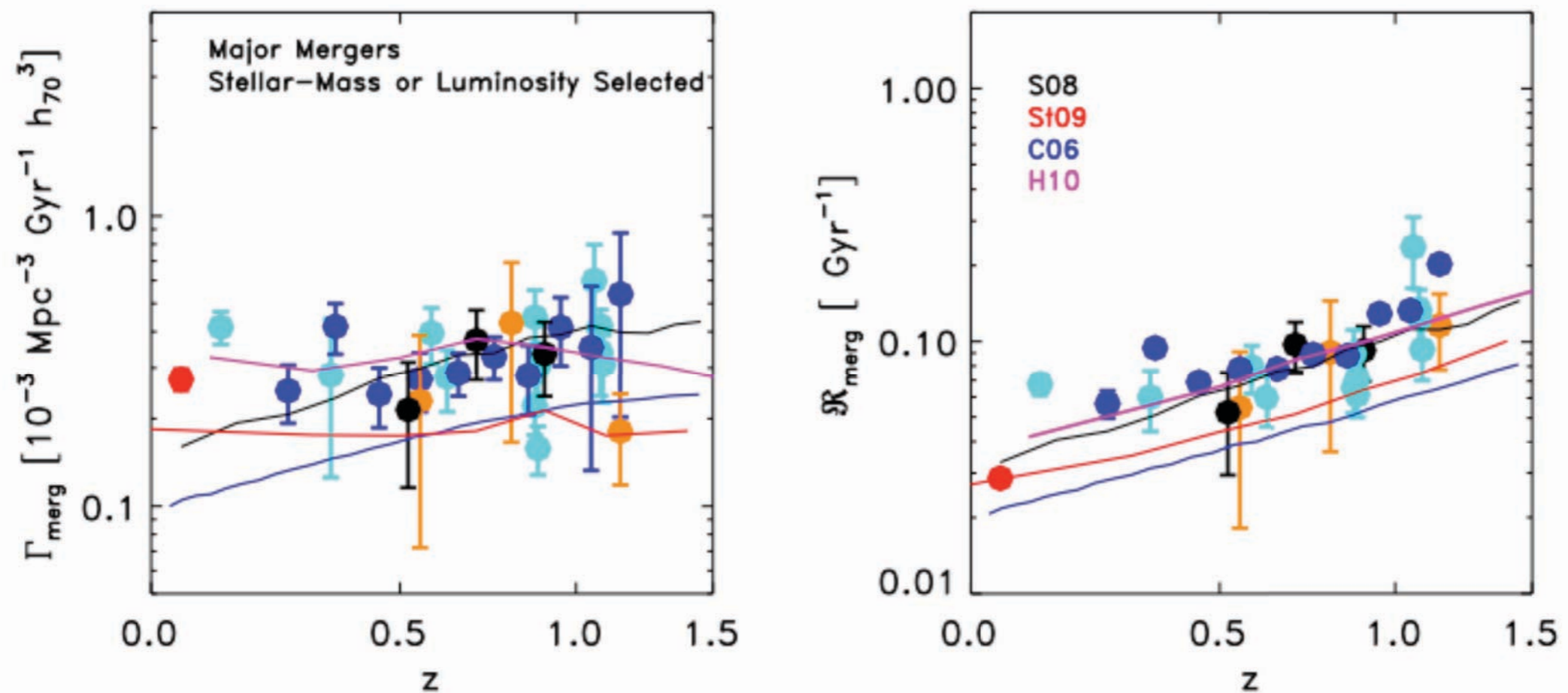


Lotz, Primack, Madau 2004

THE MAJOR AND MINOR GALAXY MERGER RATES AT $Z < 1.5$

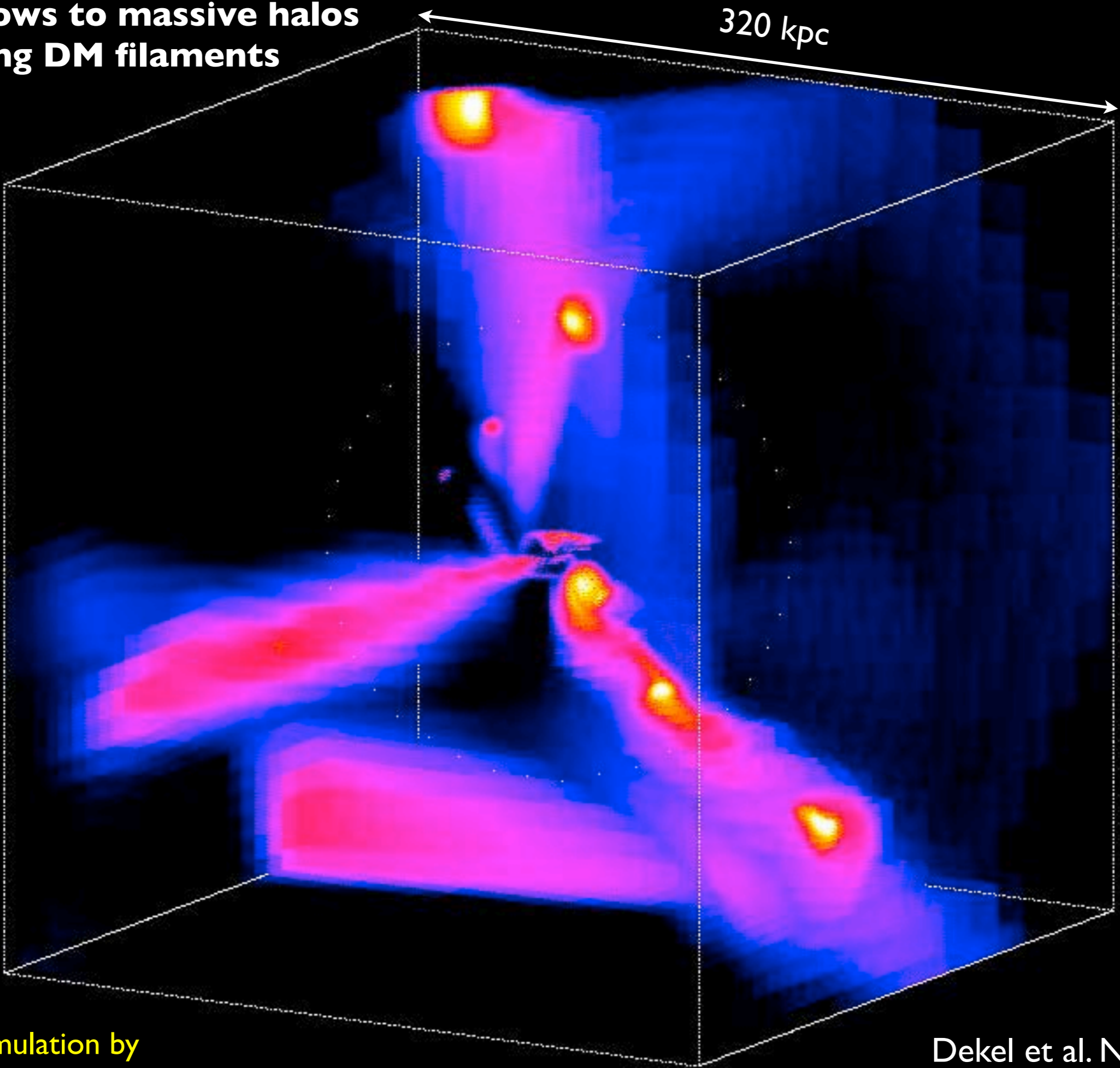
Jennifer M. Lotz, Patrik Jonsson, T.J. Cox, Darren Croton, Joel R. Primack, Rachel S. Somerville, and Kyle Stewart
Astrophysical Journal December 2011

Calculating the galaxy merger rate requires both a census of galaxies identified as merger candidates, and a cosmologically-averaged ‘observability’ timescale $\langle T_{\text{obs}}(z) \rangle$ for identifying galaxy mergers. While many have counted galaxy mergers using a variety of techniques, $\langle T_{\text{obs}}(z) \rangle$ for these techniques have been poorly constrained. We address this problem by calibrating three merger rate estimators with a suite of hydrodynamic merger simulations and three galaxy formation models. When our physically-motivated timescales are adopted, the observed galaxy merger rates become largely consistent.



Observed Galaxy Merger Rates v. Theoretical Predictions. The volume-averaged (left) and fractional major merger (right) rates given by stellar-mass and luminosity-selected close pairs are compared to the major merger rates given by the S08 (black lines), St09 (red lines), C06 (blue line), and Hopkins et al. 2010b (magenta lines) models for 1:1 - 1:4 stellar mass ratio mergers and galaxies with $M_{\text{star}} > 10^{10} M_{\odot}$. The theoretical predictions are in good agreement with the observed major merger rates.

**Gas inflows to massive halos
along DM filaments**



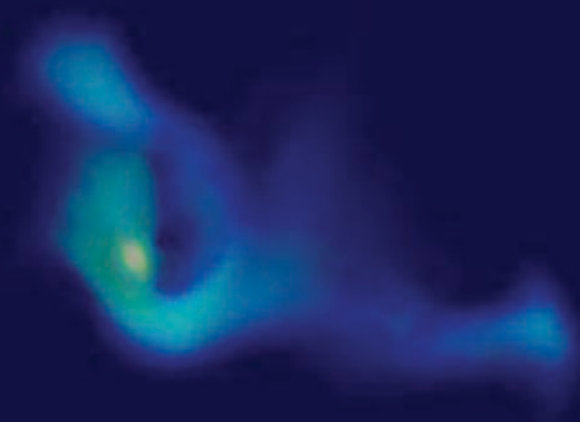
320 kpc

RAMSES simulation by
Romain Teyssier on Mare Nostrum supercomputer, Barcelona

Dekel et al. Nature 2009



● Stars



time=276

ART Simulation Daniel Ceverino;
Visualization: David Ellsworth

Simulated Evolution of an Elliptical Galaxy

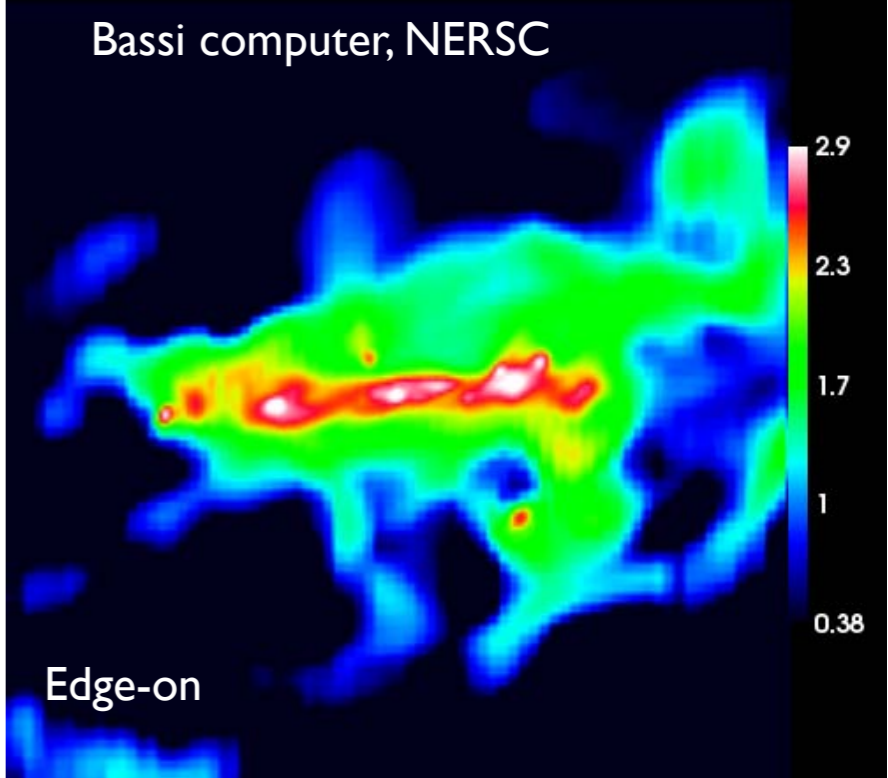
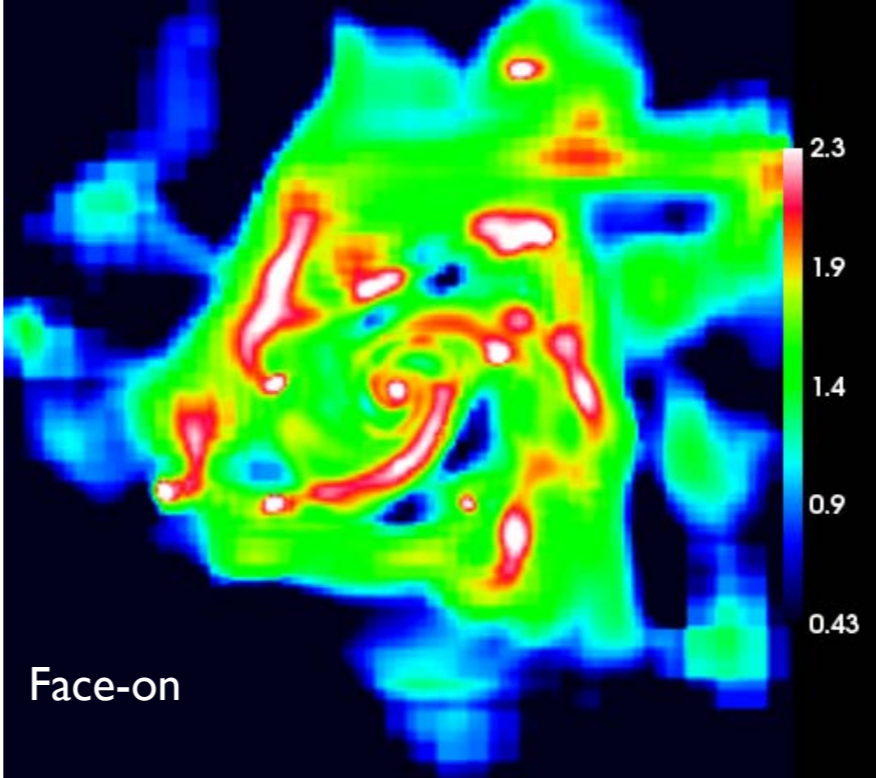
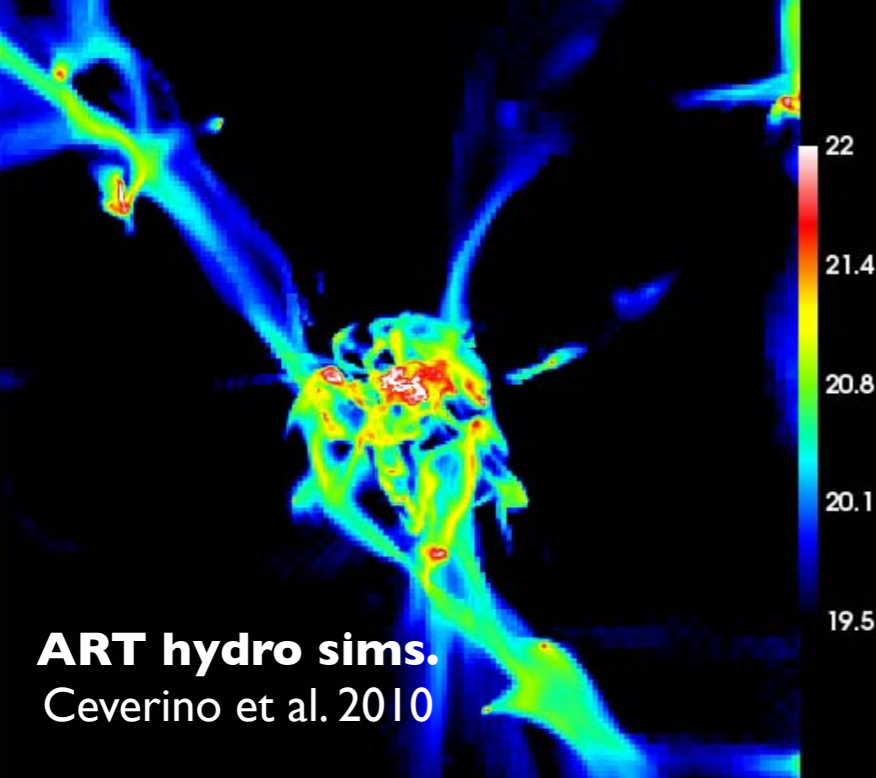
Sunrise U-V-J Images Every ~100 Million Years



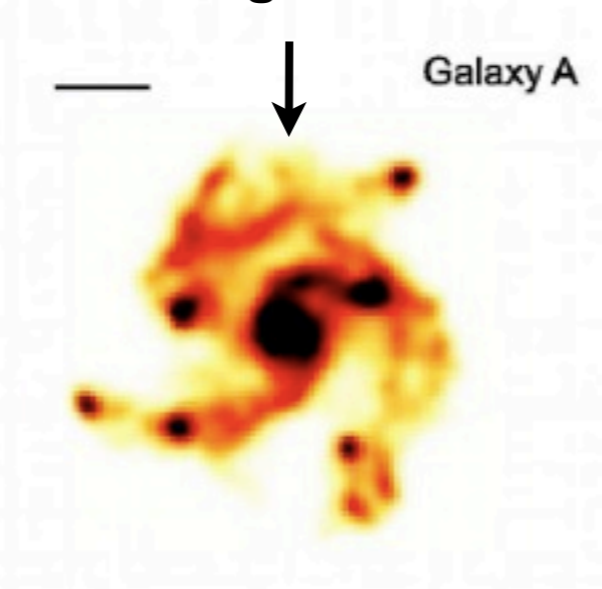
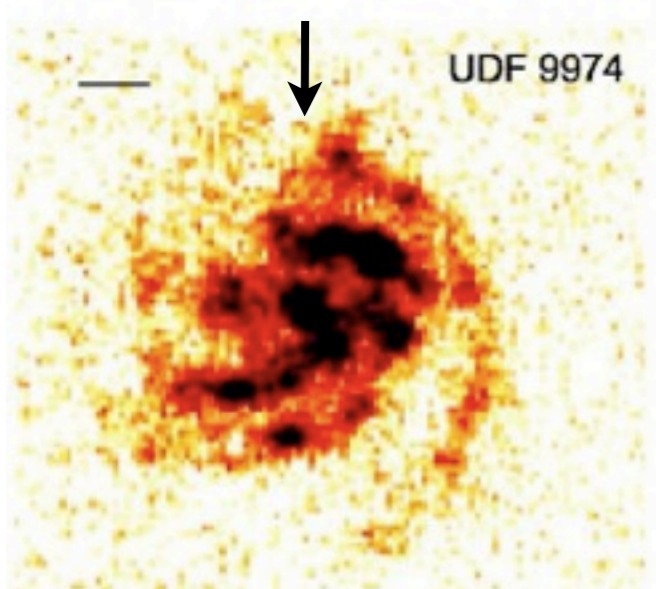
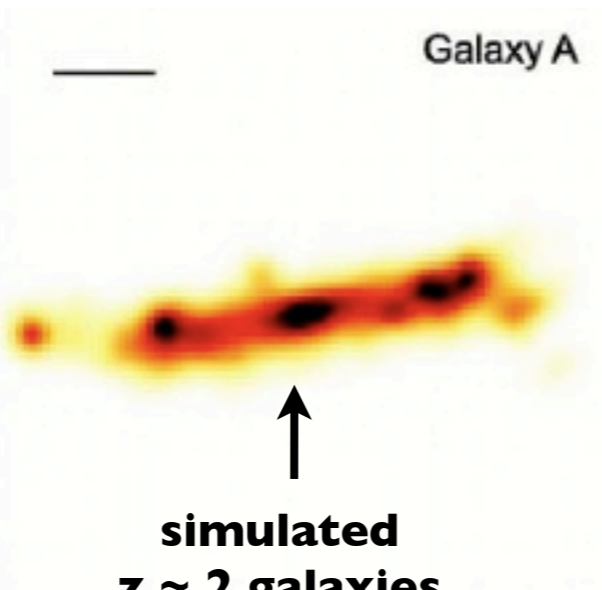
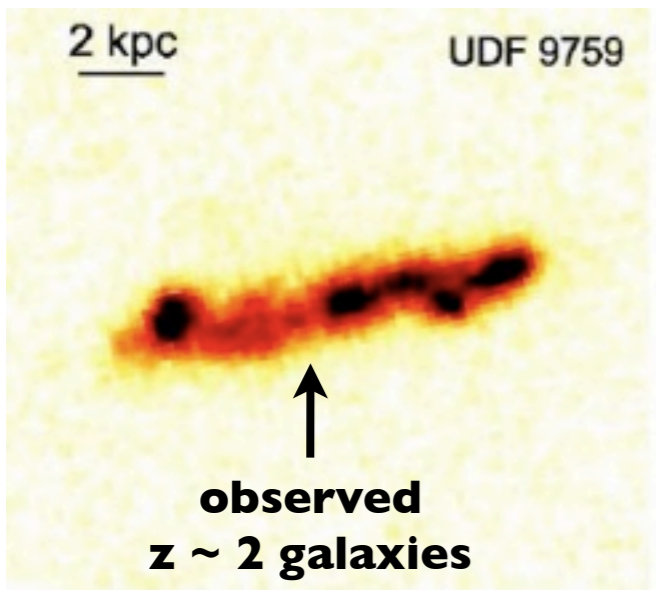
70,000 Light Years

A horizontal white double-headed arrow pointing from the left to the right, positioned below the text '70,000 Light Years'. The arrow spans the width of the text and is centered horizontally.

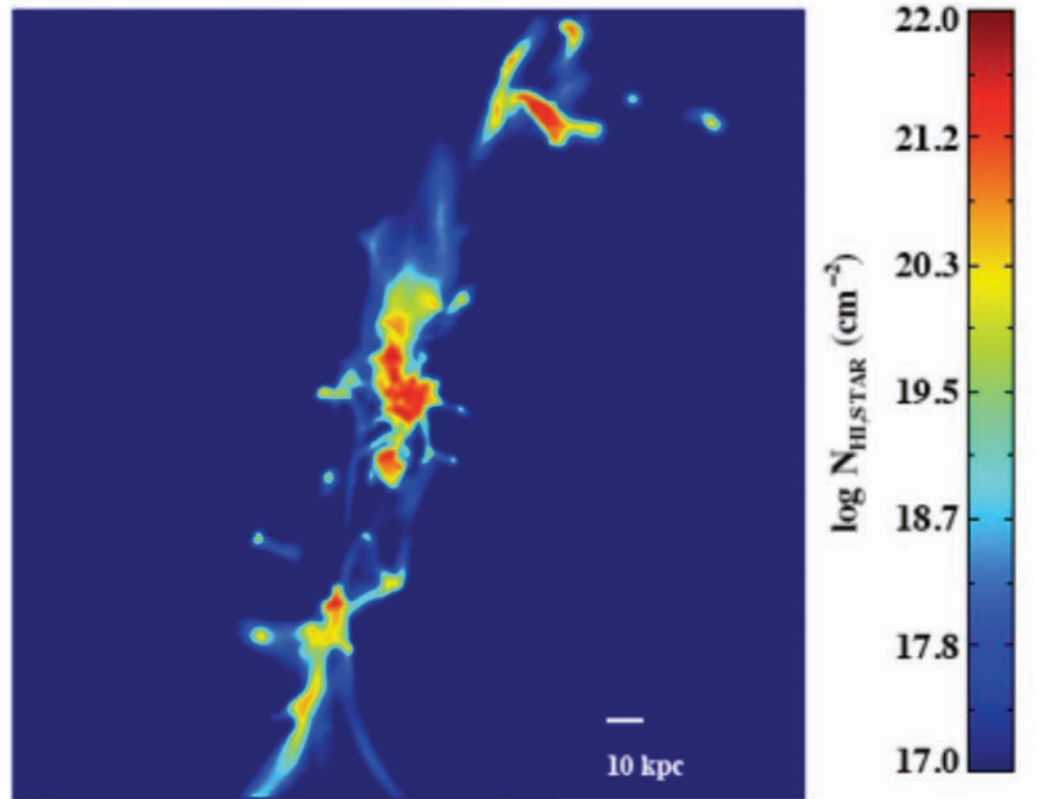
Chris Moody



now running on NERSC Hopper-II
and NASA Ames Pleiades supercomputers

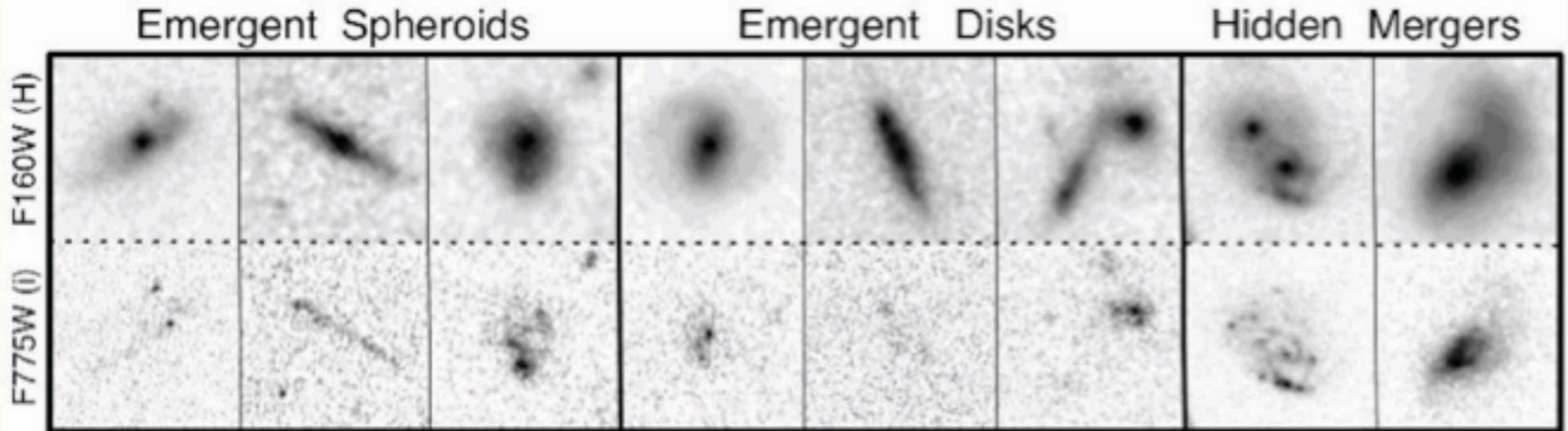


Ly alpha blobs from same simulation



Fumagalli, Prochaska, Kasen, Dekel, Ceverino, & Primack 2011

The CANDELS Survey



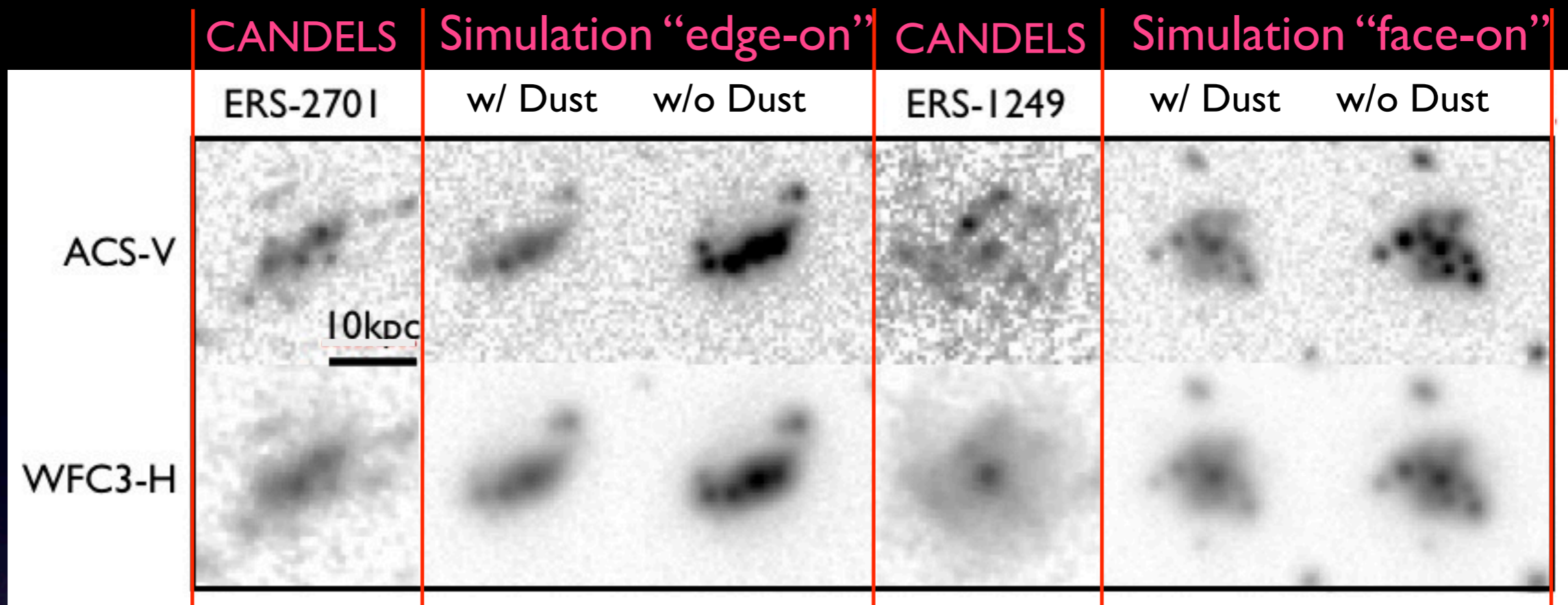
CANDELS makes use of the near-infrared WFC3 camera (top row) and the visible-light ACS camera (bottom row). Using these two cameras, CANDELS will reveal new details of the distant Universe and test the reality of cosmic dark energy.

<http://candels.ucolick.org>

CANDELS: A Cosmic Odyssey

CANDELS is a powerful imaging survey of the distant Universe being carried out with two cameras on board the Hubble Space Telescope.

- **CANDELS is the largest project in the history of Hubble**, with 902 assigned orbits of observing time. This is the equivalent of four months of Hubble time if executed consecutively, but in practice CANDELS will take three years to complete (2010-2013).
- **The core of CANDELS is the revolutionary near-infrared WFC3 camera**, installed on Hubble in May 2009. WFC3 is sensitive to longer, redder wavelengths, which permits it to follow the stretching of lightwaves caused by the expanding Universe. This enables CANDELS to detect and measure objects much farther out in space and nearer to the Big Bang than before. CANDELS also uses the visible-light ACS camera, and together the two cameras give unprecedented panchromatic coverage of galaxies from optical wavelengths to the near-IR.



Simulation shown is MW3 at $z=2.33$ ‘imaged’ to match the CANDELS observations in ACS-Vband and WFC3-Hband

- 0.06” Pixel scale
- convolved with simulated psfs
- noise and background derived from ERS observations (same field as examples shown)

MW3 was imaged at ‘face-on’ and ‘edge-on’ viewing angles both with and without including dust models

Summary: the big cosmic questions now

- The nature of the dark matter
- The nature of the dark energy (the future of the Universe)
- The early evolution of the Universe
 - Formation of the first tiny galaxies and the first stars
 - How the universe reionized
- How the entire population of galaxies forms and evolves
 - From direct observations from the ground and space
 - Interpreted with the help of cosmological simulations
 - Including star formation and feedback
 - Formation and feedback from supermassive black holes
 - etc.